

https://dspace.org/

The use of cassava waste in the removal of cobalt, chromium and vanadium metal ions from synthetic effluents

Seepe, Lizzy

2015-05-05
http://hdl.handle.net/10539/17617

Downloaded from a DSpace repository. https://dspace.org/

THE USE OF CASSAVA WASTE IN THE REMOVAL OF COBALT, CHROMIUM AND VANADIUM METAL IONS FROM SYNTHETIC EFFLUENTS

Lizzy Seepe

A dissertation submitted to the Faculty of Engineering and Built Environment, University of the Witwatersrand, Johannesburg, in fulfilment of the requirements for the degree of Masters of Science in Engineering

Johannesburg, 2015

DECLARATION

I declare that this dissertation is my own unaided work. It is being submitted for the degree of Master of Science in Engineering to the University of the Witwatersrand, Johannesburg. It has not been submitted before for any other degree or examination in any other University.

.....

(Signature of Candidate)

15th day of January 2015

ABSTRACT

This study investigated the removal of Co^{2+}, Cr^{3+} and V^{3+} from synthetic effluent using untreated and acid treated cassava waste biomass. Cassava waste biomass is a cellulosic material which possesses hydroxyl groups and sulfhydryl groups (or thiol groups) when untreated and treated with thioglycollic acid, respectively. Both these functional groups can act as binding sites for metal ions. Test works were carried out in batch flasks; semi-continuous counter current system and packed bed column.

The cassava waste biomass was characterized by using FTIR and BET. The effects of pH ranging from 2 to 7, and temperature from 30 to 50°C on the removal of metal from the solutions were investigated in a batch process. Metal concentrations from 50 to 250 mg/L, agitation speed of 50 to 200 rpm and biomass of 0.05 to 0.3g were used.

FTIR analysis proved that the thiolation process added a sulfhydryl (-SH) group onto the cassava waste resulting in an improved metal removal performance of the biomass. In the preliminary batch test works metal uptake was generally found to increase with an increase in pH, agitation speed, biomass and initial metal concentration. Adsorption of metal ions was observed to increase with pH, with an optimum removal obtained at pH of 6.0, 3.0 and 3.0 for Co^{2+}, Cr^{3+} and V^{3+}, respectively. Metal adsorption increased with an increase in temperature from 30 to 40°C at an initial metal concentration of 100 mg/L. However, there was a reduction in adsorption beyond 40°C for all the metal ions. The rate of removal of the metal ions in this study increased with an increase in dosage of the sorbent. This was attributed to the increase in surface area and in the number of available active sites for the sorption of Co^{2+}, Cr^{3+} and V^{3+}. It was found that the biomass that had been treated with a modifying agent had higher adsorption rates. Furthermore, the results showed that an increase in the concentration of the modifying reagent improved the adsorptivity of the cassava waste biomass. The capacity for the sorption of the three metal ions was found to be lower in ternary solution systems as compared to single ion systems suggesting the prevalence of a competitive adsorption effect in mixed solutions.

The presence of cations (Ca^{2+}, Mg^{2+}, Na^{+}, K^{+}) in aqueous solution decreased the amount of Co^{2+}, Cr^{3+} and V^{3+} adsorbed by cassava. The presence of Ca^{2+} was observed to have the most negative impact on the adsorption of the three metal ion systems. The equilibrium biosorption data could

be described by both Freundlich and Langmuir models, with the Freundlich isotherm describing the data better. Desorption experiments showed that at low H_2SO_4 concentration; it is possible to remove the metal ions bound to the biomass and to regenerate the biosorbent allowing its successive use. The cassava-peel biomass retained its original metal removal capacity up to six adsorption- desorption cycles. This is a good indication of cassava-peels' potential as a biosorbent material since they can be reused several times while maintaining high overall process efficiency.

Semi continuous counter current experiments showed that the adsorption of Co^{2+} needed 8 stages to meet the targeted limit of 0.05 mg/L set by the EPA. The Cr^{3+}system needed 6 stages to obtain the targeted limit of 0.05 mg/L. whilst for the V^{3+}system required 4 stages to attain the target limit of 0.1 mg/L.

The performance of the packed bed column was analysed using the effluent concentration versus time curves. The packed bed column was found to perform better with lower influent rate and high bed depth. The uptake analysis revealed a high selectivity for V^{3+}over Cr^{3+} and Co^{2+} at all conditions tested. The adsorption zone parameters and column design parameters have been determined using BDST and Thomas models. The experimental data best fitted with BSDT model than with the Thomas model for all the conditions tested with high linear correlation coefficient. This shows that the rate of adsorption is controlled by surface reaction and the unused capacity of the adsorbent. The adsorption-desorption results showed that the biosorbent can be used repeatedly without significant loss in sorption capacity reflecting its feasibility for commercial application.

PUBLICATIONS AND PRESENTATIONS

This work has produced some publications

Journal publications

1. Ndlovu, S., Simate, G.S., Seepe, L., Shemi, A., Sibanda, V., Van Dyk, L., 2013. Removal of Co^{2+}, V^{3+} and Cr^{3+} from synthetic waste water using cassava waste. South African *Journal of Chemical Engineering* 18 , 51-69

2. Simate, G.S., Ndlovu, S., 2013. The removal of heavy metals in a packed bed column using immobilized cassava peels waste biomass. *Journal of Industrial and Engineering Chemistry* 21, 635-643.

Conference proceeding

1 Seepe, L., Ndlovu, S., Simate, G.S., 2012. The removal of Co, Cr and V from synthetic waste water using cassava waste. Anglo American Hydrometallurgy Symposium August 29th- July – 1st, University of Cape Town, South Africa.

2 Seepe, L., Ndlovu, S., Simate, G., Shemi, A., Sibanda, V., Van Dyk, L., 2011. The Use of Cassava Waste in the Removal of Co (II), Cr (III) and V (III) from Effluents Streams. The 6th Africa Materials Research Society December 11-16, Victoria Falls, Zimbabwe.

DEDICATION

Dedicated to my parents and son.

ACKNOWLEDGEMENTS

Firstly, I would like to express my gratitude to my supervisors: Prof. Sehliselo Ndlovu and Dr Geoffrey S. Simate, for their advice, support, guidance and encouragement throughout the course of this work. This work would not have been possible without their supervision.

Dr Lizelle Van Dyk and Dr Vusumuzi Sibanda for the suggestions they made during research meetings.

NRF Scholarship (South Africa) and Friedel Sellschop Award (University of the Witwatersrand, South Africa) for the financial assistance with these studies.

My deepest appreciation to Bruce Mothibedi, Mthunzi Mbense, Xolani Mdletjae and all the technicians in the School of Chemical and Metallurgical Engineering for their assistance.

To My Colleagues: Alan Shemi, Reneilwe Mpana, Glawdis Tshofu, Doris Oke, Lerato Lekganya and Dominique Kyembo for showing interest in the completion of this work.

Thanks are expressed to the Wits Chemistry Department for their technical support.

Finally, I am indebted to my parents (Kamela and Tabudi), brothers (Malatela, Dibotho and Mphahlele), sisters (Mamotsiane and Mohweledi), son (Nduvho) and friend (Dakalo) for their unconditional love, encouragement and support throughout my study

TABLE OF CONTENTS

Table of Contents

DECLARATION i

ABSTRACT ii

PUBLICATIONS AND PRESENTATIONS iv

DEDICATION v

ACKNOWLEDGEMENTS vi

TABLE OF CONTENTS vii

LIST OF FIGURES xii

LIST OF TABLES xvii

CHAPTER ONE 1

1 INTRODUCTION 1

1.1 General Introduction 1

1.2 Research problem 2

1.3 Aim 2

1.4 Research methodology 3

1.5 Dissertation layout 3

CHAPTER TWO 4

2 LITERATURE REVIEW 4

2.1 Introduction 4

2.2 Toxic aspects of heavy metals 5

2.2.1 Cobalt 5

2.2.2 Chromium 6

2.2.3 Vanadium 7
2.3 Convectional Wastewater Treatment methods 7
2.3.1 Chemical precipitations 7
2.3.2 Ion exchange 8
2.3.3 Electrolytic techniques 9
2.3.4 Membrane technology 9
2.3.5 Chemical reduction 9
2.3.6 Adsorption 10
2.4 Biosorption 11
2.4.1 Mechanism of Biosorption 13
2.4.2 Cassava 14
2.5 Factors Affecting Biosorption 15
2.5.1 Solution pH 16
2.5.2 Solution temperature 17
2.5.3 Biomass concentration 17
2.5.4 Competing ions 17
2.6 Desorption and Regeneration 18
2.7 Sorption isotherm studies 19
2.8 BET surface area measurements 21
2.8.1 BET Theory 22
2.8.2 Adsorption isotherm 22
2.8.3 Pore size distribution analysis 24
2.9 Biosorption Contactors 25
2.9.1 Batch studies 25

2.9.2 Fixed bed column 26
2.9.3 Counter Current Biosorption Systems 30
CHAPTER THREE 33
3 MATERIAL AND METHODS 33
3.1 Introduction 33
3.2 Methods 33
3.2.1 Cassava 33
3.2.2 Activation 33
3.2.3 Thiolation 33
3.2.4 Stock Solution 34
3.3 Analytical Techniques 34
3.3.1 Determination of surface functional groups 34
3.3.2 Determination of the pH of the point of zero charge 34
3.3.3 Determination of surface area and pore structure (BET) 35
3.3.4 Determination of metal ion concentrations (FAAS) 35
3.4 Experimental methods 35
3.4.1 Batch adsorption 35
3.4.2 Adsorption-desorption cycle 36
3.5 Continuous adsorption system 37
3.5.1 Semi-continuous counter current adsorption studies 37
3.5.2 Adsorption- desorption experiments 38
3.5.3 Immobilization of acid treated cassava waste biomass 38
3.5.4 Characterization of immobilized cassava waste biomass 39
3.5.5 Column studies 39

3.5.6 Adsorption- desorption experiments 41

CHAPTER FOUR 42

4 BATCH STUDIES 42

4.1 Introduction 42

4.2 Results and Discussion 43

4.2.1 Fourier Transform Infrared spectroscopy (FTIR) analysis 43

4.2.2 Point of Zero Charge (pH_{PZC}) 46

4.2.3 BET analysis of untreated and acid treated biomass 46

4.2.4 Effect of acid treatment 47

4.2.5 Effect of pH 48

4.2.6 Effect of contact time 53

4.2.7 Effect of temperature 54

4.2.8 Effect of agitation 56

4.2.9 Effect of biomass and initial metal ion concentration 57

4.2.10 Effect of co-cations 60

4.2.11 Equilibrium isotherms 63

4.2.12 Adsorption-acid desorption cyclic studies 65

4.3 Summary and Conclusion 71

CHAPTER FIVE 72

5 CONTINUOUS ADSORPTION SYSTEMS 72

5.1 Introduction 72

5.2 Results and Discussion 73

5.2.1 Surface chemistry structure of immobilized cassava waste biomass 73

5.2.2 BET analysis of immobilized acid treated biomass 75

5.2.3 Semi continuous counter current system 75
5.2.4 Adsorption-desorption cycle 80
5.2.5 Packed bed column 81
5.2.6 Application of breakthrough models 88
5.2.7 Adsorption-desorption cycle 94
5.3 Comparison of batch, fixed bed and semi continuous counter current adsorption 96
5.4 Summary and Conclusion 97
CHAPTER SIX 98
6 Conclusions and Recommendations 98
6.1 Conclusions 98
6.1.1 Introduction 98
6.1.2 Batch test works 98
6.1.3 Semi- Counter current systems 99
6.1.4 Packed Column 100
6.2 Recommendations 100
CHAPTER SEVEN 102
7 REFERENCES 102
CHAPTER EIGHT 118
8 APPENDICES 118
8.1 Appendix A 118
8.2 APPENDIX B 124
8.3 APPENDIX C 127

LIST OF FIGURES

Figure 2.1 - The adsorption isotherms plot of nitrogen gas adsorption onto the surface of the adsorbent as pressure increases. ……..……..23

Figure 2.2 - Representation of a typical breakthrough curve.....28

Figure 2.3 - Multiple stage counter current adsorption……..31

Figure 2.4 - Graphic representation of multistage counter current adsorption.....32

Figure 3.1 - Experimental procedure of counter current adsorption system……..…....38

Figure 3.2 - Experimental setup for fixed bed operation…….....40

Figure 4.1(a) - Fourier transform infrared for untreated cassava waste biomass.....44

Figure 4.1(b) - Fourier transform infrared spectra for 0.5M acid treated cassava waste biomas..44

Figure 4.1(c) - Fourier transform infrared spectra for 1 M acid treated cassava waste biomass...45

Figure 4.2(a) - Effect of acid treatment on cassava waste for the removal of Co^{2+}: (pH = 4; biomass = 0.250 g; agitation speed = 150 rpm; contact time = 1h; temperature = 30°C; metal ion concentration = 100 mg/L).....47

Figure 4.2(b) - Effect of acid treatment on cassava waste for the removal of Cr^{3+}: (pH = 4; biomass = 0.250 g; agitation speed = 150 rpm; contact time = 1h; temperature = 30°C; metal ion concentration = 100 mg/L).....48

Figure 4.2(c) - Effect of acid treatment on cassava waste for the removal of V^{3+} (pH= 4; biomass = 0.250 g; agitation speed = 150 rpm; contact time = 1h; temperature = 30°C; metal ion concentration = 100 mg/L).....48

Figure 4.3(a) - Effect of initial pH on the removal of Co^{2+}, Cr^{3+} and V^{3+} using cassava waste biomass: single metal ion solutions; (pH = 2-7; biomass = 0.250 g; agitation speed = 150 rpm; contact time = 1h; temperature = 30°C; metal ions concentration = 100 mg/L)……...50

Figure 4.3(b) - Effect of initial pH on the removal of Co^{2+} and V^{3+} using cassava waste biomass: Binary metal ion systems; (pH = 2-7; biomass = 0.250 g; agitation speed = 150 rpm; contact time = 1h; temperature = 30°C; mixed metal solutions concentration = 100 mg/L).....50

LIST OF FIGURES (CONTINUED)

Figure 4.3(c) - Effect of initial pH on the removal of Co^{2+} and Cr^{3++} using cassava waste biomass: Binary metal ion systems (pH = 2-7; biomass = 0.250 g; agitation speed = 150 rpm; contact time = 1h; temperature = 30°C; mixed metal solutions concentration = 100 mg/L).....51

Figure 4.3(d) - Effect of initial pH on the removal of Cr^{3+} and V^{3+} using cassava waste biomass: Binary metal ion systems (pH = 2-7; biomass = 0.250 g; agitation speed = 150 rpm; contact time = 1h; temperature = 30°C; mixed metal solutions concentration = 100 mg/L).....51

Figure 4.3(e) - Effect of initial pH on the removal of Co^{2+}, Cr^{3+} and V^{3+} using cassava waste biomass: Ternary metal ion systems (pH = 2-7; biomass = 0.250 g; agitation speed = 150 rpm; contact time = 1h; temperature = 30°C; mixed metal solutions concentration = 100 mg/L).....52

Figure 4.4 - Effect of contact time on the removal of Co^{2+}, Cr^{3+} and V^{3+} using cassava waste biomass: Single metal ion solutions; (pH = 6 for Co^{2+}, 3 for Cr^{3+} and 3 for V^{3+}; biomass = 0.250 g; agitation speed = 150 rpm; contact time = 1h; temperature = 30°C; metal ions concentration = 100 mg/L).....54

Figure 4.5(a) - Effect of temperature on the removal of Co^{2+}, Cr^{3+} and V^{3+} ions using cassava waste biomass: Single metal ion systems; (pH = 6 for Co^{2+}, 3 for Cr^{3+} and 3 for V^{3+}; biomass = 0.250 g, agitation speed = 150 rpm; contact time = 1h; temperature = 30-50°C; concentration = 100 mg/L).....55

Figure 4.5(b) - Effect of temperature on the removal of Co^{2+}, Cr^{3+} and V^{3+} using cassava waste biomass : Ternary metal ion systems; (pH, = 4; biomass = 0.250 g, agitation speed = 150 rpm agitation speed; contact time, = 1h; temperature = 30-50°C; concentration = 100 mg/L).....55

Figure 4.6(a) - Effect of agitation speed on the removal of Co^{2+}, Cr^{3+} and V^{3+} using cassava waste biomass: Single metal ion system (pH = 6 for Co^{2+}, 3 for Cr^{3+} and 3 for V^{3+}, biomass = 0.250 g; agitation speed = 50-200 rpm; contact time = 1h; temperature = 30°C, concentration = 100 mg/L)……...…56

Figure 4.6(b) - Effect of agitation speed on the removal of Co^{2+}, Cr^{3+} and V^{3+} using cassava waste biomass: Ternary metal ion system ((pH = 4, biomass = 0.250 g; agitation speed = 50-200 rpm; contact time = 1h; temperature = 30°C, concentration = 100 mg/L).....57

LIST OF FIGURES (CONTINUED)

Figure 4.7(a) - Effect of biomass dosage on the removal of Co^{2+}, Cr^{3+} and V^{3+} using cassava waste biomass: Single metal ion systems (initial pH= 6 for Co^{2+}, 3 for Cr^{3+} and 3 for V^{3+}, biomass = 0.05 - 0.30 g; agitation speed = 150 rpm; contact time = 1h; temperature = 30°C, concentration = 100 mg/L).....58

Figure 4.7(b) - Effect of biomass dosage on the removal of Co^{2+}, Cr^{3+} and V^{3+} using cassava waste biomass: Ternary metal ion systems (initial pH= 4, biomass = 0.05-0.30 g; agitation speed = 150 rpm; contact time= 1h; temperature = 30°C, concentration = 100 mg/L).....58

Figure 4.8(a) - Effect of initial metal ion concentration on the removal of Co^{2+}, Cr^{3+} and V^{3+} using cassava waste biomass: Single metal ion systems (pH = 6 for Co^{2+}, 3 for Cr^{3+} and V^{3+}; biomass = 0.250 g; agitation speed = 150 rpm; contact time =1h; temperature = 30°C; concentration = 50-250 mg/L).....59

Figure 4.8(b) - Effect of initial metal ion concentration on the removal of Co^{2+}, Cr^{3+} and V^{3+} using cassava waste biomass: Ternary metal ion system (pH = 4; biomass = 0.250 g; agitation speed = 150 rpm; contact time =1h; temperature = 30°C; concentration = 50-250 mg/L).....60

Figure 4.9(a) - Effect of cations on the Co^{2+}removal using cassava waste biomass: Single metal ion system (pH = 6, biomass = 0.250 g, 150 rpm agitation speed; contact time, 1h; temperature 40°C, concentration 100 mg/L).....62

Figure 4.9(b) - Effect of cations on the Cr^{3+}removal using cassava waste biomass: Single metal ion systems (pH=3, biomass 0.250 g, 150 rpm agitation speed; contact time, 1h; temperature 40°C, concentration 100 mg/L).....62

Figure 4.9(c) - Effect of cations on the V^{3+}removal using cassava waste biomass: Single metal ion systems (pH=3, biomass 0.250 g, 150 rpm agitation speed; contact time, 1h; temperature 40°C, concentration 100 mg/L).....63

Figure 4.10 - Effect of H_2SO_4 concentrations on the desorption efficiency of Co^{2+}, Cr^{3+} and V^{3+} from cassava waste biomass.....66

Figure 4.11(a) - Fourier transform infrared spectrum for original cassava waste biomass before desorption with H_2SO_4……..67

LIST OF FIGURES (CONTINUED)

Figure 4.11(b) - Fourier transform infrared spectrum for 0.1M H_2SO_4 eluted cassava waste biomass……..67

Figure 4.11(c) - Fourier transform infrared spectrum for 1.5M H_2SO_4 eluted cassava waste biomass……..…68

Figure 4.11(d) - Fourier transform infrared spectrum for 2M H_2SO_4 eluted cassava waste biomass……..68

Figure 4.12 - Adsorption efficiency of cassava waste biomass for the adsorption-desorption regeneration cycles.....70

Figure 4.13 - Desorption efficiency of cassava waste biomass for the adsorption- desorption cycles using 0.1 mol/L H_2SO_4.....70

Figure 5.1(a) - Fourier transform infrared spectrum for immobilized cassava waste biomass before loading with Co^{2+}, Cr^{3+} and V^{3+}…….74

Figure 5.1(b) - Fourier transform infrared spectrum for metal loaded immobilized cassava waste biomass after loading with Co^{2+}, Cr^{3+} and V^{3+}……..…74

Figure 5.2 - Adsorption efficiency of cassava waste biomass for the adsorption-desorption cycles (semi continuous system).……..……81

Figure 5.3 - Desorption efficiency of cassava waste biomass for the adsorption- desorption cycles using 0.1 mol/L H_2SO_4 (semi continuous system)…….....81

Figure 5.4(a) - Breakthrough curves of Co^{2+} sorption by immobilized cassava waste biomass at different flow rates (Co = 100 mg/L, pH = 4 and bed depth = 10 cm)…….…83

Figure 5.4(b) - Breakthrough curves of Cr^{3+} sorption by immobilized cassava waste biomass at different flow rates (Cr = 100 mg/L, pH = 4 and bed depth = 10 cm)……..83

Figure 5.4(c) - Breakthrough curves of V^{3+} sorption by immobilized cassava waste biomass at different flow rates (V = 100 mg/L, pH = 4 and bed depth = 10 cm)……...…84

Figure 5.5(a) - Breakthrough curves of Co^{2+} sorption by immobilized cassava waste biomass at different bed depth (Co = 100 mg/L, pH = 4 and flow rate = 0.83 mL/s)……..…86

LIST OF FIGURES (CONTINUED)

Figure 5.5(b) - Breakthrough curves of Cr^{3+} sorption by immobilized cassava waste biomass at different bed depth (Cr = 100 mg/L, pH = 4 and flow rate = 0.83 mL/s…….….87

Figure 5.5(c) - Breakthrough curves of V^{3+} sorption by immobilized cassava waste biomass at different bed depth (V = 100 mg/L, pH = 4 and flow rate = 0.83 mL/s)……...87

Figure 5.6(a) - Plot of BDST equation for Co^{2+}.adsorption on immobilized cassava waste biomass (flow rate = 0.83 mL/s, initial cobalt concentration = 100 mg/L, pH = 4)…….…….....90

Figure 5.6(b) - Plot of BDST equation for Cr^{3+}.adsorption on immobilized cassava waste biomass (flow rate = 0.83 mL/s, initial chromium concentration = 100 mg/L, pH = 4)……...90

Figure 5.6(c) - Plot of BDST equation for V^{3+}.adsorption on immobilized cassava waste biomass (flow rate =0.83 mL/s, initial Vanadium concentration = 100 mg/L, pH = 4……91

Figure 5.7 - Adsorption efficiency of immobilized cassava waste biomass for the adsorption-desorption cycles (packed column)…….…….....95

Figure 5.8 - Desorption efficiency of immobilized cassava waste biomass for the adsorption-desorption cycles using 0.1 mol/L H_2SO_4 (packed column)…….…….96

LIST OF TABLES

Table 2.1 Regulation limits for some toxic metals and typical content of metal in waste water…….....4

Table 3.1 - Process parameters evaluated……..36

Table 3.2 - Flow rate and bed depth used……..40

Table 4.1 - general assignment of the FTIR spectra……..45

Table 4.2 - Structural characteristics of untreated and acid treated cassava waste biomass.....46

Table 4.3 - Linear Langmuir and Freundlich isotherm parameters for Co^{2+}, Cr^{3+} and V^{3+} sorption by cassava waste biomass.....64

Table 4.4 - Structural characteristics of original acid treated cassava waste biomass and after elution with different concentrations of H_2SO_4……69

Table 5.1 - Structural characteristics of original acid treated, 0.1M eluted and metal loaded immobilized cassava waste biomass…….….75

Table 5.2 - The adsorption of cobalt onto acid treated cassava waste biomass using semi continuous counter current in single system with initial metal ion concentration of 100 mg/L…….……..77

Table 5.3 - The adsorption of cobalt onto acid treated cassava waste biomass using semi-continuous counter current in ternary system with initial metal ion concentration of 100 mg/L…….…..78

Table 5.4 - The adsorption of chromium onto acid treated cassava waste biomass using semi-continuous counter current in single system with initial metal ion concentration of 100 mg/L…….…….….78

Table 5.5 - The adsorption of chromium onto acid treated cassava waste biomass using semi-continuous counter current in ternary system with initial metal ion concentration of 100 mg/L…….……..79

Table 5.6 - The adsorption of vanadium onto acid treated cassava waste biomass using semi-continuous counter current in single system with initial metal ion concentration of 100 mg/L…….…….….79

Table 5.7 - The adsorption of vanadium onto acid treated cassava waste biomass using semi-continuous counter current in ternary system with initial metal ion concentration of 100 mg/L……...…80

Table 5.8 - Parameters for breakthrough curves for the adsorption of Co^{2+}, Cr^{3+} and $V^{3+}$by immobilized cassava waste biomass at different flow rates……..85

LIST OF TABLES (CONTINUED)

Table 5.9 - Parameters for breakthrough curves for the adsorption of Co^{2+}, Cr^{3+} and V^{3+} by immobilized cassava waste biomass at different bed depth……..….....88

Table 5.10 - The BDST model parameters for the adsorption of Co^{2+}, Cr^{3+} and V^{3+} on immobilized cassava waste biomass…….……..…91

Table 5.11 - Thomas model parameters for the adsorption of Co^{2+}, Cr^{3+} and V^{3+} on immobilized cassava waste biomass at different flow rate (Bed depth = 10 cm, initial metal ion concentration = 100 mg/L)…….……..93

Table 5.12 - Thomas model parameters for the adsorption of Co^{2+}, Cr^{3+} and V^{3+} on immobilized cassava waste biomass at different bed depth and (Flow rate = 0.83 mL/s, initial metal ion concentration = 100 mg/L)……94

CHAPTER ONE

1 INTRODUCTION

1.1 General Introduction

Wastewater from many industries, such as metallurgical, tannery, chemical manufacturing, mining, battery manufacturing, etc., contains one or more toxic heavy metals. The concentrations of some of the toxic metals like Cr, Hg, Pb, As, etc., are sometimes higher than permissible discharge levels in these effluents. Therefore, it becomes necessary to remove these heavy metals from these wastewaters by an appropriate treatment process before releasing them into the environment (Meena *et al*., 2005).

Treatment processes for metal contaminated waste streams include chemical precipitation, ion exchange, adsorption and ultra-filtration (Volesky 1990a, b). However, most of these treatment methods have limitations because they are only economically viable at high concentrations of metal ions (Addour *et al*., 1999) and would require the use of costly chemicals and specialized equipment. For example, precipitation and ion-exchange, the two removal/recovery techniques that have found wide spread application require the use of chemicals and synthetic resins which are expensive (Mane *et al*., 2011).

A satisfactory process would be one that achieves the goal of toxic metal removal from wastewaters at a relatively low cost. Among the technologies used for water treatment is the adsorption technique which involves the use of an adsorbent such as biomass for the removal of trace amounts of toxic and valuable metals from industrial and municipal wastewater effluents has received much attention (Abia *et al*., 2002, 2003; Gardea-Torresdey *et al*., 1998; Ho *et al*., 1995; Low *et al*., 1995; Quek *et al*., 1998; Randall *et al*., 1974). Large amounts of excess plant biomass are being produced by the agricultural industry and they have been identified as potential alternatives to the existing metal removal technologies (Gurib-Fakim and Eloff, 2013). The use of agro-wastes for metal removal in aqueous solutions has attracted considerable attention because they are readily available, cheap, biodegradable, and the process involves small initial cost and land investment (Uppendra, 2006).

One of such agricultural plant of interest is cassava. Cassava waste biomass is a cellulosic material which possesses sulfhydryl groups and hydroxyl groups when acid treated and untreated, respectively. Both functional groups can act as binding sites for metal ions. Since

cassava waste biomass has negligible economic value, its conversion into adsorbents would increase its market value and ultimately benefit the millions of cassava producers.

Although the use of cassava biomass has shown much potential in the development of several bioprocesses such as bioremediation and biodegradation of hazardous compounds and products in recent years, there are still a few questions to be answered.

1.2 Research problem

Though cassava waste has proven to adsorb metals from waste water using batch adsorption processes (Abia *et al.*, 2003; Horsfall *et al.*, 2003; Suharso and Buhani, 2011), to the best of our knowledge no published work is available regarding their use for the removal of metals from aqueous solutions using continuous or semi-continuous biosorption processes on a large scale. In addition there is very little data related to the characteristics of the biomass as well as the operational system. This study therefore aims to answer the following questions;

- What is the feasibility of using a continuous process for the removal of Co^{2+}, $Cr^{3+}$and V^{3+} from effluent streams using cassava peelings?
- What operational parameters (e.g. pH, metal ion concentration, biomass: liquid ratio and temperature) would give optimum metal absorption?
- What is the possibility of regeneration and re-use of the cassava biomass?

1.3 Aim

The aim of this research is to develop a process for removal of toxic metal ions (i.e., Co^{2+}, $Cr^{3+}$and V^{3+}) from waste water solutions using cassava waste biomass. The process should be able to reliably operate on a large scale. This would involve the use of batch and continuous operations, selection of operating conditions and optimisation of process parameters.

Specific aims of the research involves:-

- Investigating the use of cassava waste in the recovery of toxic metals (Co^{2+}, Cr^{3+} and V^{3+}) from waste water solutions using batch and continuous processes.
- Investigating the effect of acid treatment on the removal efficiency of the biomass.
- Establishing the possibility of regeneration and re-use of the biomass.
- Establishing the selectivity of the process with respect to particular metals and the effect of the presence of other cations on the metal uptake ability of the biomass.
- The use of a counter current adsorption system to up scale the adsorption process.

1.4 Research methodology

The research method for this study involved the following: literature review, laboratory testing, laboratory test data analysis, conclusions and recommendations.

1.5 Dissertation layout

The dissertation will be structured as follows:

Chapter 1 Introduction: Outlines the research problem and sets out the objectives of the research work.

Chapter 2 Literature Review: This chapter reviews adsorption processes and the conventional treatment methods that are used in wastewater treatment processes.

Chapter 3 Materials and Method: Describes experimental setup and the equipment used in the study. Characterisation techniques of the cassava waste biomass and the sample preparation are also outlined.

Chapter 4-5 Results and Discussions: These chapters' describes laboratory tests and discussion of the findings.

Chapter 6 Conclusions and Recommendations: This chapter concludes the dissertation with a summary of the findings and recommendations.

List of references and appendices are given at the end of the dissertation.

CHAPTER TWO

2 LITERATURE REVIEW

2.1 Introduction

The metals found in the environment continue to increase due to industrialization. The anthropogenic sources of these metals include electroplating and metal finishing industries, metallurgical industries, tannery operation, chemical manufacturing, mine drainage, battery manufacturing and contaminated ground water from hazardous waste sites (Reed *et al*., 1994, Neal *et al*, 1990). The effluents from these sources contain trace amounts of heavy metal sufficient to humans as well as the rest of the ecosystem. At times, valuable materials are present in these effluent streams in small quantities. These elements should be removed prior re-joining the natural hydrological system. This requires treatment of the waste water. Table 2.1 shows some limits on the concentration of toxic heavy metals as established by the US Environmental Protection Agency (EPA, 2009) and typical metal ion concentrations found in waste water (Brigden *et al.,* 2009).

Table 2.1 Regulation limits for some toxic metals and typical content of metal in waste water.

Pollutant	**Regulation limits (mg/L)**	**Typical metal concentration in waste water (mg/L)**
Antimony	0.01	50
Arsenic	0.002	50
Cadmium	0.01	5
Chromium	0.02	20
Cobalt	0.02	20
Copper	1.30	372
Lead	0.10	50
Mercury	0.002	2
Selenium	0.05	200
Vanadium	0.10	20

This literature review describes the toxicity of heavy metal, conventional water treatment methods, biosorption process and continuous flow contactors.

2.2 Toxic aspects of heavy metals

The term heavy metals refers to metals and metalloids having densities greater than 5 g cm^{-3} and is usually associated with pollution and toxicity, although some of these elements (essential metals) are required by organisms at low concentrations (Adriano, 2001). When metals with no known biological function compete with, or replace a functional metal, toxicity results (Hughes and Poole, 1989). They can be toxic to microbial population at sufficiently high concentrations. However, some metals such as silver, mercury, cadmium and copper are markedly more toxic even at very low concentrations (Forstner and Wittman, 1979).

Toxic metals can exert harmful effects principally as a consequence of their strong coordinating abilities (Gadd, 1993). Toxic effects include the blocking of functional groups of biologically important molecules, the displacement and/or substitution of essential metal ions from biomolecules, conformational modification, denaturation and inactivation of enzymes and disruption of cellular and organelle integrity (Gadd, 1993). On a macro scale, effects include reduction in growth rates, extension of lag phase and perturbations in morphology and physiology (Hughes and Poole, 1989).

As discussed in section 1.2 (Research problem), this study will focus on cobalt, chromium and vanadium ions. These are some of the heavy metals found in industrial waste water.

2.2.1 Cobalt

Cobalt is an essential trace element for all animal organisms because it is an active centre of coenzymes called cobalamins (Schwaraz *et al*., 2000) which includes vitamin B-12 which is essential for mammals. Cobalt is also an active nutrient for bacteria, algae, and fungi. A deficiency of cobalt leads to pernicious anemia, a lethal disorder. One way pernicious anemia can develop is by loss of gastric parietal cells, which are responsible, in part, for the secretion of intrinsic factor, a protein essential for subsequent absorption of vitamin B_{12} in the ileum. The loss of ability to absorb vitamin B_{12} (B_{12}) is the most common cause of adult B_{12} deficiency. Impaired absorption of vitamin B_{12} may be due to a loss of intrinsic factors or to a number of other conditions that decrease production of gastric acid, which also plays a part in the absorption of B_{12} from foods. Pernicious anemia is, however, very rare, because trace

amounts of cobalt are available in most diets. The presence of 0.13 to 0.30 mg/kg of cobalt in soils markedly improves the health of grazing animals (Schwarz *et al*., 2000). Although cobalt is an essential element for life in minute amounts, it is toxic at high concentrations. Cobalt is a major cause of contact dermatitis and is considered carcinogenic. Therefore, several health and environmental organizations have set limits on the concentration of cobalt discharges. For example, the Occupational Safety and Health Administration (OSHA) have set a limit of 0.1 mg of nonradioactive cobalt per cubic meter of workplace air (0.1 mg/m^3) for an 8-hour workday and 40-hour work week. The Nuclear Regulatory Commission limits radioactive cobalt in workplace air to $1x10^{-5}$microcurie per millilitre (µCi/mL) for ^{57}Co and $7x10^{-8}$ µCi/mL for ^{60}Co. The Environmental Protection Agency (EPA) has set an average annual drinking water limit of 1000 picocurie per litre (pCi/L) for ^{57}Co or 100 pCi/L for ^{60}Co so the public radiation dose will not exceed 4 millirem (ATSDR, 2004).

2.2.2 Chromium

Chromium compounds are found in the environment, due to erosion of chromium-containing rocks and can be distributed by volcanic eruptions. The concentration range in soil is between 1 and 3000 mg/kg; in sea water 5 to 800 µg/L; and in rivers and lakes 26 to 5200 µg/L (Kotas and Stasicka, 2000). In aqueous solution chromium occurs in two forms - Cr (III) and Cr (VI). The relation between Cr (III) and Cr (VI) strongly depends on pH and oxidative properties of the location, but in most cases, the Cr (III) is the dominating species, although in some areas the ground water can contain up to 39 µg of total chromium of which 30 µg is present as Cr (VI). Cr (III) is essential in human nutrition (especially in glucose metabolism). However, Cr (VI) is more hazardous, carcinogenic and mutagenic to living organisms (Nakajima and Baba, 2004). In addition, it leads to liver damage, pulmonary congestion and causes skin irritation resulting in ulcer formation (Kobya, 2004).

While Cr (III) is relatively innocuous and immobile, Cr (VI) moves readily through soils and aquatic environments and is a strong oxidizing agent capable of being absorbed through the skin (Park and Jung, 2001). The US Environmental Protection Agency's established maximum concentration limit for Cr (VI) for discharge into inland surface waters is 0.1 mg/L and in potable water is 0.05 mg/L. In the dietary guidelines the daily chromium uptake was lowered from 50-200 µg for an adult to 35 µg (adult male) and to 25 µg (adult female) (Deans and Dixon, 1992).

2.2.3 Vanadium

Vanadium is an essential trace mineral needed for the normal functioning of the body. It is found in various amounts in the soil and several foods, and is released into the air by burning petroleum and petroleum products (Sigel and Sigel, 1995). Though vanadium is essential, high concentration of vanadium in the body has toxic effects. In fact, all vanadium compounds should be considered to be toxic (Roschin, 1967). Major effects include breathing problems, fatigue, purple-green tongue, retarded body growth, cancer and painful menstrual cycles. Excessive intake of the mineral may also lead to anaemia. The Occupational Safety and Health Administration (OSHA) has set an exposure limit of 0.05 mg/m^3 for vanadium pent oxide dust and 0.1 mg/m^3 for vanadium pent oxide fumes in workplace air for an 8-hour workday and 40-hour work week. The National Institute for Occupational Safety and Health (NIOSH) has recommended that 35 mg/m^3 of vanadium be considered immediately dangerous to life and health (OSHA, 2009).

2.3 Convectional Wastewater Treatment methods

The commonly used procedures for removing metal ions from aqueous streams include chemical precipitation, ion exchange, electrolytic techniques, membrane technology and chemical reduction (Rich and Cherry, 1987). However, many of these processes have significant disadvantages which include incomplete metal removal at low concentrations (Sag and Kutsal, 1996). The process description of each method is presented below.

2.3.1 Chemical precipitations

Chemical precipitation, including hydroxide precipitation and sulfide precipitation, is effective and by far the most widely used process in industry because it is relatively simple and inexpensive to operate (Ku and Jung, 2001). In precipitation processes, chemicals react with heavy metal ions to form insoluble precipitates. The precipitates formed can be separated from the water by sedimentation or filtration. The treated water is then decanted and appropriately discharged or reused.

Despite widespread usage, one of the main drawbacks of the chemical precipitation method is the use a large amount of chemicals needed to reduce metals to an acceptable level before discharge. Other disadvantages are its excessive sludge production that requires further treatment, increased costs, slow metal precipitation, poor settling, the aggregation of metal precipitates and the long-term environmental impacts of sludge disposal (Kurniawan, 2006).

Hydroxide Precipitation: The most widely used chemical precipitation technique is hydroxide precipitation due to its relative simplicity, low cost and ease of pH control (Huisman *et al*., 2006). The metal hydroxides can be removed by flocculation and sedimentation. A variety of hydroxides have been used to precipitate metals from wastewater. Based on the low cost and ease of handling, lime is the preferred choice used in hydroxide precipitation at industrial settings (Baltpurvins *et al*., 1997).

Although, widely used, hydroxide precipitation processes have some limitations. Firstly, hydroxide precipitation generates large volumes of relatively low density sludge, which can present dewatering and disposal problems (Kongsricharoern and Polprasert, 1995). Secondly, some metal hydroxides are amphoteric, and the mixed metals create a problem using hydroxide precipitation since the ideal pH for one metal may put another metal back into solution. Thirdly, when complexing agents are in the wastewater, they will inhibit metal hydroxide precipitation. Another drawback of the precipitation method is that the metal concentration of treated water cannot be reduced below the solubility of the precipitate (Kim *et al*., 2006a). Therefore, the use of other methods should be considered.

Sulfide Precipitation: This is also an effective process for the treatment of toxic heavy metals ions. One of the primary advantages of using sulfide is that the solubilities of the metal sulfide precipitates are dramatically lower than hydroxide precipitates and sulfide precipitates are not amphoteric. As the result, the sulfide precipitation process can achieve a high degree of metal removal over a broad pH range compared with hydroxide precipitation. Metal sulfide sludges also exhibit better thickening and dewatering characteristics than the corresponding metal hydroxide sludges.

However, there are potential dangers in the use of sulfide precipitation process. As it is known, heavy metal ions often in acid conditions and sulfide precipitants result in the evolution of toxic H_2S fumes. It is essential that this precipitation process be performed in a neutral or basic medium. Moreover, metal sulfide precipitation tends to form colloidal precipitates that cause some separation problems in either settling or filtration processes.

2.3.2 Ion exchange

Ion exchange resins are available for selective removal of some metal ions. The cation exchange resins are mostly synthetic polymers containing an active ion group such as SO_3H (Van der Heen, 1977). The cations are exchanged for H^+ or Na^+. Ion exchange is capable of reducing metal ion concentrations to parts per million levels. In the presence of large

quantities of competing mono-and divalent ions such as Na^{+} and Ca^{2+}, ion exchange is almost totally ineffective. The major limitations on the use of ion exchange for inorganic effluent treatment are primarily high cost and the requirements for appropriate pre-treatment systems (Singh and Kaushal, 2013; Sonune and Ghate, 2004) also highlighted the high cost due to the disposal of regeneration cycle salt brine.

2.3.3 Electrolytic techniques

Electrolytic techniques use an electrical current to plate out the metals (which can be recovered) and oxidize the cyanides in rinse waters from plating operations. Viggiano and Gramham (2003) showed that electrolytic recovery technology can remove more than 90% of the metal in the rinse stream and oxidize up to 50% of the cyanides thus minimizing the use of hazardous chemicals including acids, alkalis and chlorine-containing chemicals to treat rinse waters. Additionally, since the metal is recovered, the volume of metal-containing hazardous sludge at the wastewater treatment plant is reduced. The advantage of this technique is reduction in the use of treatment chemicals for cyanides and metals in the wastewater treatment plant and the recovery and reuse of metals. The disadvantages are the initial cost of purchasing the equipment which may be prohibitive and the process cannot differentiate among various types of metals for selective recovery.

2.3.4 Membrane technology

Membrane technologies, such as reverse osmosis and electro dialysis, are used commercially to recover dissolved metals from aqueous wastes generated through electroplating or metal etching processes (Ying, 2007). The technology is applicable to specific wastewaters, provided pre-treatment measures can be used to remove suspended and dissolved solids and ensure acceptable membrane lifetimes. However, current membrane processes tend to be hindered by the problems of limited flow-rates, instability of the membranes in salt and acid conditions and fouling by inorganic and organic species (Ying, 2007).

2.3.5 Chemical reduction

Chemical reduction as a waste treatment process is an established and well developed technology. For example, the reduction of hexavalent chromium's oxidation state to decrease toxicity and encourage precipitation is presently used as a treatment technology in numerous electroplating facilities (Ying, 2007). Major advantages of using chemical reduction such as in the reduction of hexalent chromium include operation at ambient conditions, automatic

controls, high reliability, and modular process equipment. The disadvantage of this process is the utilization of chemicals throughout the reduction process (Ying, 2007). Chromium needs to be readily available, and release of metals (iron, manganese, arsenic) during the process could produce undesirable water quality changes (Water Science and Technology Board, 2003).

2.3.6 Adsorption

Adsorption is defined as the mass transfer of a substance (adsorbate) from liquid onto the solid interface (adsorbent) and becomes attached by physical and/or chemical interactions (Kurniawan *et al*., 2006). Thus, adsorption can either be physical or chemical in nature, and frequently involves both (Cheremisinoff and Morresi, 1978). In chemisorption, the transfer of electrons is significant and equivalent to the formation of a chemical bond between the sorbate and the solid surface. In physisorption the interactive forces are relatively weak (Sing *et al*., 1985). In addition, physisorption involves the attraction by electrical charge differences between the adsorbent and the adsorbate.

Adsorption capacity depends on the physical and chemical characteristics of both the adsorbent and adsorbate, concentration of the adsorbate in liquid solution, experimental conditions such as temperature and solution pH, and the amount of time the adsorbate is in contact with the adsorbent (residence time) (Cheremisinoff and Morresi, 1978).

Adsorption is now recognized as an effective and economic method for heavy metal wastewater treatment. The adsorption process offers flexibility in design and operation and in many cases will produce high-quality treated effluent. In addition, because adsorption is sometimes reversible, adsorbents can be regenerated by suitable desorption process.

Below are various adsorbents which have been developed and applied for the removal of heavy metals from metal-contaminated wastewater.

Adsorption by Activated Carbon

Activated carbon (AC) is an excellent adsorbent, and it has been proven to be very effective in the removal of both inorganic and organic compounds from wastewaters. It has high specific surface area ranging between 500 and 1500 m^2/g and widely different surface functional groups (Yin *et al*., 2007). Any carbon material can be used to make activated carbon. However, commercial activated carbon is manufactured from only a few carbon sources such as wood, peat, coal, oil products, coconuts and pits (Davidson *et al*., 1968).

These are activated with steam or carbon dioxide at elevated temperature (700 – 1100°C). Unfortunately, it is not suitable for use in developing countries due to the high costs associated with production and regeneration of the spent carbon (Panday *et al*., 1985).

Adsorption by Zeolites

Zeolites are alumina silicate minerals containing exchangeable alkaline and alkaline earth metal cations (normally Na, K, Ca and Mg) as well as water in their structural framework. The physical structure is porous, enclosing interconnected cavities in which the metal ions and water molecules are contained (Yabe and Oliveira, 2003; Panday *et al*., 1985). Zeolites have high ion exchange and size selective adsorption capacities as well as thermal and mechanical stabilities (Wang *et al*., 2009). In addition, zeolites can be either synthetic (Hui *et al*., 2006) or natural. They have been used as water softeners (Ali and El- Bishtawi, 1997), chemical sieves and adsorbents (Hui *et al*., 2005) for a long time. However, zeolites become unstable at high pH (Basu *et al*., 2006) and for this reason chemicals are added to adjust the pH, making this process expensive. Furthermore, the use of zeolites does not reduce the level of most organic compounds (Johnson, 2005).

Adsorption by Activated Alumina

Activated alumina is the most widely used adsorbent because it possesses amphoteric properties allowing it to act as either an acid or a base. It is manufactured from aluminium hydroxide by dehydroxylating it in a way that produces a highly porous material (Farooqi *et al*., 2007). Activated alumina removes a variety of contaminants including excessive fluoride, arsenic, and selenium (Farooqi *et al*., 2007). The medium requires periodic cleaning with an appropriate regenerant such as alum or acid in order to remain effective. The main disadvantage of activated alumina is that the adsorption efficiency is highest only at low pH and contaminants like arsenites must be preoxidized to arsenates before adsorption (Johnson, 2005).

2.4 Biosorption

A satisfactory process for removal of trace metals from effluent streams would be one that achieves the goal of water purification by metals removal at a relatively low cost. The search for adsorption technologies involving the application of low cost and easily available adsorbent for the removal of toxic metals from wastewaters has directed attention to biosorption. Biosorption is based on binding capacities of various biological materials such as living or dead microorganisms or plants. It offers unique capabilities to concentrate and

reduce the levels of heavy metals to environmentally acceptable limits in an economically and environmentally friendly manner (Volesky, 2001). The process involves a solid phase (sorbent or biosorbent; biological material) and a liquid phase (solvent, distilled water) containing a dissolved species to be sorbed (adsorbate, metal) (Ahalya *et al*., 2003). Due to the higher affinity of the biosorbent for the adsorbate species, the latter is attracted and bound to the biosorbent by different mechanisms. The process continues until equilibrium is established between the amount of solid-bound adsorbate species and its portion remaining in the solution. The degree of adsorbent affinity for the adsorbate determines its distribution between the solid and liquid phases.

The major advantages of biosorption over conventional treatment methods include low cost, minimization of chemical or biological sludge, no additional nutrient requirement and regeneration of biosorbents and possibility of metal recovery (Sud *et al*., 2008). The cost-effective nature of the biosorption process in removing heavy metals places this technology in an interesting position of being able to open and successfully penetrate the potentially huge suppressed environmental clean-up markets.

Agricultural waste is one of the rich sources for low cost adsorbents besides industrial by-product or natural material. In fact, large amounts of excess plant biomass that possess little economic value are produced by the agri-industry creating serious disposal problems. It is desirable to use these as a renewable resource for sustainable bioremediation and biodegradation processes. If not used to generate a value-added product, the biomass would remain in the waste stream and require expensive disposal or treatments.

The basic components of the agricultural waste materials (biomass) include hemi-cellulose, lignin, extractives, lipids, proteins, simple sugars, water hydrocarbons, and starch that contain a variety of functional groups that facilitate metal complexation and help in the sequestering of heavy metals (Bailey *et al*., 1999). These promising agricultural waste materials are used in the removal of metal ions either in their natural form or after some physical or chemical modification. The use of agrowastes in a pure or chemically modified form for the remediation of contaminants in aqueous solution and industrial effluents has continued to attract considerable attention by several researchers (Abia *et al*., 2002, 2003; Gardea-Torresdey *et al*., 1998; Ho *et al*., 1995; Low *et al*., 1995; Quek *et al*., 1998; Randall *et al*., 1974). This is because agrowastes are readily available, cheap, biodegradable, sludge free and involve small initial cost and land investment.

2.4.1 Mechanism of Biosorption

The mechanisms of biosorption are generally based on physico-chemical interactions between metal ions and the functional groups present on the cell surface, such as electrostatic interactions, ion exchange and metal ion chelation or complexation (Ozer *et al*., 2004). Functional groups most commonly used in such interactions include acetomido groups of chitin, structural polysaccharides of fungi, amino and phosphate groups in nucleic acids, sulfhydryl and carboxyl groups in proteins, hydroxyls in polysaccharides and phosphoryl groups present within cell wall components such as polysaccharides, lipids and proteins (Dziwulska *et al*., 2004). For example, cassavas waste biomass which is a cellulosic material possesses hydroxyl groups when untreated, and sulfhydryl groups when treated with acids such as thioglycollic and mercaptoacetic acids (Horsfall and Abia, 2003; Horsfall *et al*., 2003 Ndlovu *et* al., 2013). Both these functional groups can act as binding sites for metal ions.

The biosorption mechanism can be divided into two; metabolism dependent and metabolism independent (Ahalya *et al*., 2003). In the metabolism dependent process transport of the metal across the cell membrane yields intracellular accumulation which is dependent on the cell's metabolism. This means that this kind of biosorption may take place only on viable cells (Ahalya *et al*., 2003). During non-metabolism dependent biosorption metal uptake is by physico-chemical interaction between the metal and the functional groups present on the cell surface (Kuyucak and Volesky, 1988). This type of biosorption, i.e., non-metabolism dependent is relatively rapid, can be reversible and requires minimal energy for activation; in the region of 21 kJ/mol, as opposed to the activation energy required for bioaccumulation (63 kJ/mol) (Kaduková and Virčíková, 2005, Kuyucak and Volesky, 1988). This allows for metal ion desorption followed by regeneration and reuse of the biosorbent in successive sorption/desorption cycles. Biosorption is based on physical adsorption, ion exchange and chemical sorption, which is not dependent on the cell metabolism.

Below are some of the physico-chemical interaction processes between metal ions and the functional groups present on the cell surface.

Physical adsorption

Physical adsorption takes place with the help of van der Waals' forces. Kuyucak and Volesky (1988) hypothesized that uranium, cadmium, zinc, copper and cobalt biosorption by dead biomasses of algae, fungi and yeasts takes place through electrostatic interactions between

the metal ions in solutions and walls of microbial cells. The principal driving force for metal ion biosorption is the net negative surface charge of the biomass. Studies have shown that a definite relationship between the electronegativity of activated sludge surfaces and their metal biosorptive capacities does exist (Bux and Kasan, 1994). From this it follows that the higher the electronegativity of the biomass the greater the attraction and adsorption of heavy metal cations.

Ion Exchange

The polysaccharides associated with microbial cell walls allow the exchange of bivalent metal ions. For example, the alginates of marine algae occur as salts of K^+, Na^+, Ca^{2+}, and Mg^{2+}. These ions can exchange with counter ions such as CO^{2+}, Cu^{2+}, Cd^{2+} and Zn^{2+} resulting in the biosorptive uptake of heavy metals (Kuyucak and Volesky, 1988).

Complexation

The metal removal from solution may also take place by complex formation on the cell surface after the interaction between the metal and the active groups. Aksu *et al* (1992) hypothesized that biosorption of copper by *Calluna vulgaris* and *Zoogloea Ramigera* takes place through both adsorption and formation of coordination bonds between metals and amino and carboxyl groups of cell wall polysaccharides. Complexation was found to be the only mechanism responsible for calcium, magnesium, cadmium, zinc, copper and mercury accumulation by *Pseudomonas syringae (*Ahalya *et al*., 2003*).*

2.4.2 Cassava

The metal adsorption capacities of different kinds of biomass have been identified as potential alternatives to the existing metal removal technologies. The much studied biosorbents include algae, seaw**e**ed, alfalfa, sago waste (Quek *et al*., 1998), banana pith (Low *et al*., 1995) and sunflower and cassava waste (Horsfall and Abia, 2003). Amongst these biosorbents, cassava waste is the main interest of this study.

Cassava is a perennial woody shrub, which is a major source of low cost carbohydrates for populations in the humid tropics. The largest producer of cassava is Brazil, followed by Thailand, Nigeria, DRC and Indonesia. Production in Africa and Asia continues to increase, while that in Latin America has remained relatively constant over the past 30 years (O'Hair, 1995).

The preparation of cassava for consumption purposes produces a large volume of waste such as peelings which create a lot of environmental problems. So far, not much effort has been made to control or manage the enormous wastes arising from processing cassava tuber into its various products, which are abundant and available in all seasons. The economic utilization of cassava tuber bark waste may not only provide a solution to its environmental nuisance, but will create employment and improve local economies. Abundant amount of non-used cassava peels fits this purpose and might be utilized as an effective and low cost adsorbent. In addition the world market for cassava starch and meal is limited, and since the cassava has negligible economic value its conversion into adsorbents would increase its market value and ultimately economically benefit the millions of cassava producers (Gurib-Fakim and Eloff, 2013).

Although the use of cassava biomass has shown much potential in the development of several bioprocesses such as bioremediation and biodegradation of hazardous compounds and products in recent years, its potential to operate reliably at a large scale has not been investigated to the same degree. Furthermore, there is very few data related to the characteristics of the biomass as well as the operational system. A possible viable system would be to employ fixed bed reactors such as conventional processes that use ion exchange resins or activated carbon. This would allow the treatment of large volumes of solutions, although limited by the loading of the biomass system. It would thus be necessary to develop a system for the regeneration of the biomass in order to employ it in a larger number of sorption cycles. Other parameters such as the adequate flow rate and residence time compatible with the process would also need to be considered.

2.5 Factors Affecting Biosorption

Past research on the sorption of metal ions by biomass has led to the findings that apart from the fundamental biosorption influences, such as the metal ions to be absorbed and the type and form of biomass to be used as the adsorbent, the conditions under which the reaction take place are largely responsible for the efficiency of the absorption process (Wang and Chen, 2006; Horsfall and Abia, 2003). Some of the factors influencing reactions biosorption include the solution temperature, the solution pH and the presence of competing ions in solution that may be adsorbed with equal or higher affinity than the target metal.

2.5.1 Solution pH

The pH seems to be the most important parameter in the biosorptive process. It affects the solution chemistry of the metals, the activity of the functional groups in the biomass and the competition of metallic ions (Friis and Myers-Keith, 1986; Galun *et al*., 1987). The pH is capable of influencing not only the binding site dissociation state, but also the solution chemistry of the target metal in terms of hydrolysis, complexation by organic and/or inorganic ligands and redox potentials (Fiol *et al*., 2006). This accounts for the specific sorption of some metal species rather than others at various conditions of pH (Godlewska-Żyłkiewicz and Kozłowska, 2005). It has been found that at low pH value, i.e., those lower than 3, adsorption of metal ions decreases. This is because at low pH values there are large amounts of H^+ ions present in the system, thus metal ions need to compete with these ions to form a bond with active sites of functional groups on biosorbents surface. Increasing the pH reduces the electrostatic repulsion, exposing more ligands carrying negative charges hence increase in adsorption. However, at much higher pH values, metal precipitation and formation of hydroxylated complexes such as chromium complexes take place, thus making the adsorption process ineffective.

Other metal-specific pH influences include precipitation, speciation and the availability of the metal for biosorption (Esposito *et al*., 2002). Successful biosorption of base metal cations usually takes place in the range of pH of 3 - 7, and is extremely pH dependent (Sharma and Sanghi, 2012). Ozer and Ozer (2003) reported an optimal pH value for lead and nickel uptake of 5.0, while Vianna *et al.* (2000) found that copper, cadmium and zinc uptake was maximal at pH 4.5, and decreased significantly when the pH was dropped to 3.5 or 2.5. This led them to suggest that an initial electrostatic attraction between the negatively charged functional groups and the metal cations was involved in the biosorption reaction.

The biosorption process is not necessarily limited by this apparent dependence on the small pH range within which optimal sorption occurs. When screening four variants of immobilized chitosan for gold binding capabilities (Arrascue *et al.,* 2003). Found that by grafting sulfur compounds onto the biosorbent they could decrease the influence of pH via modification of the uptake mechanism from pure ion exchange to a combination with sulfur chelation. This would not only increase the uptake capacity, but also allow a much broader operating range if similar modifications are made to other already successful biosorbents. Parsons *et al*. (2003)

also found that chemical modification of the alfalfa biomass resulted in an increase in the pH at which maximal platinum binding occurred at pH 6.

2.5.2 Solution temperature

The temperature at which a sorption reaction takes place is rarely important (Panda *et al*., 2006), with most reactions being temperature-independent (Bhainsa and D'Souza, 1999). However, there are exceptions where temperature does affect the interaction between the biosorbent and the metal ions, usually by influencing the stability of the metal ions in solution (Sag and Kutsal, 2000), the stability of the metal-sorbent complex, and the ionization of the cell wall chemical moieties (Özer *et al*., 2004).

2.5.3 Biomass concentration

Biomass concentration in solution seems to influence the specific uptake: for lower values of biomass concentrations there is an increase in the specific uptake (Fourest and Roux, 1992; Gadd *et al*. 1988). Gadd *et al*. (1988) suggested that an increase in biomass concentration leads to interference between the binding sites. Fourest and Roux (1992) invalidated this hypothesis attributing the decrease of the specific uptake to metal concentration shortage in solution. Hence this factor needs to be taken into consideration in any application of biomass as biosorbent.

2.5.4 Competing ions

In wastewater streams, the metal of interest is usually found in a matrix containing several other metal ions (Fourest, 1993; Tobin *et al*., 1984; Chong and Volesky, 1996). This is because most processes which lead to the deposition of metals in effluent streams involve not only one metal, which is usually washed off or used in the process, but instead the water comes into contact with a variety of other metals and compounds. These extra metal ions and compounds exist simultaneously in the effluent stream with toxic metals which are targeted by the adsorption process. These will often either compete with the metal of interest for binding sites or lower the specificity of the biosorbent by binding to sites to which the metal ions of interest do not bind. If the preference of one metal ion for a ligand is similar to that of another metal ion, a competition effect could be observed between the metals for a given binding site. In cases where such competing ions co-exist in a solution to be treated by a biosorbent, the biosorption metal uptake capacity of the targeted metal is expected to be lower than that corresponding to the single metal solution of the targeted element. Thus the

presence of certain cations is bound to have an effect on the selectivity and ultimately the adsorption capacity of the adsorbent. If, however, the metal ion species exhibit preferences for different biomass binding sites, their simultaneous presence in solution may not significantly affect their corresponding metal uptake capacities (Tsezo *et al*., 1996).

The most common ions that occur in wastewater are: sodium, magnesium and calcium (Deng *et al*., 2007). These various components can interact with heavy metals and modify their behaviour towards the sorbent material used (Tsezos, 1983; Maruca *et al*., 1982; Benguella and Benaissa, 2002b). In general, sodium ions which are bound weakly through mostly electrostatic attraction are effective in competing only with other weakly bound ions. However, even heavy metals that tend to form complexes are partially bound through electrostatic attraction as a consequence of the higher concentrations of all metals near binding sites, than in the bulk solution (Schiewer and Volesky, 2000). The presence of divalent calcium or magnesium ions exerts a stronger influence on metal uptake than in the case of sodium, which is reflected even at lower salt concentrations. This could be consequence of its higher electrostatic accumulation and its greater affinity for the binding sites (Volesky, 2003). As such, divalent ions can compete more strongly for binding site than the monovalent Na^{+} ions.

2.6 Desorption and Regeneration

If the biosorption process is to be used as an alternative to the wastewater treatment scheme, the regeneration of the biosorbent is crucially important for keeping the process costs down (Ahalya *et al*., 2003). For this purpose, it is desirable to desorb the sorbed metals and to regenerate the biosorbent material for subsequent cycles of application. The desorption process should: yield the metals in a concentrated form; restore the biosorbent close to the original condition for effective reuse with undiminished metal uptake and without physical changes or damage to the biosorbent. It has been observed that for metal ions which show marked pH dependence in binding to the biomass, stripping of bound metal(s) can be accomplished by pH adjustments (Singh and Stapleton, 2002). While the regeneration of the biosorbent may be accomplished by washing the metal-laden biosorbent with an appropriate solution, the type and strength of this solution would depend on the extent of binding of the deposited metal. Dilute solutions of mineral acids like hydrochloric acid, sulphuric acid, acetic acid and nitric acid can be used for metal desorption from the biomass (de Rome and

Zhou and Kiff, 1991; Luef *et al*., 1991; Holan *et al*., 1993; Pagnanelli *et al*., 2002; Bai and Abraham, 2003).

2.7 Sorption isotherm studies

In order to estimate the practical or dynamic adsorption capacity, it is essential to first have enough information on adsorption equilibrium. Since adsorption equilibrium is the most fundamental property, a number of studies have been conducted to determine: the amount of species adsorbed under a given set of conditions (concentration and temperature), or how selective adsorption takes place when two or more absorbable components co-exist (Aksu *et al*., 1997; Chong and Volesky, 1995; Kapoor and Viraraghavan, 1995; Liu *et al*., 2002b; Pagnanelli *et al*., 2002; Volesky and Holan, 1995). When an adsorbent is in contact with the surrounding fluid of a certain composition, adsorption takes place and after a sufficiently long time, the adsorbent and the surrounding fluid reach equilibrium. This means that the equilibrium distribution of metal ions between the sorbent and the solution is important in determining the maximum sorption capacity.

Equilibrium studies that give the capacity of the biosorbent and adsorbate are described by adsorption isotherms, which is usually the ratio between the quantity adsorbed and the remaining in solution at fixed temperature. Freundlich and Langmuir isotherms are the earliest and simplest known relationships describing the adsorption equation (Muhamad *et al*., 1998; Jalali *et al*., 2002).

The Langmuir equation is used to estimate the maximum adsorption capacity corresponding to complete monolayer coverage on the biosorbent surface and is expressed by:

$$q_e = \frac{q_{max} b C_e}{1} - b C_e \qquad (2.1)$$

where q_{max} is the maximum adsorption capacity (mg/g), b is the Langmuir constant related to adsorption energy (L/mg), C_e is the equilibrium concentration of metal remaining in solution (mg/L) and q_e is the metal uptake (mg/g).

After rearranged, the Langmuir adsorption isotherm can be expressed in the linear form as:

$$\frac{C_e}{q_e} = \frac{1}{q_{max}} C_e - \frac{1}{q_{max}} b \quad (2.2)$$

An alternative linearized Langmuir isotherm is expressed as:

$$\frac{1}{q_e} = \frac{1}{q_{max}} b \left(\frac{1}{C_e}\right) + \frac{1}{q_{max}} \quad (2.3)$$

By plotting a graph of $(1/q_e)$ versus $1/C_e$, a straight line is obtained.

According to Langmuir isotherm model, the amount of the metal bound by the biosorbent is calculated as follows:

$$q_e = \frac{V(C_i - C_e)}{m} \quad (2.4)$$

and

$$Percentage\ metal\ ion\ removal = \frac{C_i - C_e}{C_i} \times 100 \quad (2.5)$$

where q_e is the metal uptake (mg metal per g biosorbent), V is the liquid sample volume (mL), C_i is the initial concentration of the metal in solution (mg/L), C_e is the final (equilibrium) concentration of the metal remaining (residual) in solution (mg/L), and m the amount of added biosorbent on dry weight basis (g).

The experimental data is then fitted into the equation 2.2 for linearization by plotting C_e/ q_e against C_e.

The Freundlich model is an empirical equation used to estimate the adsorption intensity of the sorbent towards the adsorbate and is given by:

$$q_e = K_F C_e^{\frac{1}{n}} \quad (2.6)$$

Where, q_e is the adsorption density (mg of metal ion adsorbed/g biomass); C_e is the concentration of metal ion in solution at equilibrium (mg/L); K_F and n are the Freundlich constants which determine the curvature and steepness of the isotherm (Akgerman and

Zardkoohi, 1996). Also, the value of n indicates the affinity of the adsorbate towards the biomass. The above equation is conveniently used in linear form as:

$$\mathrm{Log}q_e = \log K_F + \frac{1}{n}\log C_e \quad (2.7)$$

A plot of log C_e against log q_e yielding a straight line indicates the conformation of the Freundlich adsorption isotherm. The constants 1/n and log K_F can be determined from the slope and intercept, respectively.

2.8 BET surface area measurements

The method for determining the surface area of a porous solid was developed by Brunner, Emmett, and Teller and is a widely used tool for determining the monolayer volume (V_m) and the specific surface area (S) (Brunauer, 1945). The BET method is based on gas sorption (both adsorption and desorption) on the surface of dry solid powders. Nitrogen (N_2) adsorption at -196.15°C and at sub-atmospheric pressures represents the most widely used technique to determine catalyst surface area and to characterize its porous texture (Leofanti *et al*., 1998). N_2 is applied over a range of relative pressures and produces adsorption isotherms that provide information in micro-, meso- and macroporosity ranges approximately 0.5-200nm (Groen, 2003). The amount of gas molecules adsorbed or desorbed is determined by the pressure variations due to the adsorption or desorption of the gas molecules by the material (the adsorbent). The total surface area of the adsorbent is calculated using the adsorption model and the total area that will be occupied by the N_2. The equation below is used to calculate the surface area, S_{bet} (Gregg and Sing, 1982):

$$S_{bet} = \frac{V_m N_a \sigma_x}{V} \quad (2.8)$$

Where V_m is the volume of gas for an adsorbed monolayer, V is the molar volume of the adsorbed gas, N_a is the Avogadro number and σ_x is the area covered by one nitrogen molecule.

2.8.1 BET Theory

The BET Theory put forward by Brunner, Emmett and Teller explained that multilayer formation is the true picture of physical adsorption (Tact9 media, 2010). One of the basic assumptions of Langmuir Adsorption Isotherm was that adsorption is monolayer in nature. Thus the Langmuir adsorption equation is applicable under the conditions of low pressure. Under these conditions, gaseous molecules would possess high thermal energy and high escape velocity. As a result of this, a lower number of gaseous molecules would be available near the surface of the adsorbent.

Under the condition of high pressure and low temperature, the thermal energy of gaseous molecules decreases and more and more gaseous molecules would be available per unit surface area. Therefore, multilayer adsorption would occur. The multilayer formation was explained by BET Theory.

According to Gregg and Sing (1982), BET theory suggests that the surface of the adsorbent is uniform thus the heat of adsorption of the first monolayer is constant. It further assumes that there is no lateral interaction of adsorbed particles and that adsorbed molecules can act as a new adsorption surface for subsequent layers; and this is a repetitive process. Finally, the heat of adsorption of all monolayers apart from the first is equal to the heat of condensation. From this BET theory, the derived BET equation is (Leofanti *et al*., 1998):

$$V_{ads} = V_m \frac{cp/p_o}{1-p/p_o(1+(c-1)p/p_o} \qquad (2.9)$$

Where p and p_o are the equilibrium and saturation pressures of the adsorbate at the temperature of adsorption; V_{ads} is the adsorbed gas volume; V_m is the monolayer adsorbed gas volume; and c is the BET constant, which is related to the heats of adsorption and liquefaction.

2.8.2 Adsorption isotherm

The process of adsorption is usually studied through graphs known as adsorption isotherm. It is the graph between the amounts of the adsorbate (x) adsorbed on the surface of the adsorbent (m) and the pressure at constant temperature.

Types of adsorption isotherm

Five types of adsorption isotherm and their characteristics are explained below.

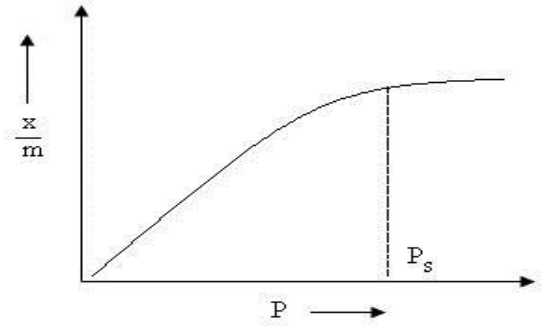

a) Type I

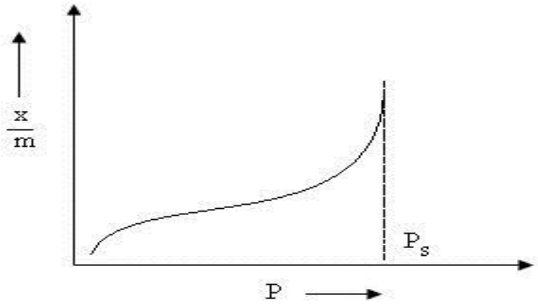

b) Type II

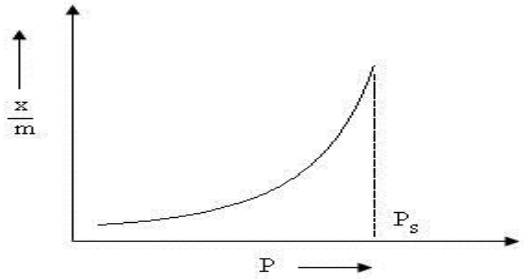

c) Type III

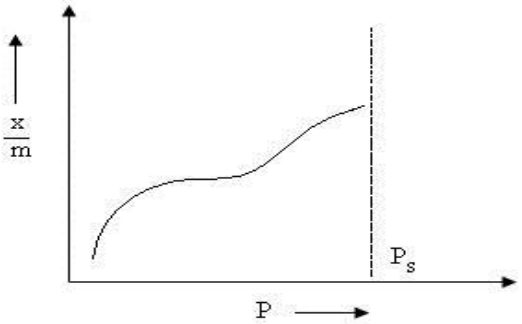

d) Type IV

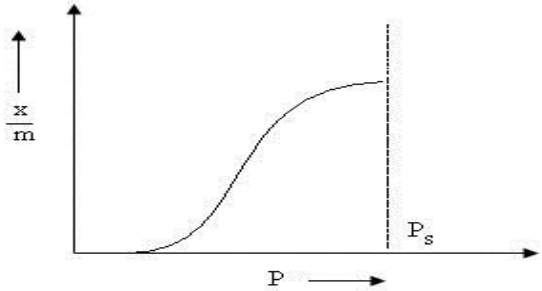

e) Type V

Figure 2.1 The adsorption isotherms plot of nitrogen gas adsorption onto the surface of the adsorbent as pressure increases (Tact9 media, 2010).

An inherent property of Type I isotherms (Figure 2.1a) is that adsorption is limited to the completion of a single monolayer of adsorbate at the adsorbent surface. Type I isotherms are observed for the adsorption of gases on microporous solids whose pore sizes are not much

larger than the molecular diameter of the adsorbate. The characterization of micro-porous materials, those with pore diameters less than 2 nm, gives this type of isotherm. Complete filling of these narrow pores corresponds to the completion of a molecular monolayer. A type I isotherm is obtained when $P/P_o < 1$ and $c > 1$ in the BET equation, where P/P_o is the partial pressure value and c is the BET constant, which is related to the adsorption energy of the first monolayer and varies from solid to solid.

A type II isotherm Figure 2.1(b) shows a very large variation from the Langmuir model of adsorption. A type II isotherm is obtained when $c > 1$ in the BET equation. The flatter region in the middle represents the formation of a monolayer. Type II isotherms do not exhibit a saturation limit as Type I. This type of isotherm indicates an indefinite multi-layer formation after completion of the monolayer and is found in adsorbents with a wide distribution of pore sizes. This is the most common isotherm obtained when using the BET technique.

A type III isotherm Figure 2.1(c) is obtained and shows the formation of a multilayer. Type III isotherm is obtained when the $c < 1$ and when the amount of gas adsorbed increases without limit as its relative saturation approaches unity. There is no flattish portion in the curve which indicates that monolayer formation is missing and therefore BET is not applicable since type III isotherm has weak interaction between the gas and adsorbent.

Type IV isotherm (Figure 2.1(d)) is similar to Type II at lower pressure. At the lower pressure regions, it shows the formation of a monolayer followed by a formation of multilayers. The saturation level reached at a pressure below the saturation vapor pressure. This can be explained on the basis of a possibility of gases condensing in the tiny capillary pores of the adsorbent at pressure below the saturation pressure of the gas. BET surface area characterization of mesoporous materials, which are materials with pore diameters between 2 - 50 nm, gives this type of isotherm.

Type V isotherms (Figure 2.1(e)) are very similar to type IV isotherms and are not applicable to BET because the adsorbent-adsorbent interactions are weak.

2.8.3 Pore size distribution analysis

Pore size distribution (PSD), a very important property of adsorbents, determines the fraction of the total pore volume accessible to molecules of a given size and shape (Zhu, 2007). Pores can have a regular and/or irregular shape. In most cases these pores are of different sizes (Leofanti *et al*., 1998). According to the International Union of Pure and Applied Chemistry

(IUPAC) definitions, the pore sizes of activated carbon can roughly be classified as micropores (< 2 nm), mesopores (2 – 50nm) and macropores (> 50 nm) (Gregg and Sing, 1982; Roquerol *et al*., 1994; Stoeckli *et al*., 2002). The macropores act as transport pathways, through which the adsorptive molecules travel to the mesopores, from where they finally enter the micropores. Thus, macro- and mesopores can generally be regarded as the highways into the adsorbent particle, and are crucial for kinetics. The micropores usually constitute the largest proportion of the internal surface of the adsorbent and contribute most to the total pore volume (Rodriguez-Reinoso and Linares-Solano, 1989).

2.9 Biosorption Contactors

The process of metal recovery using biosorbent derived from biomass is basically a solid-liquid contact process consisting of the metal uptake (sequestering) cycle and the metal desorption (elution) cycle. In its technological configuration, it would be very similar to that used in the ion-exchange process. The metal solution is contacted with the solid sorbent phase in a batch, semi-continuous, or continuous-flow arrangement. Appropriate contact between the solution and the solid phase can be accomplished routinely in any modification of the following apparatuses (Volesky, 1990): Batch-stirred tank contactor and Continuous-flow stirred-tank contactor. Both can be coupled or combined with a solid-liquid separation operation: fixed packed bed contactor, pulsating-bed contactor, fluidized-bed contactor and multiple-bed contact arrangement.

2.9.1 Batch studies

In a batch adsorption process the feed solution and the adsorbent particles are brought into contact until equilibrium is achieved. The spent solution, which also contains the impurities, is separated from the adsorbent by using an appropriate solid-liquid separation technique, e.g., filtration or centrifugation (Ghosh, 2006). These studies are used to obtain equilibrium sorption isotherms and to evaluate the sorption capacity of sorbents for given metals present in fluid phases (Fonseca *et al*., 2009). The solid material obtained (i.e. the adsorbent with the bound solute) is frequently washed for complete removal of impurities. The adsorbed solute can then be eluted from the adsorbent by adding a liquid which favours desorption of the solute. The solute is then separated from the adsorbent by using appropriate solid-liquid separation technique (Ghosh, 2006).

2.9.2 Fixed bed column

The cyclic-batch operating mode using a fixed bed is widely used in adsorption systems. Separation in a fixed bed is, in virtually all practical cases, an unsteady state rate-controlled process. This means that conditions at any particular point within the fixed bed vary with time. Adsorption only occurs in a particular region of the bed, known as the mass transfer zone (MTZ), which moves through the bed.

Sorption systems which use fixed packed bed columns have certain advantages in comparison with batch arrangements; this is because rates of adsorption depend on the concentration of metal ion in the solution being treated. In the column, the biosorbent is continuously in contact with fresh solution and this is the reason why the concentration of metal in solution, which is in contact with a defined layer of biosorbent in the column, is relatively stable. For batch treatment, the concentration of the metal in contact with specific quantity of biosorbent decreases much more rapidly as adsorption proceeds, thereby decreasing the effectiveness of the adsorbent for removing the metal.

The factors which determine the number and arrangement of fixed beds include total feed flow rate, allowable pressure drop, energy demands, length of the MTZ, method of adsorbent regeneration, and the capital investment. In order to achieve a steady flow of product, most applications include at least 2 beds such that one is in the adsorption mode while the other is in the regeneration mode. Multiple beds in parallel would be used with a relatively high flow rate and a short MTZ length while multiple beds in series would be used if the MTZ were long. For high flow rates and large MTZ lengths the choice is likely to be multiple beds in series and parallel.

The main requirement of an industrial sorption system is that the sorbent can be utilized as a fixed or expanded bed and it should not cause much pressure drop across the bed. This will necessitate some degree of pretreatment, sizing, pelleting, chemical modification or immobilization. These are aimed at obtaining a suitable structure for use in a bed reactor and may enhance metal-specific binding sites. In order to retain the ability of biomass to sorb metals during the continuous industrial process, it is important to utilize an appropriate immobilization technique (Gupta *et al*., 2000).

The use of biomass in powder form has a preferred choice of numerous studies on adsorption of metal ions from aqueous solutions. Powdered biomass has been conveniently used in batch adsorption studies without considering the difficulties that an actual industrial system

operating in fixed bed mode may faces in separating the biomass from aqueous solution after the adsorption of heavy metals is complete. On contact with water the biomass becomes soft. The small particle size, low density and strength can cause difficulties in column applications, and separation of biomass from treated effluent (Tsezos, 1990). These problems can be overcome by immobilization of biomass powder in a solid matrix. Biomass can be immobilized in a synthetic polymer matrix and/or grafted onto an inorganic support material like silica to yield particles with the required mechanical properties. In this way the biosorbents can be manipulated for better efficiency and for multiple reuses to increase their economic attractiveness, compared with conventional adsorbents like ion-exchange resins or activated carbons.

Most previous research using biosorbents for metal ions is based on batch equilibrium studies using a continuous stirred tank reactor system. However, in the practical operation of full-scale biosorption processes, continuous-flow fixed bed columns are often preferred. Due to the fact that in fixed bed systems, the concentration profiles in the liquid and adsorbent phases vary in both space and time, design and optimization of fixed bed columns are difficult to carry out without a quantitative approach. From the perspective of process modelling, the dynamic behaviour of a fixed bed column is described in terms of a breakthrough curve (Chu, 2004).

A breakthrough curve is the dynamic behavior of columns described in terms of effluent concentration-time profiles. A typical breakthrough curve is illustrated in Figure 2.2. The breakthrough curves show the loading behaviour of metal to be removed from solution in a fixed bed and is usually expressed in terms of adsorbed metal concentration (C_{ad}), concentration of metal removal (C_r), inlet metal concentration (C_i), outlet metal concentration (C) or normalized concentration defined as the ratio of effluent metal concentration to inlet metal concentration (C/C_i) as a function of time or volume of effluent for a given bed height (Aksu and Gönen, 2004).

In packed-bed contactor due to the continuous adsorption, the flow of the solution creates a wave front as it flow through the bed. This wave front is better known as the mass transfer zone (MTZ). This is where active adsorption happens in a packed-bed reactor. Within the MTZ, the degree of saturation with adsorbent varies from 100 percent to effectively zero. As the adsorbent reaches its equilibrium capacity i.e. becomes exhausted, the MTZ will travel further through the bed. When the MTZ moves across the packed bed it leaves behind a

section of the bed which is completely exhausted and in front of the leading edge of the MTZ lays fresh adsorbent. The MTZ will continue to travel through the bed until the bed hits its breakthrough point. The breakthrough point shown in Figure 2.2 is defined when a preset concentration emerges in the effluent, and the effluent quality no longer meets predetermined treatment objectives. The breakthrough concentration can be taken as the minimum detectable or maximum allowable solute concentration in the effluent fluid, e.g. as dictated by downstream processing unit. As breakthrough continues, the concentration of the adsorbate in the effluent increases gradually up to the feed value C_i. When this has occurred no more adsorption can take place in the bed and the adsorbent will need to be replaced to keep excessive concentrations of impurities out of the effluent.

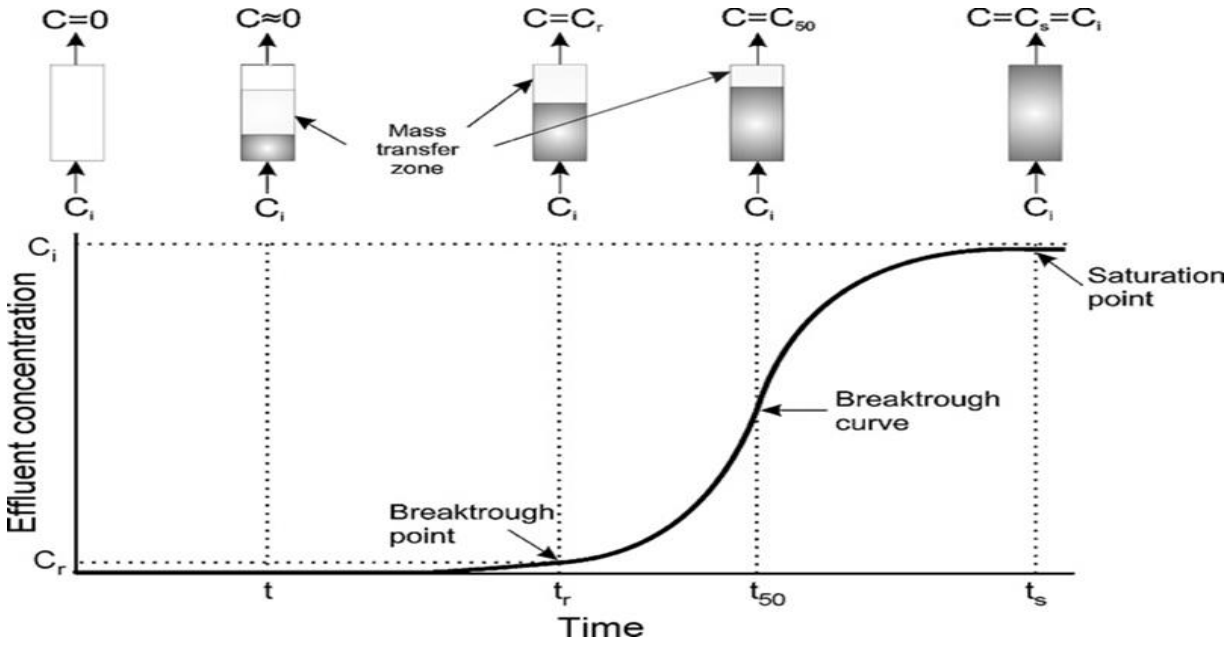

Figure 2.2 Representation of a typical breakthrough curve (Calero *et al*., 2000).

Where t (min) is the time

t_s (min) is the saturation time

t_r (min) is the breakthrough time

t_{50} (min) is the time required to obtain 50% breakthrough

C_i (mg/L) is the influent concentration

C (mg/L) is the effluent concentration

C_r (mg/L) is the metal concentration at breakthrough point

C_s (mg/L) is the metal concentration at saturation point

C_{50} (mg/L) is the metal concentration at 50% recovery

The time for breakthrough appearance and the shape of the breakthrough curve are very important characteristics for determining the operation and the dynamic response of an adsorption column (Aksu and Gönen, 2004).). As a general rule, the time to breakpoint is decreased by: (1) increased particle size of the adsorbent; (2) increased concentration of solute in the influent; (3) increased pH of the water; (4) increased flow rate; and (5) decreased bed depth (Walter and Weber, 1974). An important design consideration is the length of the MTZ. Minimizing the length of the MTZ allows for more of the capacity of the adsorbent to be utilized for any predetermined treatment objective. The length of the MTZ is a function of the influent flow rate and the rate of adsorption. This means that any parameter that changes the rate of adsorption will also change the length of the MTZ to some extent.

The length of the MTZ can be calculated as;

$$L_{MTZ} = \frac{L\,(t_s - t_b)}{t_s} \qquad (2.10)$$

where L_{MTZ} (cm) is the length of the MTZ

L (cm) length of the entire biomass bed in packed bed contactor

t_b (min) is time taken for the biomass bed to reach breakthrough point

t_s (min) is time taken for the biomass bed to reach complete exhaustion

At the same time the Effluent volume (V_{eff}) can be calculated as:

$$V_{eff} = Qt \qquad (2.11)$$

where t and Q are the total flow time (min) and volumetric flow rate (mL min^{-1}), respectively. The area under the breakthrough curve (A), obtained by integrating the plot of adsorbed concentration (C_{ad}; mg L^{-1}) versus t (min), can be used to find the total adsorbed

metal quantity (maximum column capacity). Total adsorbed metal quantity (q_{total}) in the column for a given feed concentration and flow rate is calculated as (Han *et al*., 2006).

$$q_{total} = \frac{QA}{1000} = \frac{Q}{1000}\int_{t=0}^{t=t_{total}} C_{ad}\, dt \qquad (2.12)$$

Total amount of metal ion sent to column (m_{total}, g) is calculated as:

$$m_{total} = \frac{C_0 Q t_{total}}{1000} \qquad (2.13)$$

Total removal is calculated as:

$$\text{Total removal } \% = \frac{q_{total}}{m_{total}} X\ 100 \qquad (2.14)$$

Equilibrium metal uptake (q_{eq}) (or maximum capacity of the column) in the column is defined by Equation (2.15) as the total amount of metal adsorbed (q_{total}) per g of adsorbent (X) at the end of total flow time (Aksu and Gönen, 2004).

$$q_{eq} = \frac{q_{total}}{X} \qquad (2.15)$$

2.9.3 Counter Current Biosorption Systems

Multi-stage counter current adsorption operations are superior to both batch and fixed bed operations. This is because counter current flow maximizes the average driving force for mass transfer between the fluid and adsorbent. The saturated spent biomass emerging from the last reactor enters the regenerator, in which the adsorbed metals are removed, the biomass reactivated and then returned to the adsorption circuit. The main advantage of such processes is that the adsorbent can be regenerated as soon as its role in the adsorption step has been completed. Thus, in theory at least, the inventory of the adsorbent can be kept to a minimum. The quantity of adsorbent required for a given separation can also be reduced by increasing the number of stages.

Figure 2.3 illustrate how such system would operate. It is operated at steady state in a continuous manner. Adsorption of metal ions on cassava waste biomass occurs in the nth number of stages. This technique involves contacting metal ion solution with the cassava in a series of gently agitating tanks with a sufficient retention time. The cassava and metal ion solution are transferred in a counter current flow arrangement. The cassava with cassava loading (Y_{n+1}) enters the nth stage and moves from nth stage to the (n-1) stage and then to the first stage (stage 1) as the metal loading on the cassava increases. The solution phase with metal ion concentration (X_F) enters the first stage and moves in the opposite direction to the nth stage. The metal ion concentration decreases as it moves to the nth stage and the outlet metal ions concentration (X_n) is obtained after the nth stage. The loaded cassava (Y_1) is sent to the stripping column for desorption of metals from the biomass and the biomass is regenerated and sent to the nth stage (Richardson and Harker, 2002).

$$(X_F - X_n) = B(Y_1 - Y_{n+1}) \qquad (2.16)$$

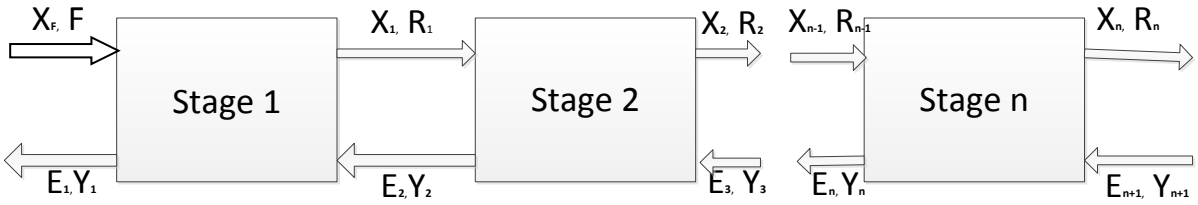

Figure 2.3 Multi stage counter current operation.

where X_F = concentration of metals in the feed solution, X_n = concentration of metal ions after the nth stage, n = is the number of theoretical stages, Y_{n+1} = concentration on the adsorbent feed, Y_1 = concentration on the adsorbent after the first stage, R = the solution from which undesired metal ions have been removed and E = adsorbent (becomes concentrated as it contacts in a stage wise fashion with the increasing solute rich solution).

It is also assumed that each stage is an equilibrium stage, and therefore the cassava and metal ions solution leaving each stage are in equilibrium. A mass balance of the solute in the entire unit is:

Equation 2.16 is the equation of straight line of slope A / B. This is the operating line whose coordinates are (X_F, Y_1), X_n, Y_{n+1} and has a slope of A/B as shown in Figure 2.4. The equilibrium line is drawn using the solid-liquid equilibrium data points of the aqueous

solution. The ideal or theoretical stages required to obtain a certain outlet concentration are constructed from top (Figure 2.4). Construction starts by stepping off stages from top of the tower (P (X_F, Y_1)), between operating line and equilibrium curve and continues until the other end (Q (X_n, Y_{n+1})) of the operating line is reached. The steps represent the equilibrium stages; and in this particular example in Figure 2.4, the required number of equilibrium stages is 4 (Richardson and Harker, 2002).

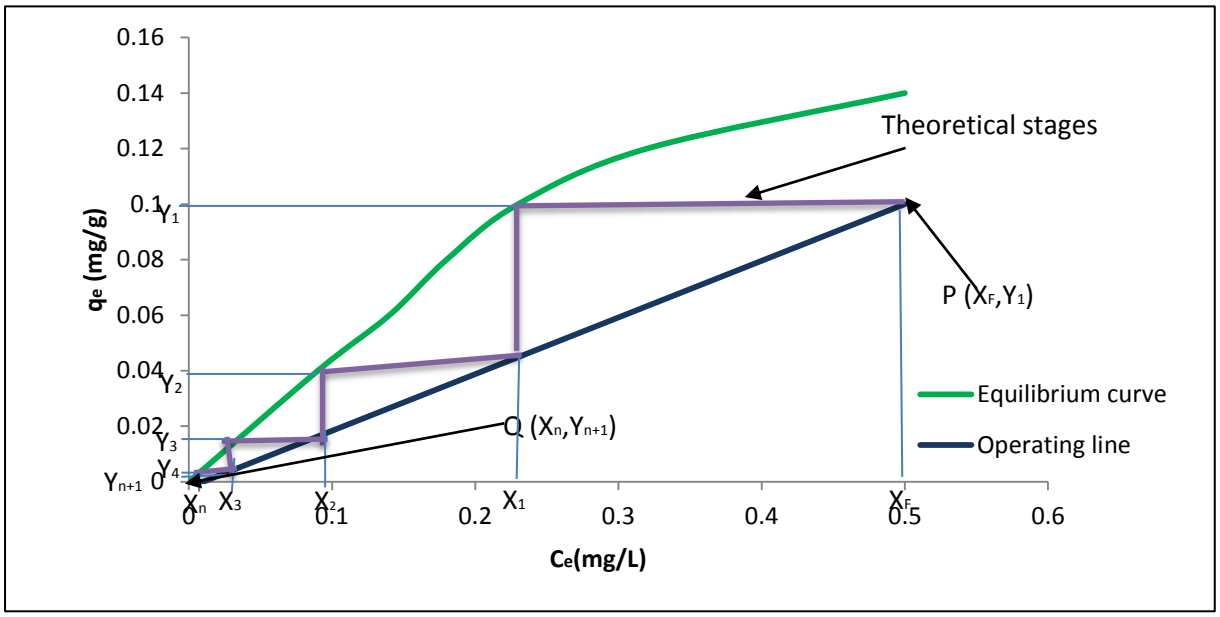

Figure 2.4 Graphic representation of multistage counter current adsorption.

CHAPTER THREE

3 MATERIAL AND METHODS

3.1 Introduction

This chapter presents the materials, experimental methods and analytical techniques used during this research.

3.2 Methods

3.2.1 Cassava

The cassava tubers were obtained from local wholesalers in South Africa. After the cassava tubers were washed with distilled water, cut into smaller pieces and carefully peeled to obtain the cassava-peel wastes. The cassava-peel waste was dried in the oven for 24 hours and was subsequently ground and sieved to 100 µm sizes using a blender and a standard sieve.

3.2.2 Activation

Initially, the cellulose biomass was activated by soaking 500 g of cassava-peel waste in 0.3M Nitric acid (HNO_3) for 24 hours, and then filtered. The filtrate was discarded and the residue was washed with distilled water until a pH of 7.0 was obtained. Later, the paste obtained was air-dried (Horsfall and Abia, 2003).

3.2.3 Thiolation

The air-dried activated biomass was divided into 3 equal portions. The first portion was left untreated. The other two portions were treated with 0.5M and 1.0M thioglycollic acid, respectively, as follows: a 25 g portion was mixed with 250 mL of the required concentration of thioglycollic acid solution in the presence of hydroxylamine (NH_2OH). The mixture was mechanically stirred for 6 hours at 30°C. This allowed the thiolation of the methylene hydroxyl group of the cellulose pyran ring (Abia *et al*., 2002). The process led to the exchange of the hydroxyl groups by the sulfhydryl (-SH) groups in the presence of hydroxylamine (NH_2OH) according to the following equation:

$$B-CH_2OH + HSCH_2CO_2H + NH_2OH \rightarrow B-CH_2-SH + CH_2CO_2H + HONH + H_2O \qquad (3.1)$$

where B represents the biomass. The mixture was then allowed to settle overnight and then centrifuged at 2500 x g for 10 minutes. The supernatant was discarded and the paste was air-dried.

3.2.4 Stock Solution

Stock solutions of Co^{2+}, V^{3+} and Cr^{3+} (1000 mg/L) were prepared from cobalt(II) sulfate ($CoSO_4.7H_20$), vanadium(III) chloride (VCl_3) and chromium(III) nitrate($Cr\ (NO_3)_3.9H_2O$) salts (Merck (chemical (Pty) Ltd), respectively. The stock solutions of the metals were diluted appropriately to prepare the different metal concentration required for biosorption studies.

3.3 Analytical Techniques

3.3.1 Determination of surface functional groups

Fourier transform infrared (FTIR) spectroscopy (Tensor 27 Bruker) was done to identify the chemical functional groups present in the untreated and variously modified cassava waste biomass. Infrared absorbance data were obtained for wave numbers in the range of 500-3500 cm^{-1}.

3.3.2 Determination of the pH of the point of zero charge

When cassava-peel biomass is mixed with a solution, it forms a colloidal suspension. The particles in a colloidal suspension usually carry an electrical charge. The surface charge depends greatly on the pH of the solution, with positive values at low pH and negative values at high pH. There is a characteristic pH value at which the surface charge is zero, corresponding to equal number of positive and negative surface groups. This pH value required to give zero net surface charge is designated the point of zero charge (pH_{PZC}) or isoelectric point (IEP). In this study, the pH_{PZC} was determined using the procedure of mass titration (Noh and Schwarz, 1988; Noh and Schwarz, 1990) as follows: solution of 0.1M $NaNO_3$ was prepared and was adjusted to different pH (pH 3, 6 and 11) using 0.1 M HNO_3 and 0.1M NaOH. For each initial pH, six containers were filled with 100 mL of solution and different amount of cassava waste biomass (0.05%, 0.1%, 0.5%, 1%, 5% and 10% by weight/volume of solution). The solutions were agitated at 150 rpm and equilibrium pH was measured after 24 hrs.

3.3.3 Determination of surface area and pore structure (BET)

The Brunauer Emmett Teller (BET) surface area and pore structural parameters of the adsorbents were determined from the adsorption-desorption isotherm of nitrogen at -196.15°C using Micrometrics (Tristar 3000) surface area and porosity analyzer. All the samples were degassed at 180°C for 4 hours, prior to adsorption- desorption experiments.

3.3.4 Determination of metal ion concentrations (FAAS)

Flame atomic absorption spectroscopy (Spectro AA, 55B Varian) was used to analyse metal ion solutions. Instrument parameters such as lamp current, fuel, support gas and wavelength were used for the analysis of the metal of interest were as recommended in the FAAS analytical methods working manual.

3.4 Experimental methods

3.4.1 Batch adsorption

Factors affecting the adsorption process were examined in a batch system. The effect of parameters such as initial metal ion concentration, solution temperature, solution pH, biomass concentration, acid treatment and the presence of co-cations on the metal adsorption by the cassava biomass were examined as tabulated in Table 3.1. Unless otherwise stated, adsorption experiments were performed in 250 mL Erlenmeyer flasks with 50 mL of solution at 100 mg/L metal ion content and 0.25 g biomass. The suspensions were agitated in a rotary shaker at 150 rpm under constant temperature (30°C) for one hour. These values were chosen based on literature (Pundir and Dastidar, 2010; Horsfall *et al*, 2006). Experiments were carried out for single, binary and ternary metal ion systems. Samples were taken every 5 minutes and then centrifuged for 10 minutes at 1000 rpm and the supernatant analysed for metal ion concentration using flame atomic absorption spectrophotometer (FAAS).

The amount of metal adsorbed by the cassava-peel wastes was calculated using the following equations:

$$q_e = V\left(\frac{C_i - C_e}{m}\right) \quad (2.4)$$

and

$$\text{Percentage metal ion removal} = \left(\frac{C_i - C_e}{C_i}\right) \times 100 \quad (2.5)$$

where q_e is the metal uptake (mg metal per g biosorbent), V is the solution sample volume (mL), C_i the initial concentration of the metal in solution (mg/L), C_e is the final (equilibrium) concentration of the metal in solution (mg/L), and m is the amount of added biosorbent on dry weight basis (g).

Table 3.1 Process parameters evaluated.

Process parameters	**Level**
Contact time	5-60 minutes
Solution pH	2-7
Temperature	30-50°C
Agitation speed	50-200 rpm
Biomass dosage	0.05-0.30 g
Initial concentration of metal ions	50-250 mg/L
Influence of commonly found cations (Ca^{2+}, Mg^{2+}, K^+ and Na^+)	0.2-2.0 g/L

3.4.2 Adsorption-desorption cycle

The amount of dried cassava with the highest metal loading (from metal adsorption capacity experiments) was used for the adsorption-desorption experiments. Metal adsorbed cassava peel waste was first washed with distilled water to remove any metals loosely attached to the adsorbent. Sulphuric acid (H_2SO_4) was used as an eluent for desorption studies. The H_2SO_4 was used as an eluent over HNO_3 or HCl because it contains high concentrations of protons present in the recovery reagent which may displace bound metal ion from the active sites on the cassava waste biomass than hydronium ions and sulphuric acid is readily available and much cheaper than the other two. Different concentrations of H_2SO_4 were studied (0.1 to 2.0M) to define an optimal value. Approximately 0.250 g of metal-adsorbed cassava peel waste was eluted with 50 mL of H_2SO_4 of appropriate concentrations.

The adsorbed and desorbed metal ions were analysed, and desorption efficiency was calculated as follows:

$$\text{Desorption efficiency} = \frac{\text{released metal ion (mg)}}{\text{initially sorbed metal ion (mg)}} \times 100 \qquad (3.2)$$

After each desorption stage, the cassava peels were washed with distilled water and reactivated with HNO_3 to remove any debris or soluble biomolecules that might interact with metal ions for the next adsorption cycle.

3.5 Continuous adsorption system

3.5.1 Semi-continuous counter current adsorption studies

Semi continuous counter current experiments were conducted on acid treated biomass. The maximum parameters obtained from batch experiments were used to set- up the semi continuous counter current process. 8, 6 and 4 stages were obtained for Co^{2+}, Cr^{3+} and V^{3+}, respectively as shown in Figure C4 to 6 in the Appendix. 0.500 g of cassava waste biomass was brought into contact with 100 mL of the influent solution in each reactor. Mixing was provided by agitation at 150 rpm. After 30 minutes, agitation was stopped and the biosorbent separated from metal ion solution by filtration. The biosorbent and effluent solutions were then transferred to the next respective reactor in a counter current manner.

The procedure was as shown in Figure 3.1. Firstly, 100 mL of fresh influent was transferred to reactor 1 from the influent solution tank. After continuous stirring for 30 minutes, the solution from reactor 1 was transferred to reactor 2. This procedure was followed from one reactor to the other until the final effluent was transferred to discharge tank from reactor n. Secondly, 0.500 g of fresh biosorbent was transferred from the biosorbent tank to reactor n. The biosorbent was then transferred in the opposite direction of the solution from rector n. This procedure was followed from one reactor to the other until the final adsorbent was transferred from reactor 1 to desorption tank. As the acid treated cassava moved up the train, it was loaded with higher concentration of the metal ions, since it came into contact with a higher grade solution.

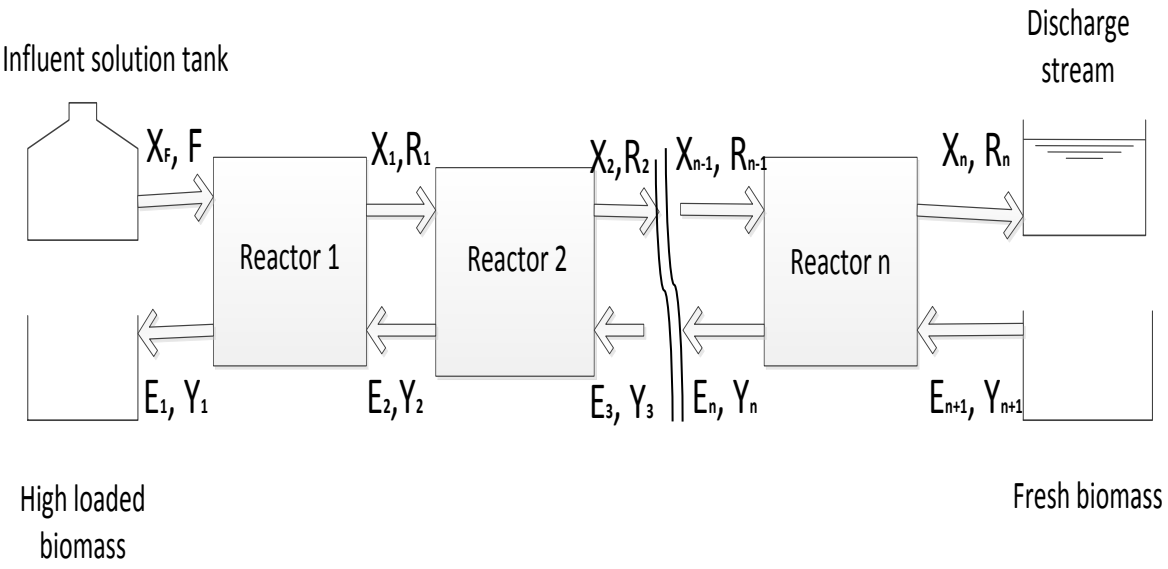

Figure 3.1 Experimental procedure of counter current adsorption system.

(where X_F = concentration of metals in the feed solution, X_n = concentration of metal ions after the nth stage, n = is the number of theoretical stages, Y_{n+1} = concentration of the metal ions on the adsorbent feed, Y_1 = concentration on the adsorbent after the first stage, R = the solution from which undesired metal ions have been removed and E = adsorbent (becomes concentrated as it contacts in a stage wise fashion with the increasing solute rich solution).

3.5.2 Adsorption- desorption experiments

After adsorption, the metal-loaded cassava waste was washed with distilled water to remove loosely attached metals ions. Thereafter, 0.500 g metal-loaded cassava was placed in contacted with 50 mL of 0.1M H_2SO_4 for 1 hr. This acid concentration was chosen from previous batch experiments as an effective eluent of cobalt, chromium and vanadium. The samples were analysed for metal ion concentration using FAAS. In order to determine the reusability of cassava waste biomass, the same cassava waste biomass was used in consecutive adsorption-desorption cycles. In each cycle, the cassava was washed with distilled water and reactivated with 0.3M HNO_3.

3.5.3 Immobilization of acid treated cassava waste biomass

Although simple cutting and/or grinding of dried biomass may yield stable biosorbent particles, the free biomass generally has low mechanical strength and is not suitable for use in column applications (Ross and Townsey, 1986). Furthermore, whilst excessive hydrostatic pressures are required to generate suitable flow rates, high pressures can cause disintegration

of free biomass. These problems can be avoided by the use of immobilized biomass systems (Gadd, 1990; Leusch *et al*., 1995). Immobilized biomass offers many advantages including better reusability, high biomass loading and minimal clogging in continuous flow systems (Holan and Volesky, 1994; Gourdon *et al*., 1990; Gupta *et al*., 2000).

The immobilization of the acid treated cassava waste was carried out according to the method of Champague and Gardner (2001). The cassava waste biomass was immobilised into small sized beads by mixing the free biomass with 250 mL distilled water and left to hydrate for 10 minutes at room temperature. The slurry was then mixed with equal volume of 4% sterile sodium alginate. This mixture was added drop wise into 0.1M calcium chloride ($CaCl_2$) solution using a syringe so as to get even-sized beads. Alginate-cassava mixture droplets solidified upon contact with $CaCl_2$, forming beads and thus entrapping biosorbent particles. The beads were allowed to harden for 30 minutes and were then washed with 0.9% sodium chloride (NaCl) solution to remove excess calcium ions. The beads generated had a diameter ranging from 3-4 mm. The cost effectiveness of the beads depend upon their regeneration and the number of cycles that they could be put in use. Taking into account the simplicity in biomass bead production, it is recommended that large quantities of beads could be generated using a slurry mixing tank which would pump out the slurry through nozzles of different diameters.

3.5.4 Characterization of immobilized cassava waste biomass

Determination of surface functional groups (FTIR)

FTIR spectra was done to identify the chemical functional groups present on immobilized cassava before and after adsorption of metals and also on 0.1M eluted immobilized cassava waste biomass.

Determination of surface area and pore structure (BET)

The immobilized cassava waste biomass was characterized before and after adsorption by measuring the surface area and pore volume. The surface area, pore size and pore volume were measured using BET analyser with nitrogen gas as an adsorbate.

3.5.5 Column studies

The column experiments were conducted in a glass column with inner diameter of 5 cm and length of 50 cm, packed with immobilized cassava waste to various heights. The metal

solution of 100 mg/L concentration at a pH of 4 was pumped through the column using a peristaltic pump (Watson Marlow 504S) as shown in Figure 3.2 with variable speed adjustment. The residence time of waste water in the column was 96.40, 64 and 49.7 s for flow rates of 0.83, 1.25 and 1.61 mL/s, respectively. The calculations are included in the appendix A. Samples from the column effluent were collected at regular time intervals and analysed by FAAS. The operating flow rates and bed depths are tabulated in Table 3.2.

Table 3.2- Flow rate and bed depth used.

Process parameters	**Level**
Flow rate	0.83-1.61 mL/s
Bed depth	5-15 cm

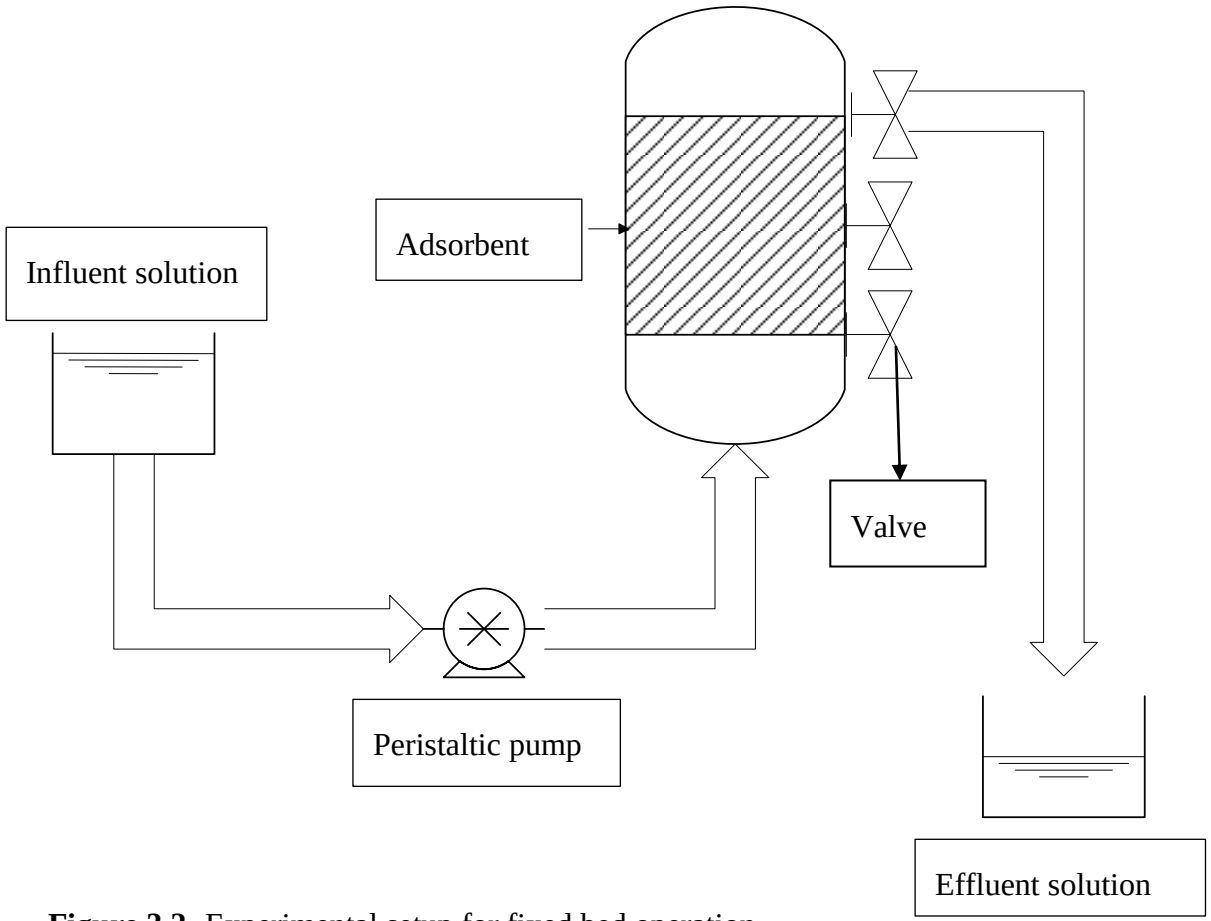

Figure 3.2- Experimental setup for fixed bed operation.

3.5.6 Adsorption- desorption experiments

After exhaustion of the immobilized acid treated cassava waste, it was necessary to regenerate it for further use. Regeneration was carried out by pumping 0.1M H_2SO_4 solution through the bed in the upward direction for 5 hours, to allow Co^{2+}, Cr^{3+} and V^{3+} to be released from the adsorbent. Subsequently, the column was washed with distilled water followed by activation of biomass with 0.3M HNO_3. After each desorption stage the same immobilized cassava waste biomass was used in consecutive adsorption-desorption cycles.

CHAPTER FOUR

4 BATCH STUDIES

4.1 Introduction

Batch biosorption processes are relatively simple operations, requiring easily available equipment. Batch operation is especially suited for treating low concentration and high volume waste streams containing toxic metal contaminants. A typical batch operation comprises of a series of steps. First, a vessel containing metal laden solution in contact with the biosorbent is agitated for a period of time to allow waste water to reach discharge limits. Secondly the treated solution is withdrawn for discharge; thirdly a small amount of the eluent is added to the vessel which is agitated for a period of time to elute the adsorbed metal. Forthly, the spent eluent containing the eluent metal is withdrawn; lastly a wash step may be used to condition the biosorbent for reuse in the next cycle for treatment.

Although most industrial applications prefer a continuous mode, batch experiments have often been used to obtain fundamental information, such as biosorbent efficiency, optimum experimental conditions, biosorption rate and possibility of biomass regeneration (Vijayaraghavan and Yun, 2008b). Batch experiments usually focus on the study of factors affecting biosorption, which are important in the evaluation of the full biosorption potential of any biosorbent. These include the pH of metal polluted solution to be studied, temperature at which the biosorption process would be carried out, ionic strength of metal ions to be adsorbed, biosorbent dosage and size, initial metal ion concentration, the speed of agitation and time required to reach equilibrium (Iqbal and Edyvean, 2004; Vijayaraghavan and Yun, 2008b).

Earlier studies have shown that the most critical parameter in the treatment of heavy metal with biosorbent material is the initial pH of the sorption medium (Esposito *et al*., 2002; Vijayaraghavan and Yun, 2008b). It affects the solution chemistry of the metal ions and the activity of the functional groups of the biosorbent. The pH strongly influences the speciation and biosorption availability of the metal ions. Some of the metal ions precipitate at high pH values, which may complicate the biosorption process (Vijayaraghavan and Yun, 2008b). The different biosorbents also exhibit different pH optima for the sorption of the different metals during biosorption which means that a further increase or reduction of pH reduces the metal uptake.

Adsorption isotherms have been commonly used to describe experimental results for the sorption of metal ions by cassava and other biosorbents. Although there are a number of adsorption isotherms (Kuyucak and Volesky, 1990), the most commonly used adsorption isotherms are the Langmuir and Freundlich equilibrium models (Liu *et al*., 2004; Rangsayatorn *et al*., 2004; Febrianto *et al*., 2009). Characterization of biosorbent using Fourier Transform Infrared spectroscopy (FTIR), Brunauer-Emmett-Teller (BET) and Point of Zero Charge (pH_{PZC}) is necessary for analysis of functional groups for metal sorption, to determine the specific surface area and to determine pH at which biosorbent has a zero charge, respectively. The experimental procedure and methodology applied to generate the results is described in detail in Chapter 3. Some of the works presented in this study have been published by Ndlovu *et al.* (2013). The results for this publication were generated by the author of this dissertation as presented in this chapter.

4.2 Results and Discussion

4.2.1 Fourier Transform Infrared spectroscopy (FTIR) analysis

The infrared spectra of the untreated and treated cassava waste biomass are shown in Figure 4.1(a), (b) and (c), respectively. As mentioned earlier in section 3.3.1, the FTIR is used to identify the existence or absence of functional groups on the surface of the cassava waste biomass. Figures 4.1(a) to (c) reveals the increase of symmetrical and asymmetrical stretching at wavelength range of 700-610, 1000-650, 1137-1280, 1588-1640 and 2800-3700 cm^{-1} for untreated and acid treated cassava waste biomass samples. Based on Table 4.1 for FTIR assignment of functional groups on biomass surface these band were assigned to C-H bending, out of plane C-H bend, -C-O stretching, -C=O and -OH stretching, respectively. The wavelength range of 2550-2600 which was assigned to -SH group only appeared in the acid treated biomass shown in Figure 4.1(b) and (c).

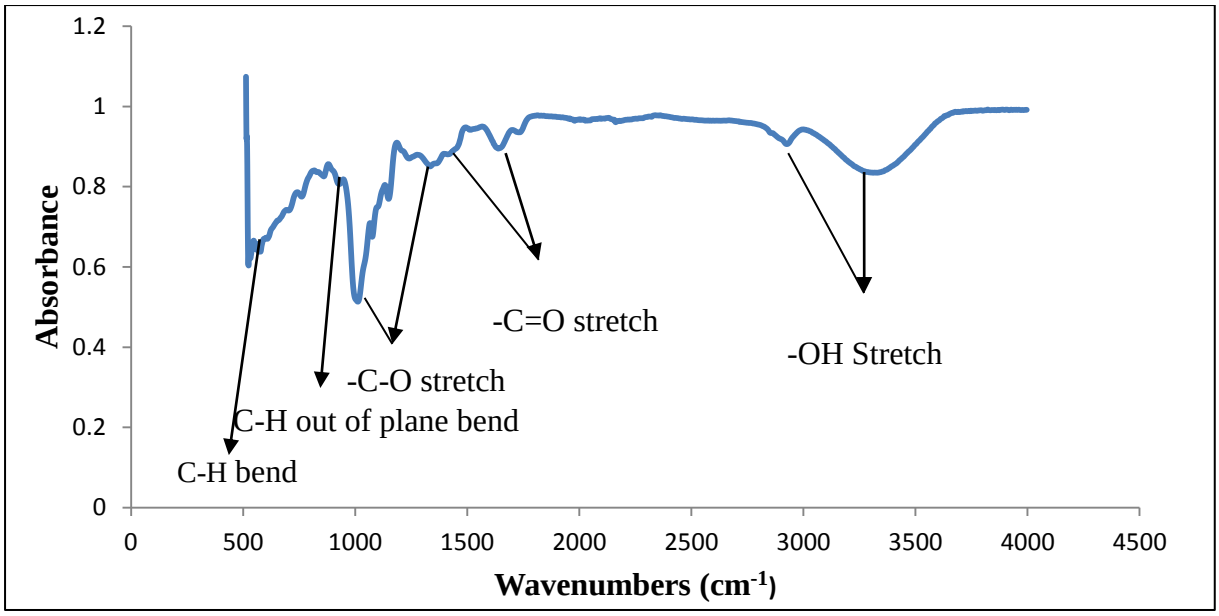

Figure 4.1(a) - Fourier transform infrared for untreated cassava waste biomass

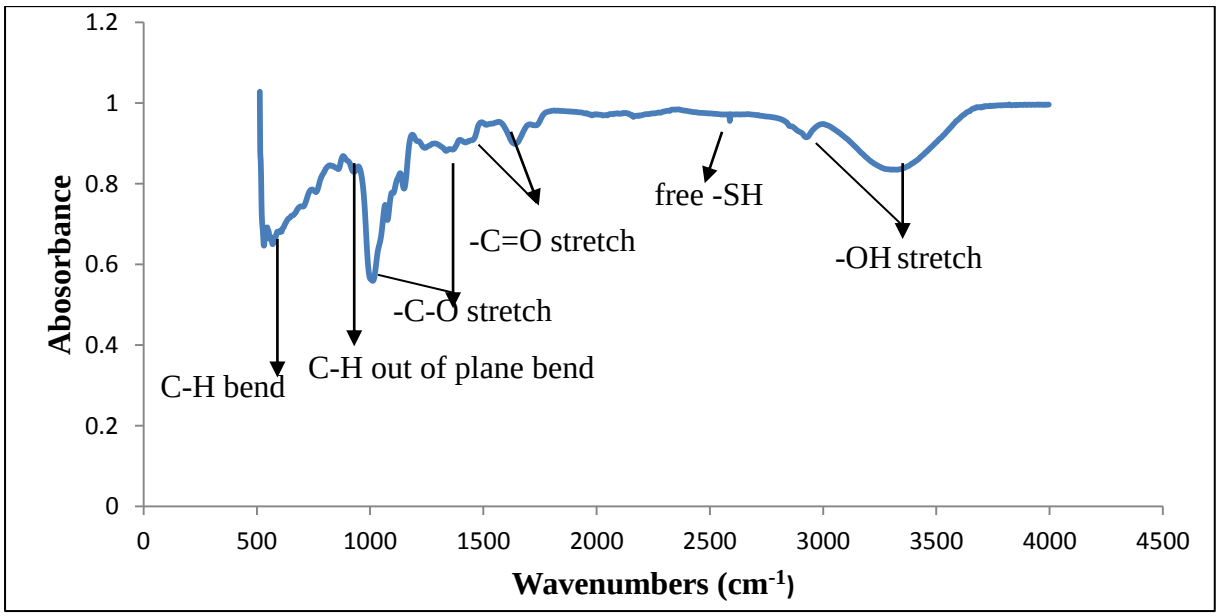

Figure 4.1(b) - Fourier transform infrared spectra for 0.5M acid treated cassava waste biomass

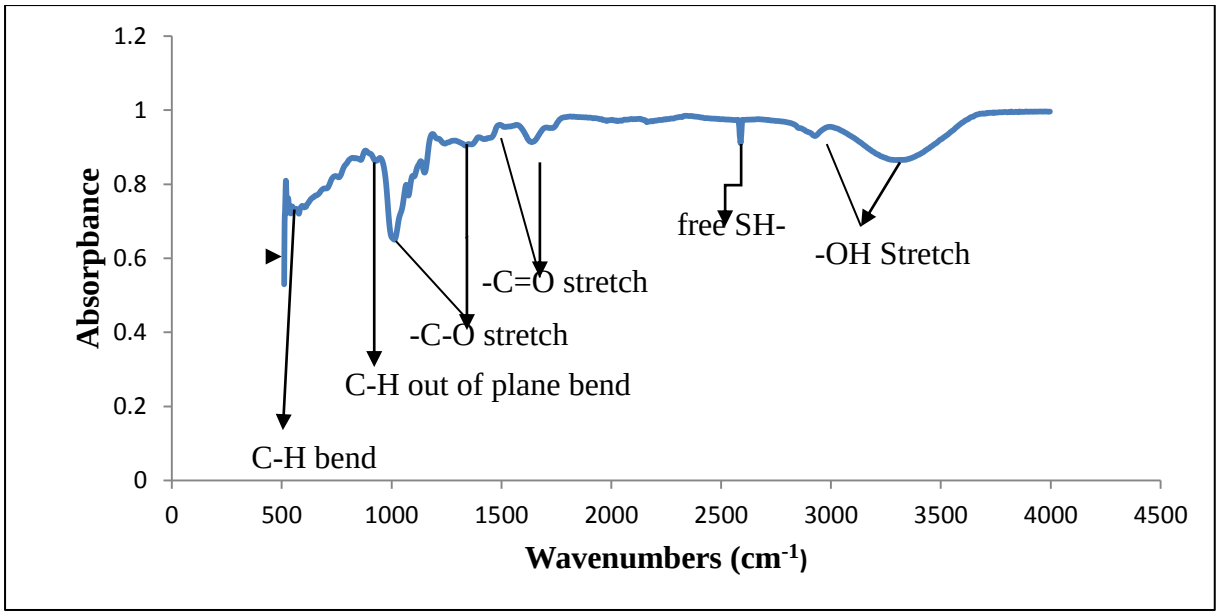

Figure 4.1(c) - Fourier transform infrared spectra for 1M acid treated cassava waste biomass.

Table 4.1 General assignment of the FTIR spectra (Morrison and Boyd, 1992)

Wavelength (cm^{-1})	**Assignment**
3700-2800	Hydrogen bonded OH groups, free OH, intermolecular bonded OH
3077-3030	Aromatic C-H stretching
2850-2500	Carboxylate ion
2550-2600	S-H thiols stretching vibration
1725-1640	C=O stretching of carboxylic acids
1640-1585	C=O stretching vibration of double bonds in cyclic and acyclic compounds, ketones and quinine
1400-1390	OH deformation and C-O stretching of phenolic OH, C-H deformation of CH3 groups
1280-1137	C-O stretching of esters, ethers and phenols
1090-1040	C-O stretching of alcoholic compounds
1000-650	C-H out of plane (OOP) bending vibration
700-610	C-H bending vibration

It can be seen from Figures 4.1(a), (b) and 4.1(c) that the major difference between the three biomasses is the presence of the sulfhydryl group (-SH). The presence of sulfhydryl group confirmed with FTIR suggests that the thiolation process adds sulfhydryl functional groups on the cassava-peel biomass. Figure 4.1(c) has a longer band as compared to Figure 4.1(b);

the difference between these bands was due to an increase in concentration of the modifying acid i.e. from 0.5M to 1.0M.

4.2.2 Point of Zero Charge (pH_{PZC})

The pH_{PZC} for both the untreated and treated cassava waste biomass were determined as 4.9 and 3.1, respectively. It has been reported by earlier researchers (Anirdvan and Krishan, 2004) that the pH_{PZC} of an adsorbent decreases with an increase in the acidic groups on the surface of the adsorbents. From the results, it can be concluded that acid modification of the adsorbent gave a positive (acidic) surface charge since the pH_{PZC} for the treated biomass was found to be lower than that of the untreated surface. Therefore, these results confirm that more acidic functional groups were incorporated into the cassava waste biomass during thiolation. These results concur well with the results shown in Figure 4.1(b) and (c) which shows the introduction of an acidic sulfhydryl group after thiolation.

4.2.3 BET analysis of untreated and acid treated biomass

Surface measurements were determined by nitrogen adsorption fitted to the BET equation 2.8 (Brunauer, 1943), using the Tristar 300 apparatus from micromeritics. A summary of the BET surface area, pore volume and pore size is presented in Table 4.2.

Table 4.2 Structural characteristics of untreated and acid treated cassava waste biomass.

Adsorbent	**Surface area $S_{BET}(m^2/g)$**	**Pore volume V_t (cm^3/g)**	**Pore size (nm)**
Untreated biomass	0.4427	0.001817	11.68
0.5 M acid treated biomass	0.4649	0.001357	11.60
1 M acid treated biomass	0.6263	0.001074	9.70

The BET surface area obtained for untreated, 0.5 M and 1 M acid treated biomass was 0.4427, 0.4649 and 0.6263 m^2/g, respectively. A specific surface area for the cassava follows the sequence 1 M acid treated> 0.5 M acid treated > untreated biomass. It has been reported that acid modification of the biomass provides the adsorbent with a larger surface area and smaller porosity so that binding of metal ions may occur on the surface of the adsorbent

(Horsfall *et al*., 2004). Thus, the increase in the specific surface area of the adsorbent with acid modification is expected to enhance the removal of metals from aqueous solution.

4.2.4 Effect of acid treatment

Figures 4.2(a) to (c) show the effect of acid treatment on the adsorption of Co^{2+}, V^{3+} and Cr^{3+} from single metal ion systems. From the figures, it can be seen that, in all cases, the metal ions adsorption by the chemically modified biomass was greater than the unmodified biomass. The improved level of the metal ion sorption is due to the availability of the incorporation of more binding groups (-SH) on the cellulosic matrix as shown in Figure 4.1 (b) and (c). From Table 4.2 it is also seen that treatment of the biomass at higher acid concentration (1.0M) resulted in better adsorption capacities than the biomass treated at lower acid concentration (0.5M). The non-treated biomass gave the least adsorption levels for the 3 metal ion systems. The difference in adsorption capacities between 0.5 and 1.0M thioglycollic acid concentrations is as a result of increase in sulfhydryl groups, –SH, as the modifying reagent concentration increased. Since 1.0M acid treatment was found to give higher adsorption capacities, subsequent experiments were conducted using the biomass that had been acid treated using this level of concentration.

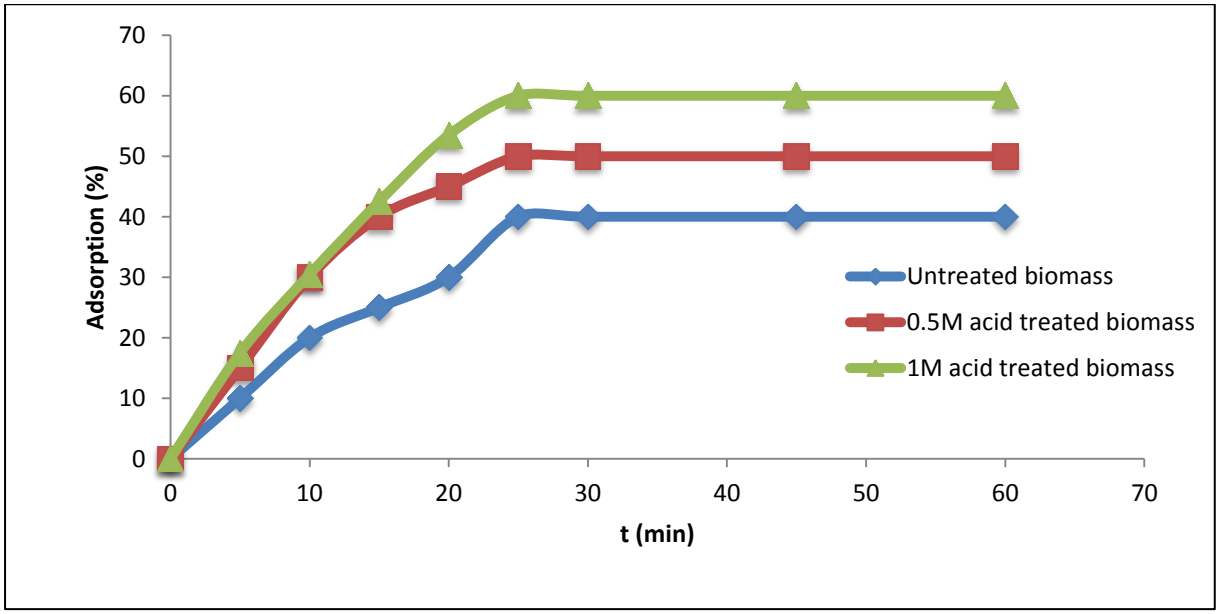

Figure 4.2(a) - Effect of acid treatment on cassava waste for the removal of Co^{2+}: (pH = 4; biomass = 0.250 g; agitation speed = 150 rpm; contact time = 1h; temperature = 30°C; metal ion concentration = 100 mg/L).

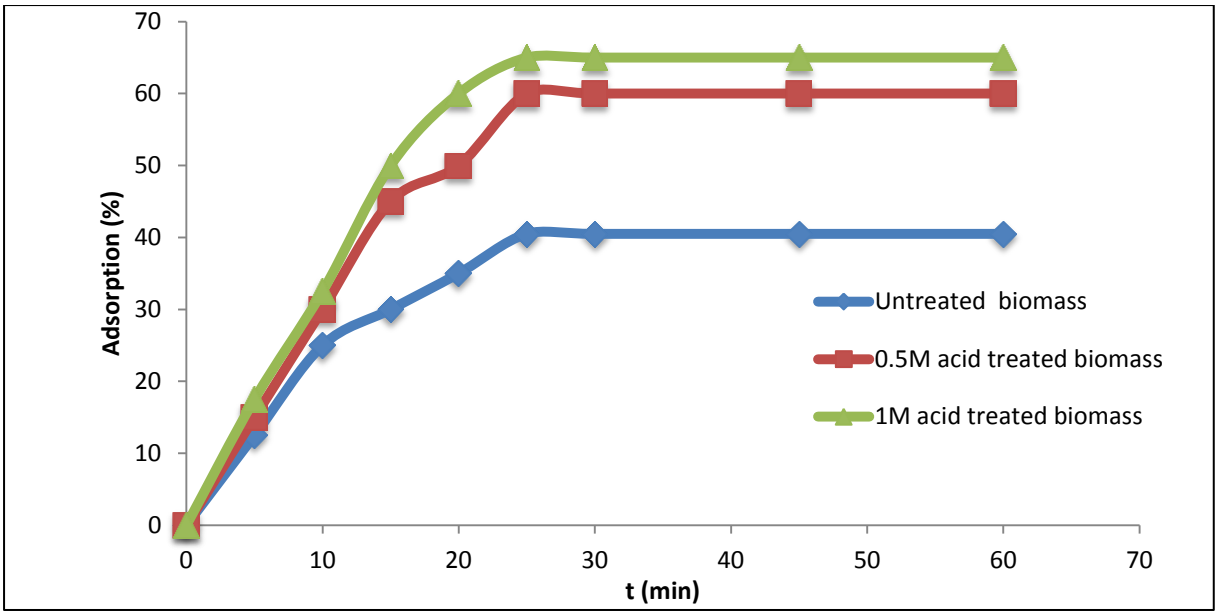

Figure 4.2(b) - Effect of acid treatment on cassava waste for the removal of Cr^{3+}: (pH = 4; biomass = 0.250 g; agitation speed = 150 rpm; contact time = 1h; temperature = 30°C; metal ion concentration = 100 mg/L).

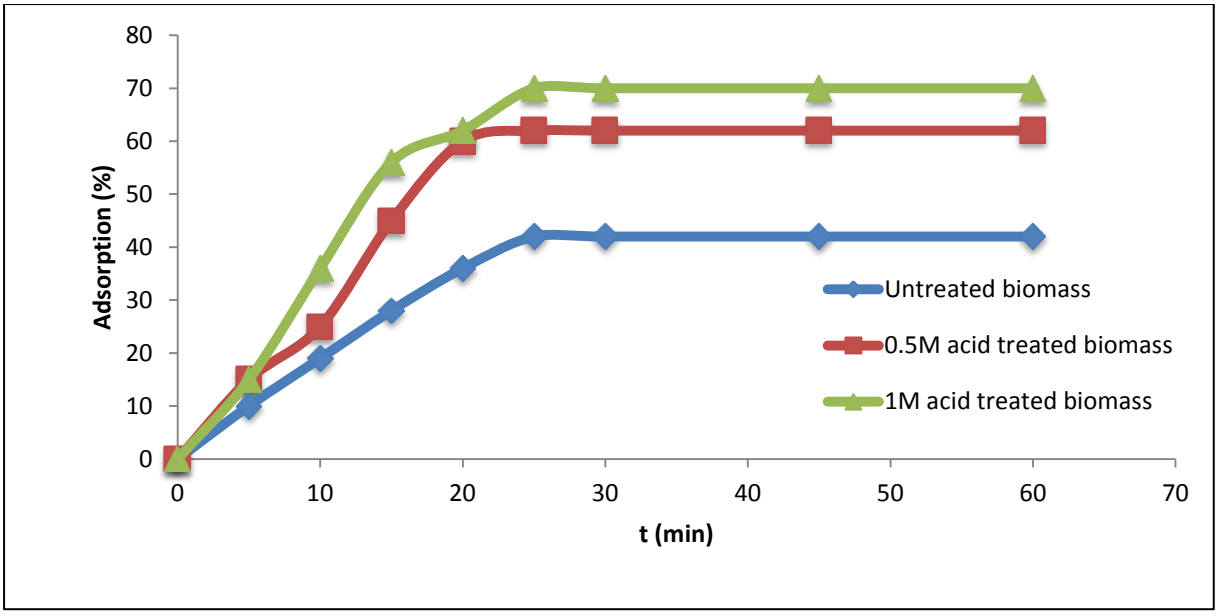

Figure 4.2(c) - Effect of acid treatment on cassava waste for the removal of V^{3+} (pH = 4; biomass = 0.250 g; agitation speed = 150 rpm; contact time = 1h; temperature = 30°C; metal ion concentration = 100 mg/L).

4.2.5 Effect of pH

One of the most important factors affecting adsorption of metal ions is the pH of the solution. The sorption of Co^{2+}, V^{3+} and Cr^{3+} onto acid treated cassava waste biomass was studied at

metal ion concentration of 100 mg/L. The effect of pH was tested on solutions of single, binary and ternary metal ion systems. Calculations of minimal pH required to precipitate Co^{2+}, Cr^{3+} and V^{3+} were done. Co^{2+}, Cr^{3+} and V^{3+} started to precipitate above pH of 7.9, 5.0 and 4.1, respectively. The calculations are included in the appendix. This implies that chemical precipitation would start to play a significant role above these pHs. In other words, the metal ions were stable at lower pHs, and unstable at higher pHs.

The results of the effects of pH are presented in Figures 4.3(a) to (e). The results in all cases show that the removal of Co^{2+}, V^{3+} and Cr^{3+} by the adsorbent is highly dependent on the pH of the solution suggesting that the metal binding occurs through an ion exchange type mechanism. In the single metal ion systems (Figure 4.3(a)) it can be seen that the maximum adsorption of V^{3+} and Cr^{3+} is obtained at pH 3. At pHs higher than 3, adsorption of both metal ion system decreases significantly. Figure 4.3(a) also shows that the adsorption of Co^{2+} ions increased with increase in pH with maximum adsorption attained at pH 6. The results show that metal ion adsorption of V^{3+} and Cr^{3+} are mostly favoured at low pHs, and unfavourable at extremely lowest and highest pHs. This trend in pH dependency confirms that sulfhydryl groups (-SH) play a role in the metal binding by cassava-peel biomass. At the lowest pHs, the free sulfhydryl groups are protonated and thus reduce any metal binding. In other words, at very low pHs, the concentration of protons is high, so the metal cations and protons compete for the binding sites on the cassava biomass which results in lower adsorption of the metal ions. As the pH is increased, the sulfhydryl groups are deprotonated and thus attract positively charged metal ions. As the pH is further increased, however, the trivalent (V^{3+} and Cr^{3+}) ionic systems are gradually substituted by the insoluble hydroxylated forms which precipitate out of solution resulting in the observed decrease in metal adsorption under alkaline conditions and the divalent (Co^{2+}) ionic system increase with increase in pH with maximum adsorption obtained at pH 6.

The pH of point of zero charge of the acid treated cassava is 3.1, meaning that the adsorbent's surface is positively charged at solution pHs below 3.1. However, the maximum adsorption of Cr^{3+} and V^{3+} were found at pH 3. This causes competition between protons and metal ion for adsorption binding sites. These cations (Cr^{3+} and V^{3+}) have higher charge densities and smaller radii which can overcome the electrostatic repulsion of the positively charge surface to bind on the surface of the biomass and displace surface protons (Wesolowski *et al*., 2008). Above the value of point of zero charge, a negative charge is present on the surface of the adsorbent causing better Co^{2+} adsorption through the electrostatic attraction.

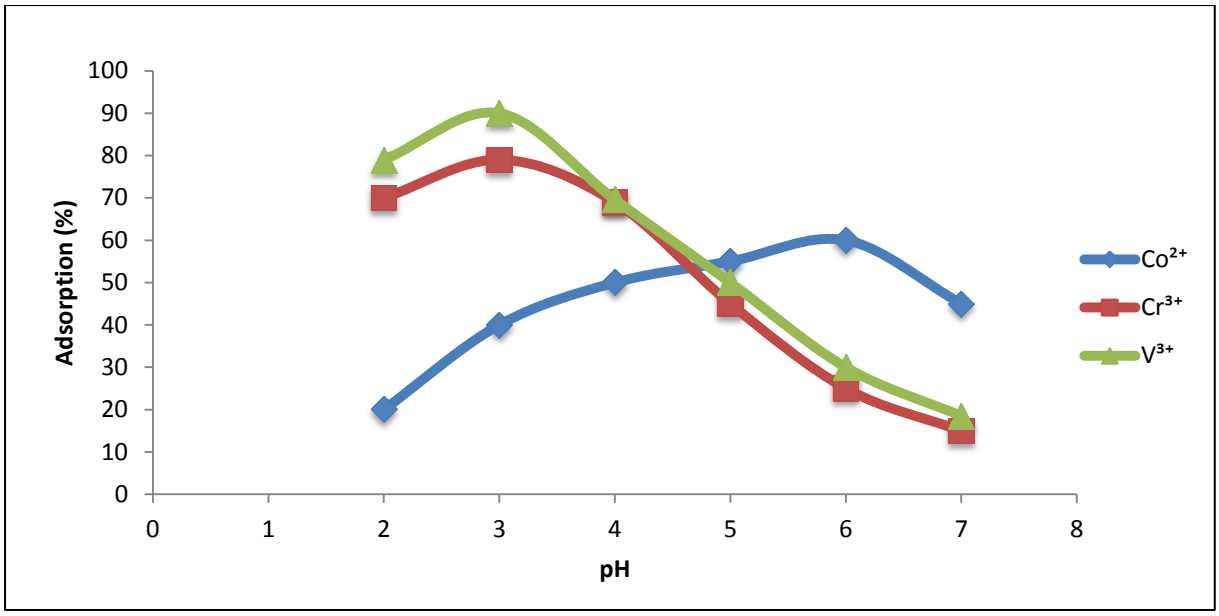

Figure 4.3(a) - Effect of initial pH on the removal of Co^{2+}, Cr^{3+} and V^{3+} using cassava waste biomass: single metal ion solutions; (pH = 2-7; biomass = 0.250 g; agitation speed = 150 rpm; contact time = 1h; temperature = 30°C; metal ions concentration = 100 mg/L).

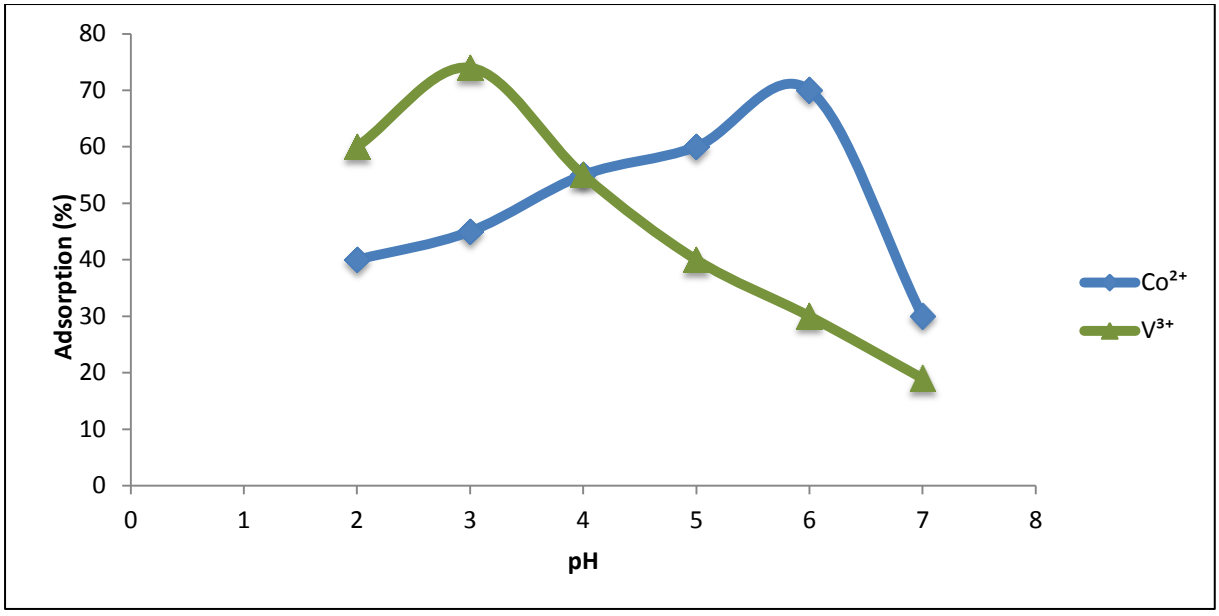

Figure 4.3(b) - Effect of initial pH on the removal of Co^{2+} and V^{3+} using cassava waste biomass: Binary metal ion systems; (pH = 2-7; biomass = 0.250 g; agitation speed = 150 rpm; contact time = 1h; temperature = 30°C; mixed metal solutions concentration = 100 mg/L).

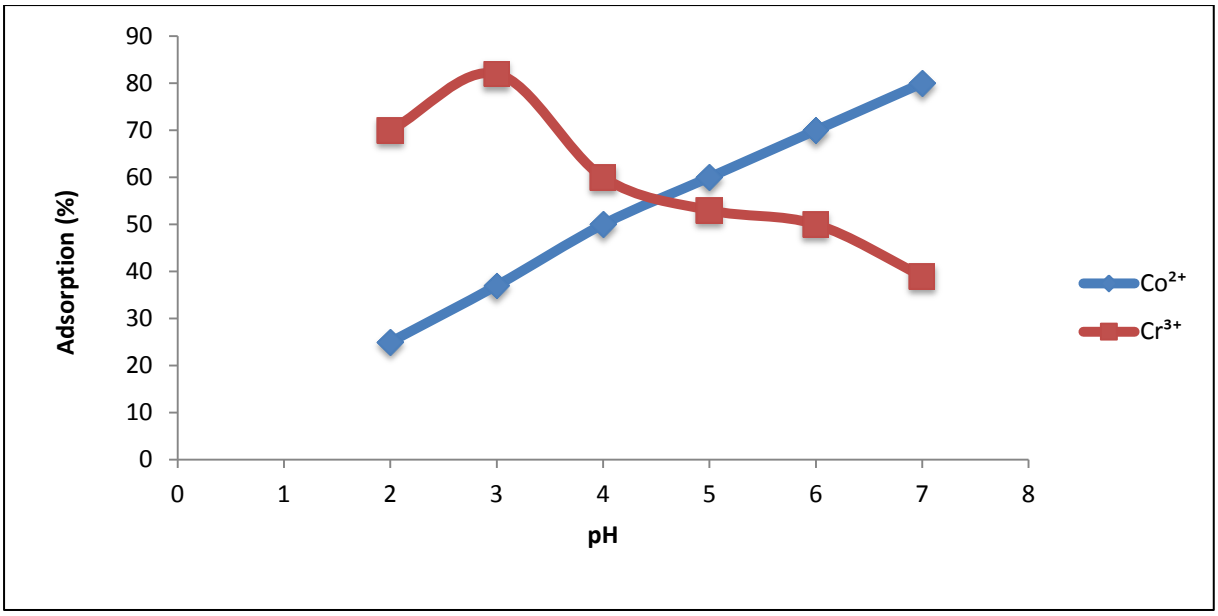

Figure 4.3(c) - Effect of initial pH on the removal of Co^{2+} and Cr^{3+} using cassava waste biomass: Binary metal ion systems (pH = 2-7; biomass = 0.250 g; agitation speed = 150 rpm; contact time = 1h; temperature = 30°C; mixed metal solutions concentration = 100 mg/L).

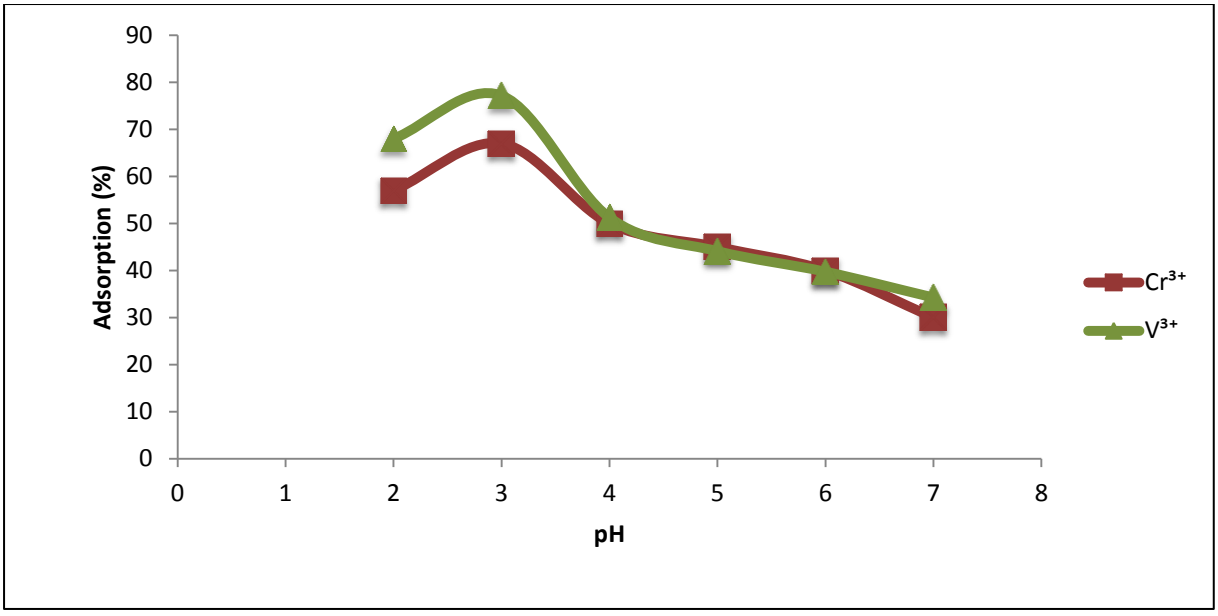

Figure 4.3(d) - Effect of initial pH on the removal of Cr^{3+} and V^{3+} using cassava waste biomass: Binary metal ion systems (pH = 2-7; biomass = 0.250 g; agitation speed = 150 rpm; contact time = 1h; temperature = 30°C; mixed metal solutions concentration = 100 mg/L).

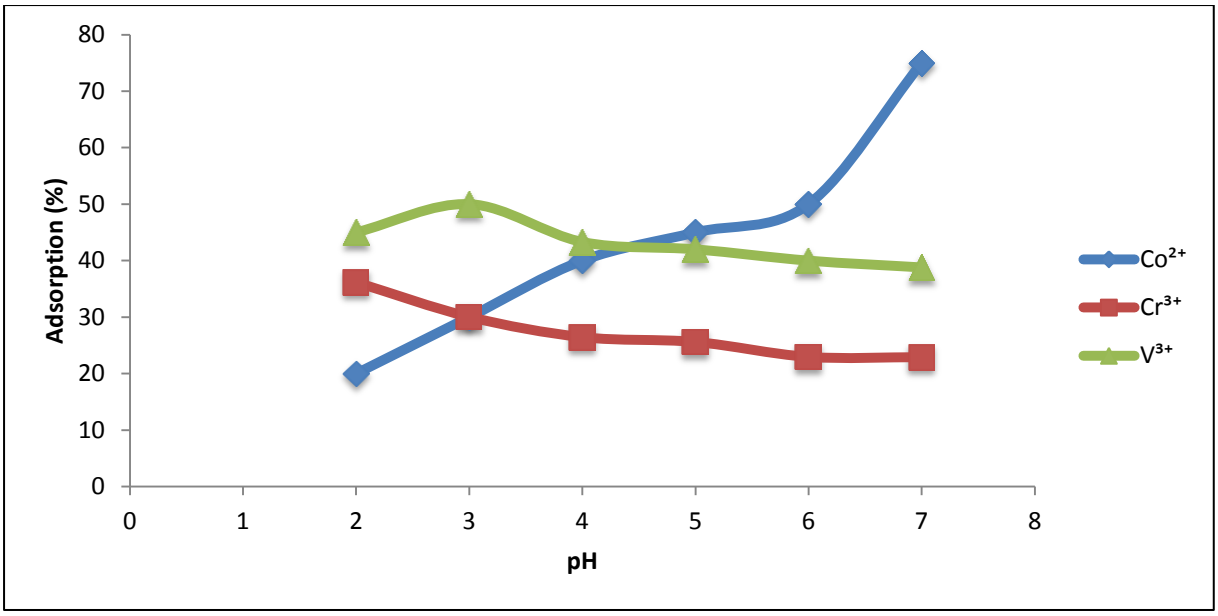

Figure 4.3(e) - Effect of initial pH on the removal of Co^{2+}, Cr^{3+} and V^{3+} using cassava waste biomass: Ternary metal ion systems (pH = 2-7; biomass = 0.250 g; agitation speed = 150 rpm; contact time = 1h; temperature = 30°C; mixed metal solutions concentration = 100 mg/L).

These results suggest that metal ions bind to the sulfhydryl groups through an ion-exchange type mechanism. At pHs around 3-6, adsorption can be considered to be an effective mechanism for removal of metal ions from aqueous solutions. As would be observed later (desorption studies), it follows that, if sulfhydryl groups do play a role in binding metal ions, by significantly lowering the pH, the metal ions would be released back into solution.

Figures 4.3(b) to (d) show the results for the binary metal ion systems. The V^{3+}- Co^{2+} (Figure 4.3(b)) and V^{3+}- Cr^{3+} (Figure 4.3(d)) systems show the same trend in adsorption as in the single metal ion systems. The pH for maximum adsorption is also similar to the single metal ion system although the percentage metal ion removal is slightly lower. This indicates that interference or competitive adsorption effect when these metal ion systems co-exist in solution is minimal. The Co^{2+}- Cr^{3+} system, however, shows a different trend. The results for this binary system show that whilst the Cr^{3+} keeps the same adsorption trend as in the single system, Co^{2+}, however, behaves differently. The presence of Cr^{3+} ions has a significant effect on the adsorption trend of Co^{2+} ions. The adsorption of Co^{2+} was seen to increase beyond pH 6 in the presence of Cr^{3+}. Since the solubility of the hydroxides of Cr^{3+} is lower than that of Co^{2+}, it is possible that when hydroxide ions are introduced into the system they will preferentially react with the Cr^{3+} ions forming, $Cr(OH)_3$. This means that the divalent Co^{2+}

ions exist in solution for longer before its maximum solubility is attained and precipitation commences.

Figure 4.3(e) shows the result for the ternary system. The results indicate a lower percentage of adsorption for Cr^{3+} and V^{3+} as compared to both the single and binary systems. A maximum of 50% at pH 3 is recorded for V^{3+} whilst a value of 35% at pH 2 is attained for Cr^{3+}. The percentage adsorption of Co^{2+} ions was seen to increase with increasing pH maintaining a trend similar to that observed in the Co^{2+}, Cr^{3+} binary system. This suggests that the Cr^{3+} ions have a more significant effect on the adsorption trend of Co^{2+} than the V^{3+} ions. These results also suggest that developing a process for the one step removal of the three metal ions systems (ternary) from waste streams would be problematic due to the observed lower adsorption efficiency of Cr^{3+} and V^{3+}. However, selective removal of Co^{2+} ions would be enhanced in a binary or ternary system in the presence of Cr^{3+}.

4.2.6 Effect of contact time

Contact time is an important factor that has an effect on the duration of a given reaction. The required contact time is also important for sorption processes as it provides information on the minimum time required for considerable adsorption to take place and the possible diffusion controlling mechanism for the metal ion as it moves from the bulk solution towards the adsorbent surface (Augustine *et al*., 2007). The effect of contact time for various metal ions is given in Figure 4.4. As can be seen from Figure 4.4, the adsorption of all the metal ions are higher at the beginning. This is due to larger number of surface sites on the biomass available for the adsorption of metal ions at the beginning of the process. As the surface sites for adsorption become exhausted, the adsorption rate is controlled by the rate at which the adsorbate is transported from the exterior to the interior sites of the adsorbent cassava biomass, thus low rates are observed over time. The equilibrium time was reached after 25 minutes for Co^{2+} and Cr^{3+}, and 30 minutes for V^{3+}. The metal ion adsorption then remained constant after equilibrium was reached for all the metal ion systems.

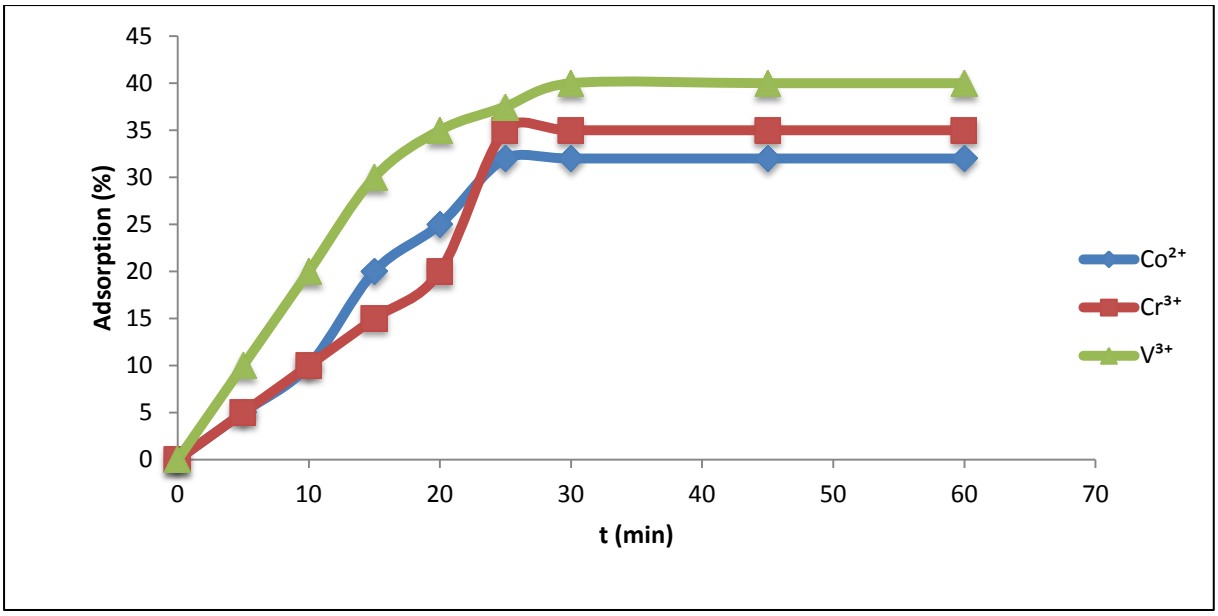

Figure 4.4- Effect of contact time on the removal of Co^{2+}, Cr^{3+} and V^{3+} using cassava waste biomass: Single metal ion solutions; (pH = 6 for Co^{2+}, 3 for Cr^{3+} and 3 for V^{3+}; biomass = 0.250 g; agitation speed = 150 rpm; contact time = 1h; temperature = 30°C; metal ions concentration = 100 mg/L).

The results from Figure 4.4 and the previous results in Figure 4.2 (a) and Figure 4.3(a) show that the capacity for the sorption of $Co^{2+}$is lower in comparison to the V^{3+} and Cr^{3+} ions. The low adsorption by Co^{2+} can be attributed to the high ionic radius and low charge density. (Brauckmann, 1990; Horsfall *et al*., 2003; Abia and Asuquo, 2008). As such the affinity of Co^{2+} ion towards the active binding site is lower.

4.2.7 Effect of temperature

Temperature is an important factor in any given reaction. It is a measure of the speed with which the reacting atoms, molecules and ions move. In other words, temperature is a measure of the kinetic energy of reacting species. Normally, the higher the temperature, the faster the reacting atoms, molecules or ions move, and the higher the rate of reaction. The temperature dependence of Co^{2+}, Cr^{3+} and V^{3+} sorption on acid treated cassava waste biomass was studied in the temperature range of 30 to 50°C and results are presented for single and ternary metal ion systems as shown in Figures 4.5(a) and (b), respectively. The results show that an increase in temperature from 30 to 40°C resulted in enhanced sorption of Co^{2+}, Cr^{3+} and V^{3+} from solution. The highest removal was observed at 40°C indicating that, at this temperature, a higher affinity of metal ions for the binding sites on the cassava occurs. The adsorption

capability of cassava-peel waste was observed to decrease beyond 40°C, possibly due to the destruction of the biomass active binding sites at higher temperatures.

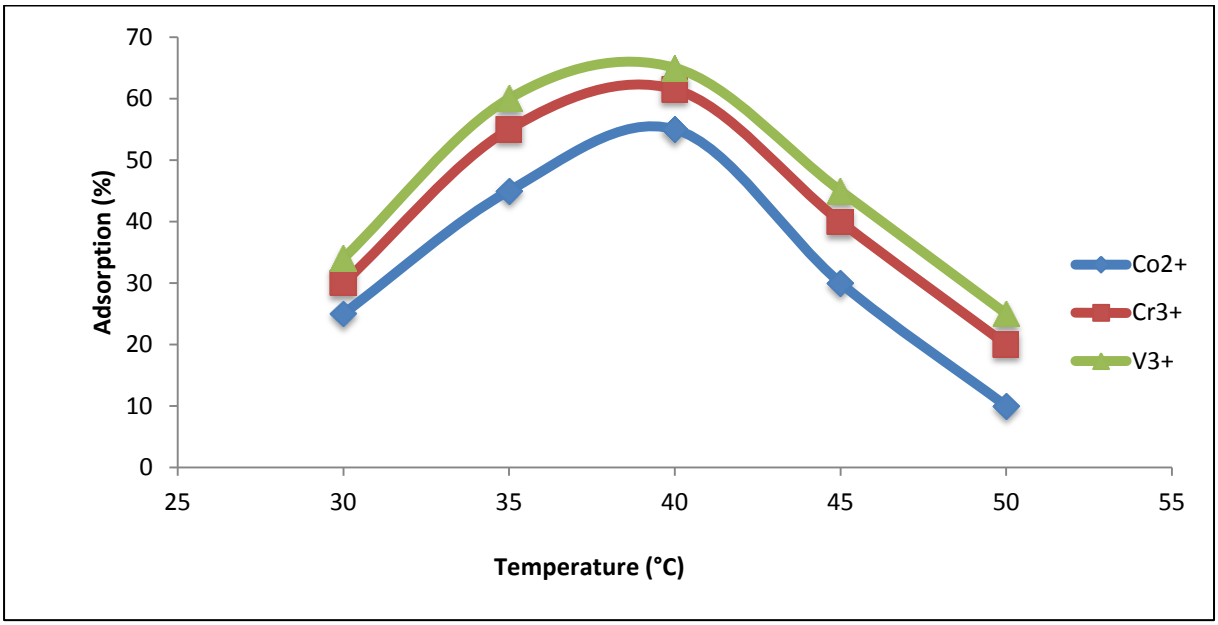

Figure 4.5(a) - Effect of temperature on the removal of Co^{2+}, Cr^{3+} and V^{3+} ions using cassava waste biomass: Single metal ion systems; (pH = 6 for Co^{2+}, 3 for Cr^{3+} and 3 for V^{3+}; biomass = 0.250 g, agitation speed = 150 rpm; contact time = 1h; temperature = 30-50°C; concentration = 100 mg/L).

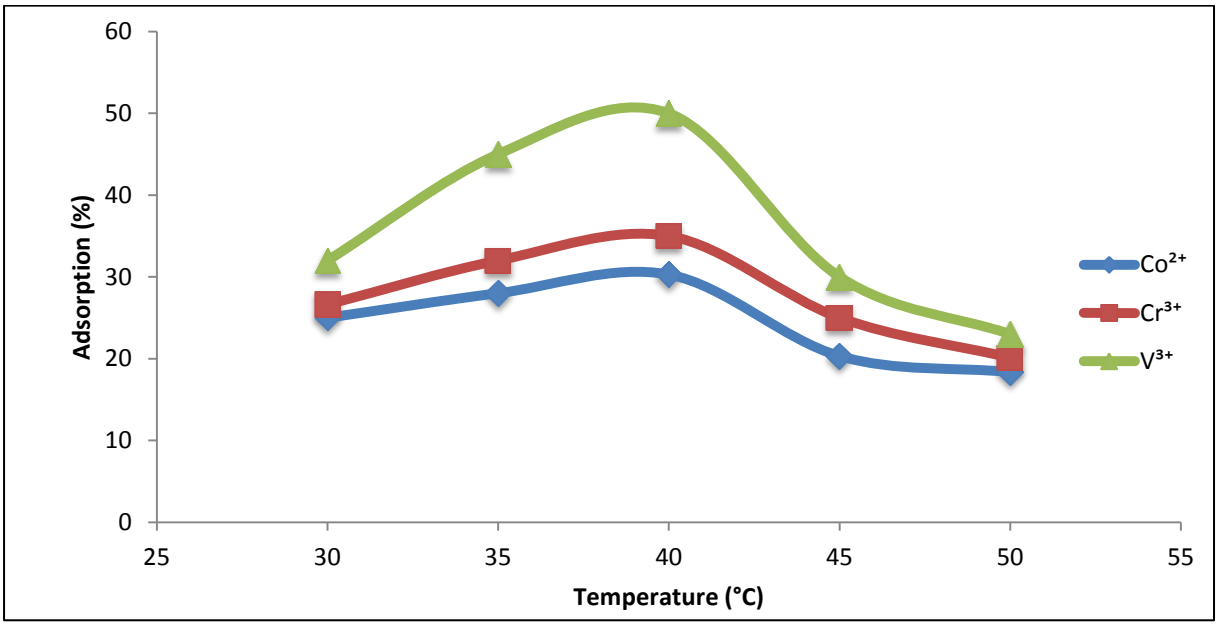

Figure 4.5(b) - Effect of temperature on the removal of Co^{2+}, Cr^{3+} and V^{3+} using cassava waste biomass : Ternary metal ion systems; (pH, = 4; biomass = 0.250 g, agitation speed = 150 rpm agitation speed; contact time = 1h; temperature = 30-50°C; concentration = 100 mg/L).

The results also show that higher adsorption was obtained in single metal ion systems as compared to ternary metal ion system. At the optimum temperature of 40°C, the loading efficiency of Cr^{3+} and Co^{2+} on the biomass was seen to decrease by almost 50% in the ternary system compared to the single metal ion systems. On the other hand, the loading efficiency for V^{3+} only decreased by about 25%. The lower adsorption efficiency in the ternary systems seems to indicate a competitive adsorption effect when the three metal ions co-exist in solution. The cassava waste biomass adsorbed the metal ion in the following order: V^{3+}>Cr^{3+}>Co^{2+}.The metal ion with the smaller ionic radius has a higher affinity towards the biomass active binding site.

4.2.8 Effect of agitation

The effect of agitation speed on the removal of Co^{2+}, Cr^{3+} and V^{3+} by cassava waste was studied at different agitation speeds from 50 to 200 rpm. Here, biomass of 0.25g, and optimum pH and temperature obtained in sections 4.2.5 and 4.2.6 respectively were kept constant. The results as given in Figure 4.6(a) and (b) show that there was an increase in sorption as the agitation speed increased from 50 to 150 rpm. This is because an increase in agitation speed maximizes the mass transfer rate of metal ion to the surface of the biomass. However, the sorption reduced as agitation increased from 150 to 200 rpm. This is because at severe turbulence the bonding between the metal ions and the adsorbent gets broken resulting in the metal ions desorbing from the surface sites. The results also imply that physical adsorption rather than chemical adsorption is taking place.

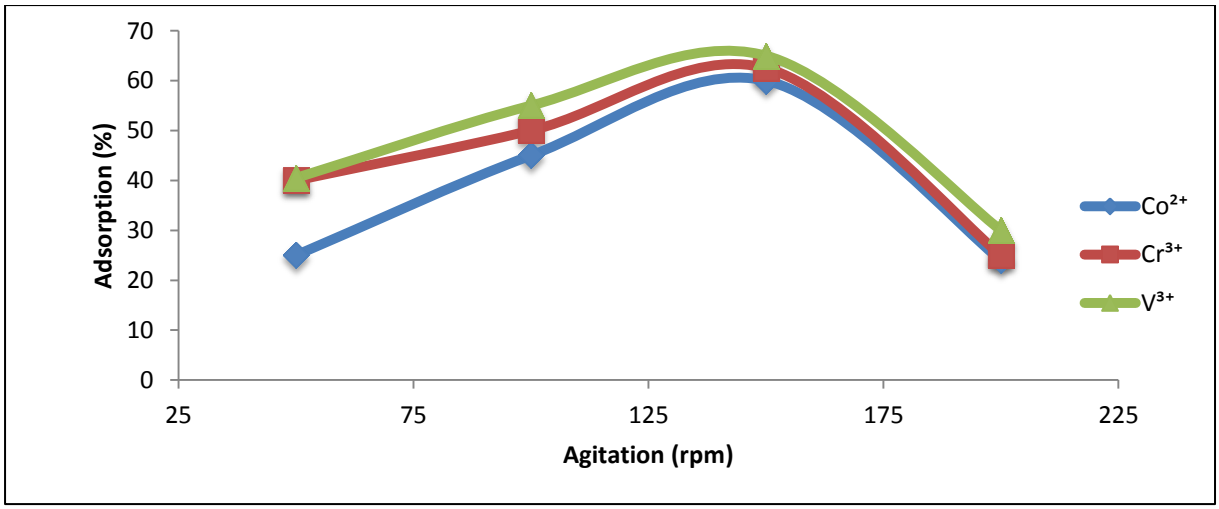

Figure 4.6(a) - Effect of agitation speed on the removal of Co^{2+}, Cr^{3+} and V^{3+} using cassava waste biomass: Single metal ion system (pH = 6 for Co^{2+}, 3 for Cr^{3+} and 3 for V^{3+}, biomass = 0.250 g; agitation speed = 50-200 rpm; contact time= 1h; temperature = 30°C, concentration = 100 mg/L).

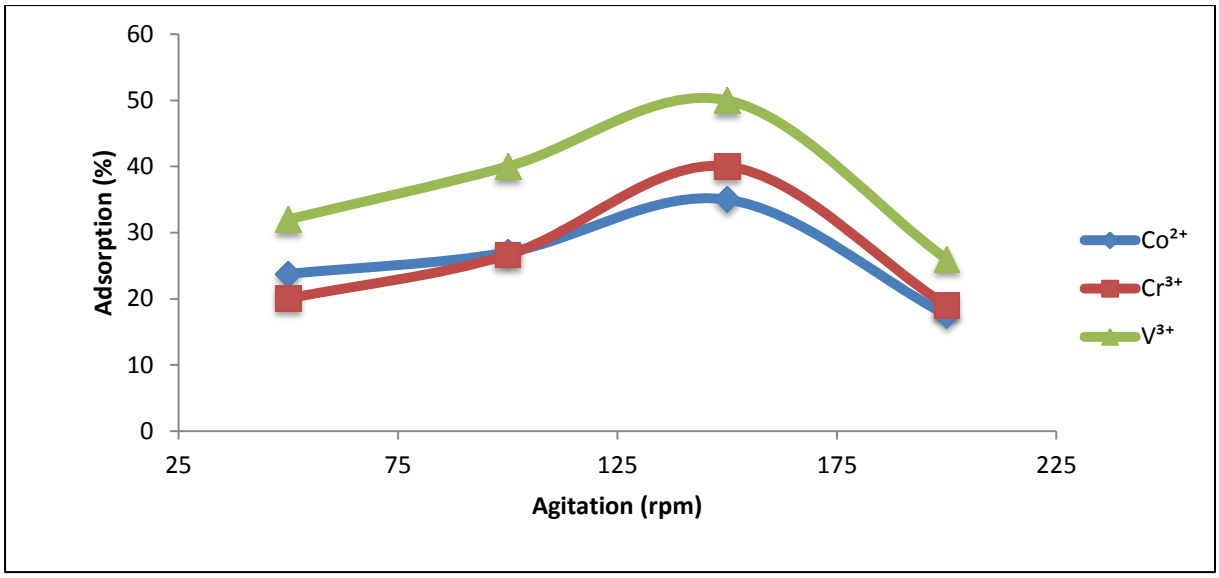

Figure 4.6(b) - Effect of agitation speed on the removal of Co^{2+}, Cr^{3+} and V^{3+} using cassava waste biomass: Ternary metal ion system (pH = 4, biomass = 0.250 g; agitation speed, = 50-200 rpm; contact time, = 1h; temperature = 30°C, concentration = 100 mg/L).

The results show lower adsorption in ternary metal ion system as compared to the single metal ion system, which was due to competitive effect between the metal ions. V^{3+} has higher affinity for adsorption on the cassava waste biomass as compared to the other metals. This was due to its lower ionic radius.

4.2.9 Effect of biomass and initial metal ion concentration

The concentration of both the metal ions and the biomass is a significant factor to be considered for effective bioremediation (Sudha and Abraham, 2001). It determines the sorbent/sorbate equilibrium of the system, because the rate of adsorption is a function of the initial metal ion concentration, and biomass quantity. Furthermore, the initial metal ion concentration provide the necessary driving force needed to overcome the resistances to mass transfer between the aqueous phase and the solid biomass phase (Kumar *et al*., 2010).

The effect of biomass dosage: The effect of the biosorbent concentration on the metal removal efficiency is presented in Figures 4.7(a) and (b). The rate of removal of the metal ions in this study increased with increase in dosage of the sorbent. This may be due to the increase in surface area and in the number of available active sites for the sorption of Co^{2+}, Cr^{3+} and V^{3+}. In other words, the higher the number of surface sites available, the higher the quantity of metal ions adsorbing on to the surfaces.

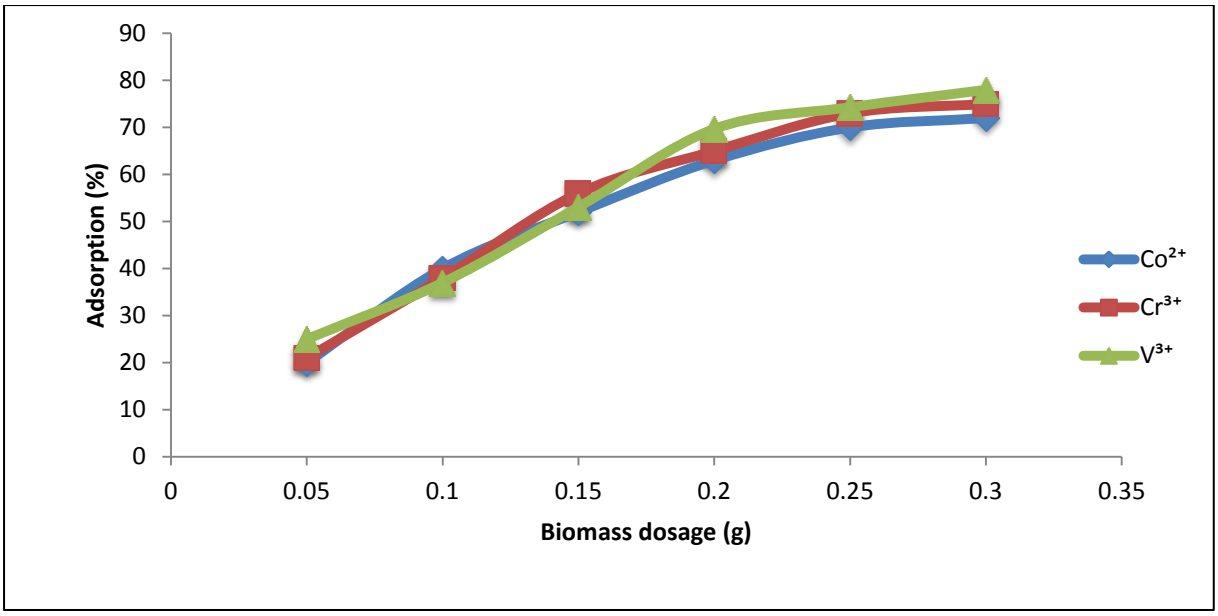

Figure 4.7(a) - Effect of biomass dosage on the removal of Co^{2+}, Cr^{3+} and V^{3+} using cassava waste biomass: Single metal ion systems (initial pH = 6 for Co^{2+}, 3 for Cr^{3+} and 3 for V^{3+}, biomass = 0.05-0.30 g; agitation speed = 150 rpm; contact time = 1h; temperature = 30°C, concentration = 100 mg/L).

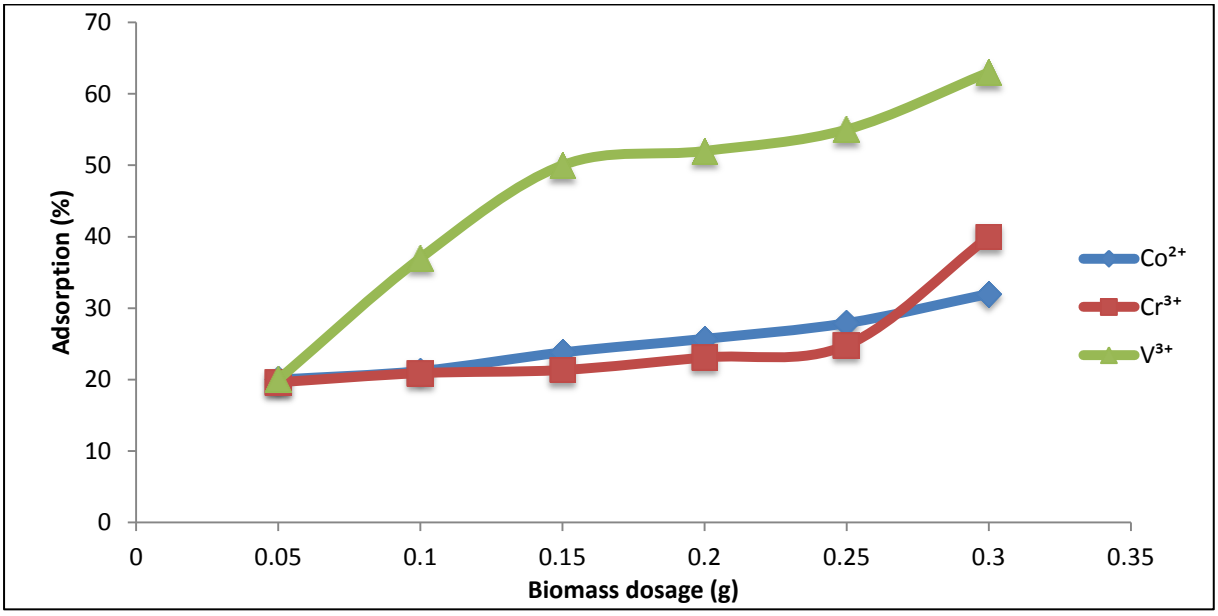

Figure 4.7(b) - Effect of biomass dosage on the removal of Co^{2+}, Cr^{3+} and V^{3+} using cassava waste biomass: Ternary metal ion systems (initial pH = 4, biomass = 0.05-0.30 g; agitation speed = 150 rpm; contact time = 1h; temperature = 30°C, concentration = 100 mg/L).

In the ternary system (Figure 4.7(b)) the capacity for the sorption of the three metal ion systems is significantly lower in comparison to the single systems indicating the prevalence of the competitive adsorption effect in mixed ions solution systems.

Effect of initial metal ion concentration: Figures 4.8(a) and (b) show the effect of initial metal ion concentration for single and ternary metal ion systems, respectively. As can be observed from the figures, the rate of Co^{2+}, Cr^{3+} and V^{3+} ions removal decreases above the ion concentration of 100 mg/L. This may be due to limited number of available active sites on the surface of the cassava waste biomass to accommodate higher concentration (Horsfall *et al*., 2003).

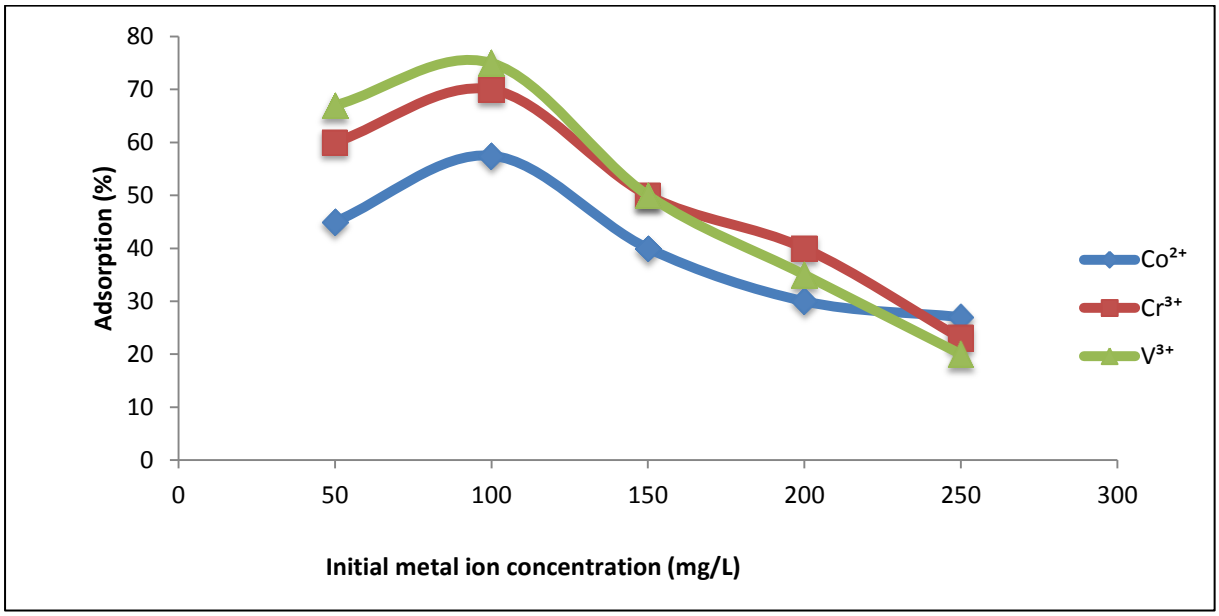

Figure 4.8(a) - Effect of initial metal ion concentration on the removal of Co^{2+}, Cr^{3+} and V^{3+} using cassava waste biomass: Single metal ion systems (pH = 6 for Co^{2+}, 3 for Cr^{3+} and V^{3+}; biomass = 0.250 g; agitation speed = 150 rpm; contact time = 1h; temperature = 30°C; concentration = 50-250 mg/L).

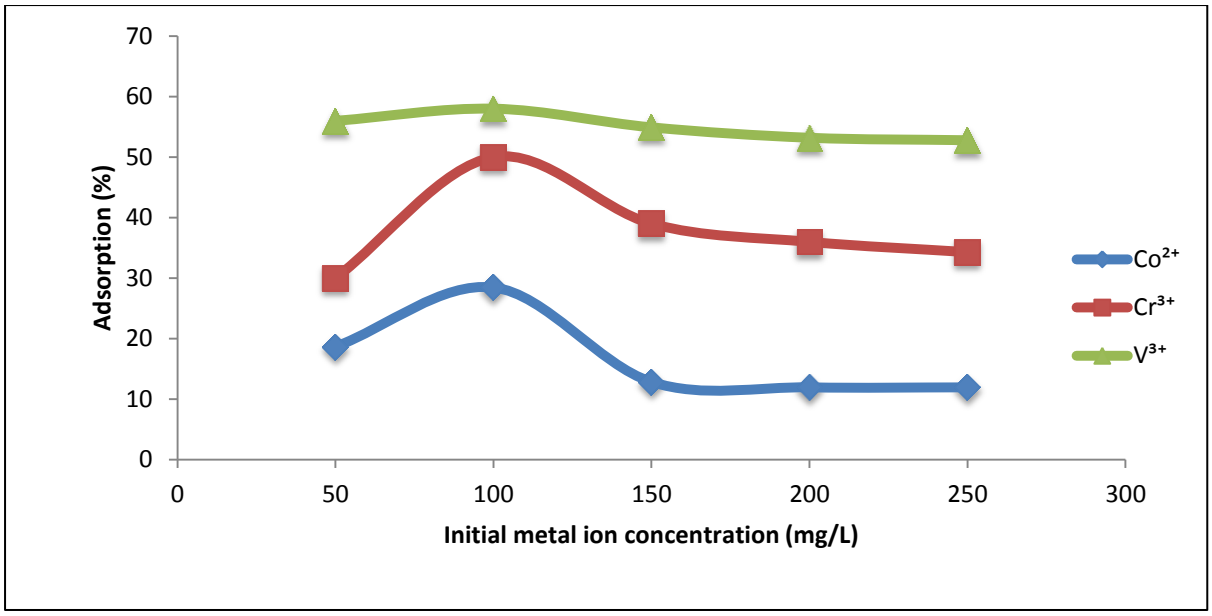

Figure 4.8(b) - Effect of initial metal ion concentration on the removal of Co^{2+}, Cr^{3+} and V^{3+} using cassava waste biomass: Ternary metal ion system (pH = 4; biomass = 0.250 g; agitation speed = 150 rpm; contact time = 1h; temperature = 30°C; concentration = 50-250 mg/L).

The efficiency of cassava waste biomass to adsorb Co^{2+}, Cr^{3+} and V^{3+} in ternary systems was lower than in single metal solutions. This drop in adsorption of metal ions as observed in the previous ternary systems results may be attributed to the greater competitive effects of the metal ions for the occupancy of the binding surfaces on the cassava waste. In ternary systems equilibrium was reached at metal ion concentration of around 150 mg/L. This was an indication of the unavailability of further adsorption sites for metal ions on the cassava waste due to saturation, i.e. the adsorption capacity limit of the cassava wastes had been reached. This also means that when a certain threshold concentration level is reached in a ternary system the biomass can only take a certain amount of each corresponding cation thus making the effect of initial metal ion concentration insignificant.

4.2.10 Effect of co-cations

In wastewater streams, the metal of interest is usually found in a matrix containing several other metal cations. The presence of certain cations in the system may influence the adsorption capacity of the cassava waste biomass since the driving force of the whole adsorption process is the electrostatic attraction between charged species and the functional groups on the biomass surface. The cations can also modify the specificity of the cassava waste biomass due to the change in the ionic strength of the aqueous phase. This is bound to have an effect on the selectivity and ultimately the adsorption capacity of the adsorbent.

Thus, industrial application of a biosorption process must deal with the fact that metal bearing waste streams often contain other ions that may interfere in the uptake of the metal ion of interest by acting as competing adsorbate, limiting the available binding sites for metal ion sorption.

Equilibrium experiments were conducted to evaluate the effect of common cations such as sodium (Na^{+}), potassium (K^{+}), magnesium (Mg^{2+}) and calcium (Ca^{2+}). Within the concentration range examined, it is evident that Co^{2+}, Cr^{3+} and V^{3+} ion uptake was not greatly affected by the presence of the chloride salts of sodium and potassium (Figures 4.9(a) to 4.9(c)). Tsezos *et al.* (1996) indicated that if metal ion species exhibit preferences for different biomass binding sites, their simultaneous presence in solution may not significantly affect their corresponding metal uptake capacities. On this basis it can be proposed that there was no direct competition for adsorption sites on the biomass in the presence of sodium and potassium, especially at low concentrations, suggesting that preferential binding to different sites of the cassava was probably involved. However, higher concentrations of magnesium and calcium had a significant effect on the adsorption of these three metal ion systems by cassava-peel biomass. In the presence of magnesium and calcium, plots of adsorption of Cr^{3+}, Co^{2+} and V^{3+} ions show lower metal ion adsorption implying that there was competitive adsorption for the binding sites on cassava-peel biomass.

The effect of calcium towards the sorption of the three metal ion systems is far more pronounced than that of magnesium. This is because hydronium ions that are found at the surface of the positively charged calcium ions in the aqueous system (Villegas-Jimenez and Mucci, 2009) significantly increased the electrostatic force of attraction between the adsorbent and the calcium cations present in solution. This resulted in calcium occupying a significant amount of binding sites on the surface of the adsorbent.

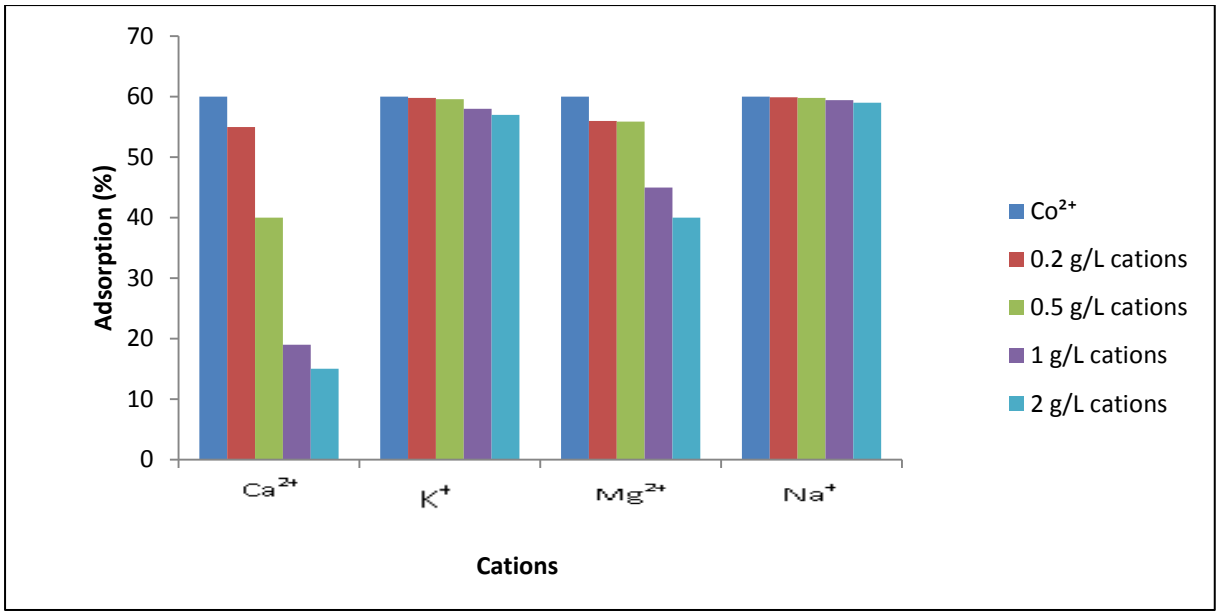

Figure 4.9(a) - Effect of cations on the Co^{2+}removal using cassava waste biomass: Single metal ion system (pH = 6, biomass 0.250 g, 150 rpm agitation speed; contact time, 1h; temperature 40°C, concentration 100 mg/L).

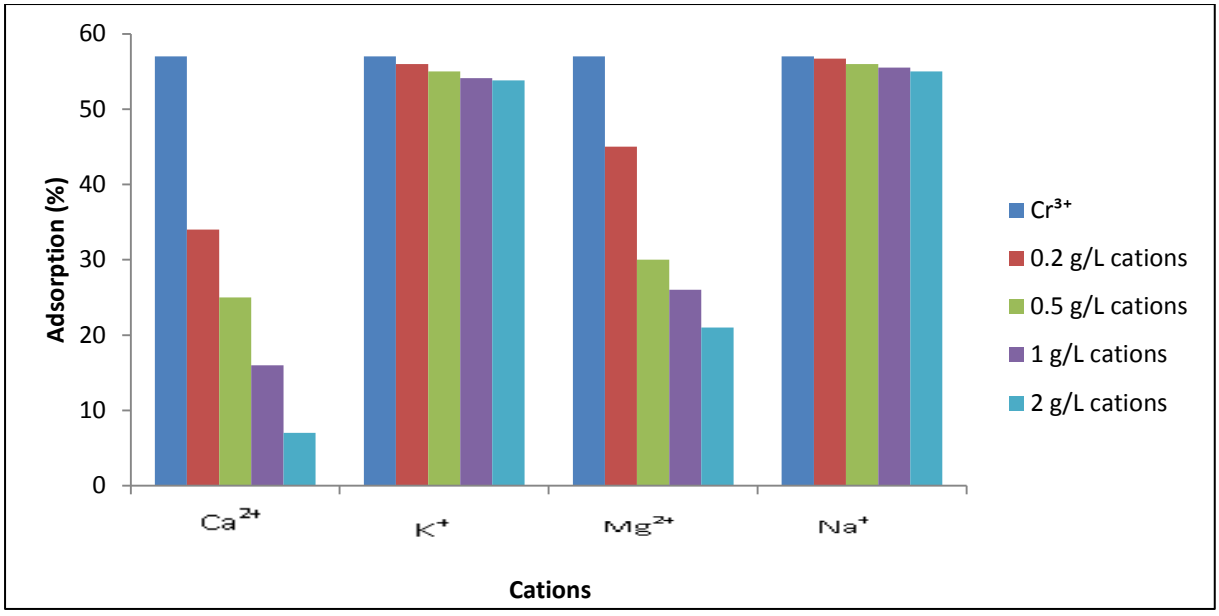

Figure 4.9(b) - Effect of cations on the Cr^{3+}removal using cassava waste biomass: Single metal ion systems (pH = 3, biomass 0.250 g, 150 rpm agitation speed; contact time, 1h; temperature 40°C, concentration 100 mg/L).

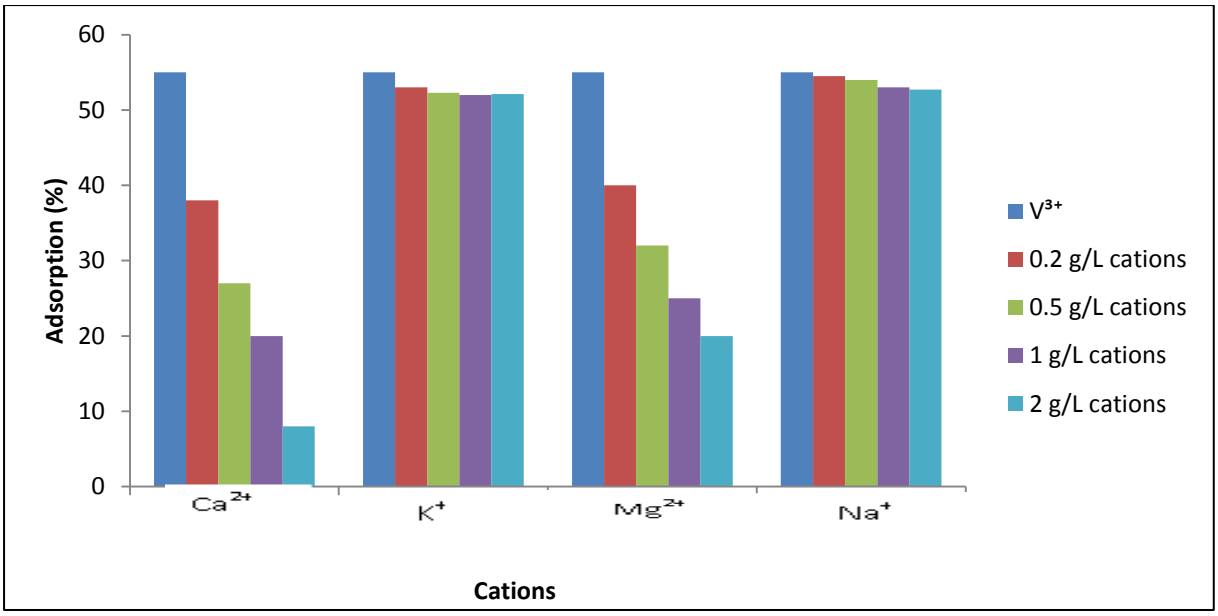

Figure 4.9(c) - Effect of cations on the V^{3+}removal using cassava waste biomass: Single metal ion systems (pH = 3, biomass 0.250 g, 150 rpm agitation speed; contact time, 1h; temperature 40°C, concentration 100 mg/L).

The results presented in this section showed that in general, the presence of cations in a solution system decreased the amount of metal ion adsorbed, due to competition for binding sites between the metal ions and the cations in question. In addition, the presence of cations in the solution resulted in an increase in the ionic strength of the aqueous phase. Adsorption is known to decrease with increasing ionic strength of the aqueous phase (Wan Ngah and Hanafiah, 2008).

The divalent Ca^{2+} or Mg^{2+} ions exert a stronger influence on the metal uptake than in the case of monovalent Na^{+} or K^{+} ions, which is reflected even at lower salt concentrations. In general, the greater the electronegativity; the greater is the affinity for the binding sites (Ansari et al., 2011). As such, divalent Ca^{2+} or Mg^{2+} ions compete more strongly for binding sites than the monovalent Na^{+} or K^{+} ions.

4.2.11 Equilibrium isotherms

Adsorption isotherms aid in the quantitative evaluation of the metal uptake from experimental data. The isotherms play an important role in the determination of the maximum capacity of adsorption. They also provide a panorama of the course taken by the system under study in a concise form, indicating how efficiently an adsorbent will adsorb and allows an estimate of the economic viability of the adsorbent's commercial applications for the specified solute

(Kumar *et al*., 2010). The Langmuir and Freundlich isotherm equilibrium models were used to evaluate the experimental results. The Langmuir sorption model served to estimate the maximum theoretical metal uptake not reached in the experiments, and the Freundlich adsorption model was used to estimate the adsorption intensity of metal ions on the cassava biomass.

The isotherm constants and correlation coefficients of Langmuir model for Co^{2+}, Cr^{3+} and V^{3+} are given in Table 4.3 From the Langmuir isotherm, the adsorption affinity constant, b, and the maximum adsorption capacity, q_{max}, of Co^{2+}, Cr^{3+} and V^{3+} forming a complete monolayer on the surface of the cassava waste biomass were estimated at 0.590 L/mg and 6.709 mg/g, 0.033 L/mg and 10.516 mg/g, and 0.037 L/mg and 12.250 mg/g, respectively. The small value of b (for V^{3+} and Cr^{3+}), which represents the affinity between sorbent and sorbate, suggests a weaker binding between the ions and the biomass surface, indicating a physisorption process (Volesky, 2004).

Table 4.3 Linear Langmuir and Freundlich isotherm parameters for Co $^{2+}$, Cr^{3+} and V^{3+} sorption by cassava waste biomass.

	Langmuir isotherm			**Freundlich isotherm**		
	$\mathbf{1/q_e=(1/q_{max}.b).1/C_e+ 1/q_{max}x}$			$\mathbf{logq_e= logK_F +1/n\ logC_e}$		
Metals	$\mathbf{q_{max}}$ (mg/g)	**b** (L/mg)	$\mathbf{R^2}$	**n**	$\mathbf{K_F}$(mg/g)	$\mathbf{R^2}$
Co	6.7088	0.59	0.455	21.905	11.669	0.555
Cr	10.5158	0.0332	0.998	12.4766	8.984	0.999
V	12.250	0.037	0.923	0.0876	6.715	0.980

The parameters for the Freundlich equation are given in Table 4.3. The Freundlich adsorption coefficient K_F and the intensity n were determined as 11.669 mg/g and 21.905 for Co^{2+}, 8.984 mg/g and 12.477 for Cr^{3+}, and 6.715 mg/g and 0.088 for V^{3+}, respectively. The Freundlich equation was found to be more suitable as indicated by the higher correlation coefficient (R^2 = 0.555) for Co^{2+}, (R^2 = 0.999) for Cr^{3+} and (R^2 = 0.980) for V^{3+}, compared to the Langmuir equation (R^2 = 0.455) for Co^{2+}, (R^2 = 0.998) for Cr^{3+} and (R^2 = 0.923) for V^{3+}.

4.2.12 Adsorption-acid desorption cyclic studies

Treatment of large volumes of solutions is usually limited by the loading capacity of the adsorbent system. With rising prices of most raw materials employed as adsorbent in effluent and wastewater treatment processes, the attractiveness of a process becomes defined by the reuse of the adsorbent in successive adsorption/desorption cycles with no marked effect on the structural characteristics and adsorption capabilities of the adsorbent. This means that throughout the successive cycles of metal uptake and acid elution, the adsorbent must be able to maintain its metal recovery capacity thus allowing its employment in larger numbers of adsorption cycles.

An evaluation of the behaviour of the cassava-peel waste regarding its reusability for Co^{2+}, Cr^{3+} and V^{3+} sorption was carried out by conducting ten sorption/desorption cycles. Elution of the loaded cassava waste was done using H_2SO_4 at concentrations varying from 0.1 to 2M. It should be mentioned that after each desorption cycle, distilled water and nitric acid were used to rinse the surface of the adsorbent so as to remove residual ions on the surface and to reactivate the cassava, respectively.

The effect of the concentration of eluent on desorption of metal ions from the cassava biomass is shown in Figure 4.10. It can be seen from the Figure that they are no significant differences in desorption efficiency when the eluent concentration is increased. However, further examination of the cassava waste after desorption indicated some significant changes in the material's appearance. The biomass that had been exposed to lower concentrations of the eluent (0.1, 0.5 and 1 mol/L H_2SO_4) remained soft and appeared suitable for subsequent cycles. In contrast, the biomass treated with 1.5 and 2 mol/L H_2SO_4 had become fragile and lost its original color (from brown to black); its weight was also found to have decreased. The weight loss was in the range of 2.3 to 17% as the eluent concentration increased from 1-2 mol/L. This deterioration of the cassava waste indicated that highly concentrated eluent dissolved and/or degraded parts of the polysaccharides of the material, destroying some of the binding sites which would then affect its recyclability.

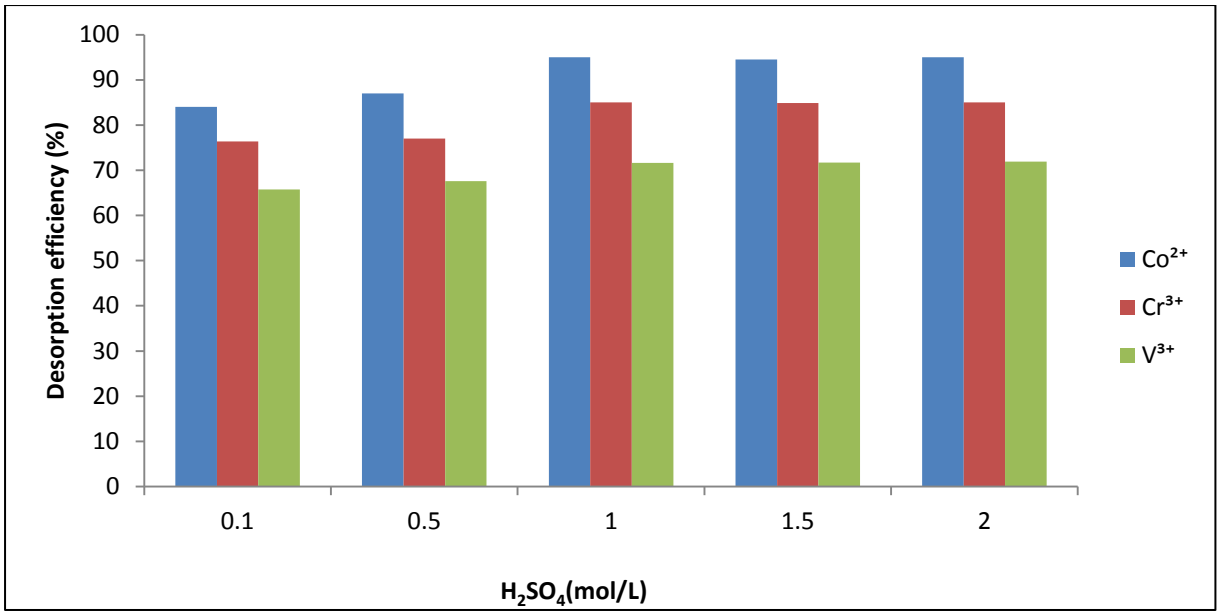

Figure 4.10- Effect of H_2SO_4 concentrations on the desorption efficiency of Co^{2+}, Cr^{3+} and V^{3+} from cassava waste biomass.

The results shown in Figure 4.10 further suggest that there is no economic gain in using a highly concentrated acid eluent as there was no significant difference in desorption efficiency observed with increasing concentration of the eluent from 0.1 to 1.0 mol/L. It can thus be concluded that 0.1 mol/L H_2SO_4 will be more suitable for desorption of Co^{2+}, Cr^{3+} and V^{3+} as it allows less mass loss and shows more compatibility with the requirements of adsorption-desorption operation. This concentration was used in the subsequent studies for determining the number of cycles for biomass regeneration.

Surface chemistry of original and eluted biomass

The FTIR spectra of the original chemically modified biomass and differently eluted cassava biomass are shown in Figure 4.11(a) to (d). The broad band at the range of 3300-2960 cm^{-1} corresponded to the stretching of –OH. A peak at 2572 cm^{-1} shown in Figures 4.11 (a) to (c) corresponded to the stretching of –SH. The peaks at the range of 1674-1586 cm^{-1} are attributed to the stretching of –C=O and the bands at the range of 1391-1028 cm^{-1} corresponded to the stretching of –C-O. The peaks at 875 and 612 cm^{-1} corresponded to the out of plane bending of C-H and C-H bend, respectively. At 2M eluent concentration (Figure 4.11d), the peaks representing stretching of –SH and the out of plane of C-H bend disappeared and the bending of –C-H and stretching of –C-O shifted. This is expected to

reduce the adsorption capacity of cassava waste biomass. Therefore, all desorption and regeneration studies were carried out using 0.1M H_2SO_4.

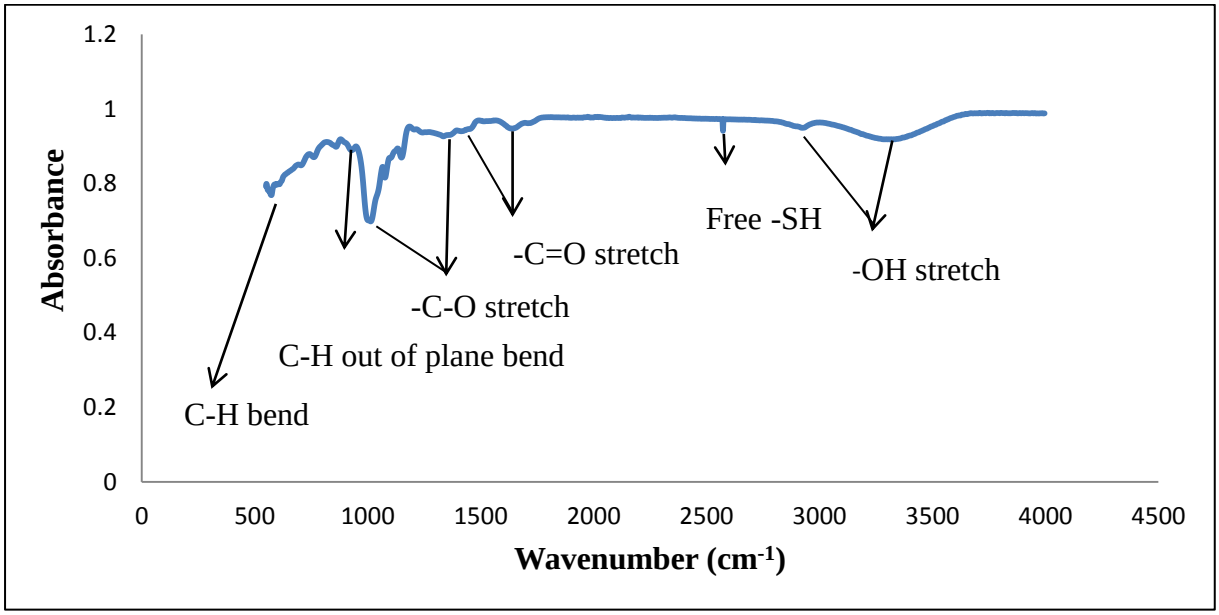

Figure 4.11(a) -Fourier transform infrared spectrum for original chemically modified cassava waste biomass.

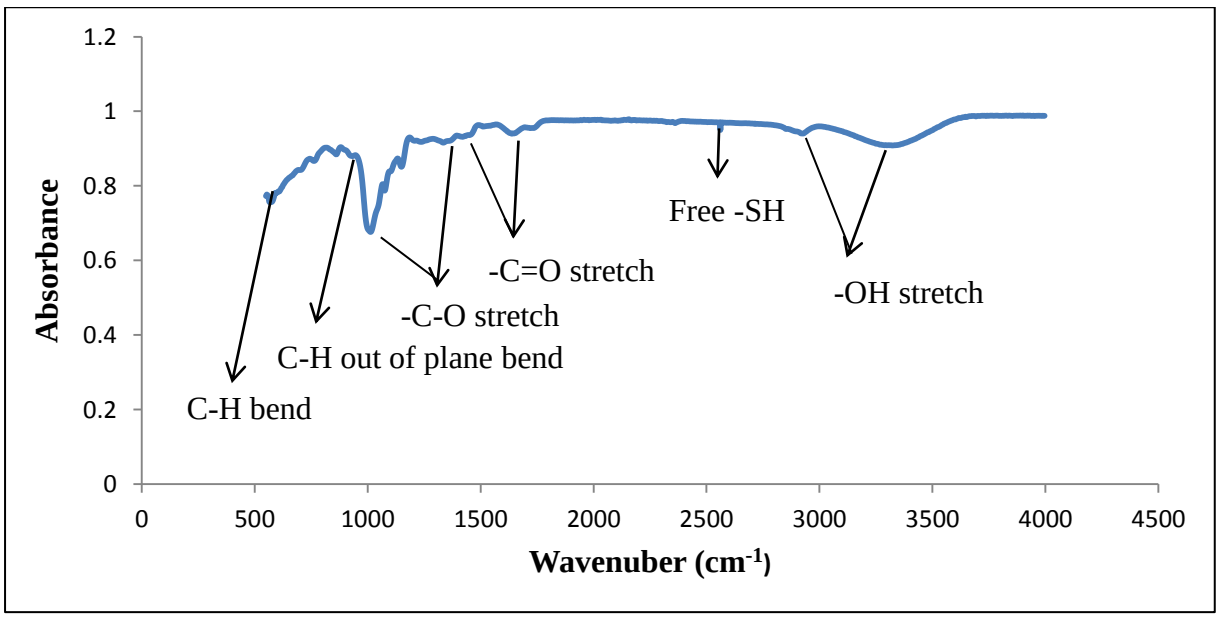

Figure 4.11(b) -Fourier transform infrared spectrum for 0.1M H_2SO_4 eluted cassava waste biomass.

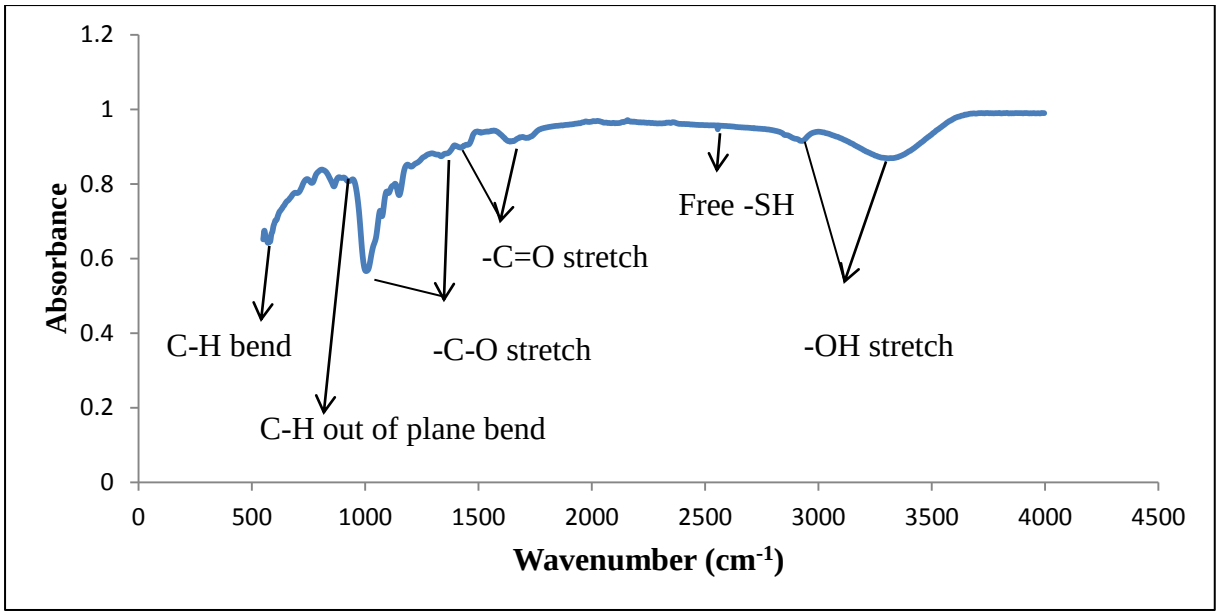

Figure 4.11(c) -Fourier transform infrared spectrum for 1.5M $H2SO_4$ eluted cassava waste biomass.

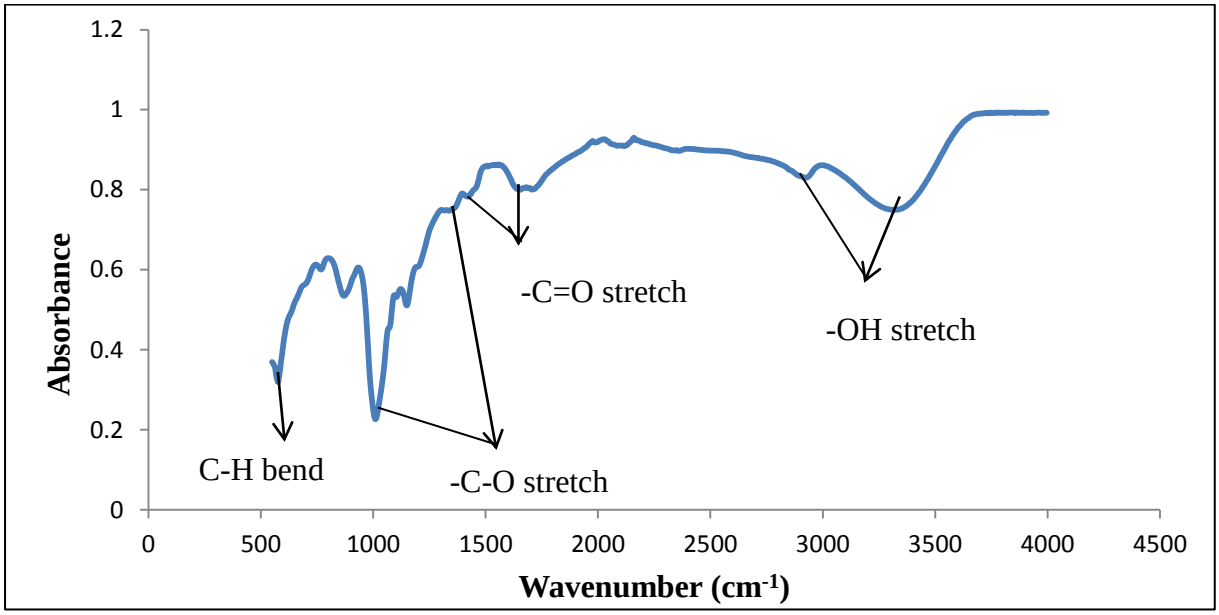

Figure 4.11(d) -Fourier transform infrared spectrum for 2M H_2SO_4eluted cassava waste biomass.

BET analysis of original and differently eluted biomass

The maximum amount of adsorption is proportional to the amount of surface area with pores that are accessible to the adsorbate. A relatively large volume of a pore corresponds to a large surface area and a large adsorption capacity for small molecules. Table 4.4 shows the effect

of eluent concentration on the BET surface area, pore volume and pore size of the cassava waste biomass. When H_2SO_4 was used as an eluent, increasing the solution concentration increased the surface area, pore volume and pore size of cassava waste biomass. The role of the eluent was to remove adsorbed metals on the cassava waste biomass and any other liquids that possibly clog up the pores and inhibit the development of a porous structure in the cassava waste biomass. Therefore, the increased solution concentration enhanced this important function of the H_2SO_4. This results in an increase in the binding sites which are responsible for metal binding. As the concentration of H_2SO_4 increased the number of protons in solution increased which further opened up the pores and increased the surface area of the adsorbent (Muhammad *et al.*, 2006). But it has been shown in Figure 4.11 (d) that at high eluent concentration some functional groups that are responsible for adsorption were destroyed. Therefore, 0.1M H_2SO_4 eluted cassava waste biomass was used for the subsequent adsorption -desorption cycle.

Table 4.4 Structural characteristics of original acid treated cassava waste biomass and after elution with different concentrations of H_2SO_4.

Adsorbent	**Surface area $S_{bet}(m^2/g)$**	**Pore volume $V_t(cm^3/g)$**	**Pore size (nm)**
Original acid treated cassava waste biomass	0.8580	0.00244	7.53810
0.1 H_2SO_4 eluted cassava waste biomass	1.6259	0.00306	11.2624
1.5M H_2SO_4 eluted cassava waste biomass	3.1052	0.01130	13.5127
2M H_2SO_4 eluted cassava waste biomass	3.4590	0.01350	15.6111

Adsorption- desorption cycles

Figure 4.12 and 4.13 show the efficiencies of the adsorption and desorption cycles, respectively. As can be seen from the figures both the adsorption and desorption capacities of cassava almost remained constant for the first six cycles, which indicated that there were no irreversible sites on the surface of the adsorbent. However, at more than six (cycles), both the adsorption and desorption efficiencies decreased. This can be attributed to the deterioration and loss of biomass that resulted in the decreased number of metal-binding sites. It can also

be seen from Figure 4.12 that the adsorption efficiency increased in the order V^{3+}>Cr^{3+}>Co^{2+}. This trend concurs with the previous observations on the effect of pH. However, it is noticed from Figure 4.13 that desorption efficiency is in the reverse order to the adsorption efficiency trends, i.e., Co^{2+}> Cr^{3+}> V^{3+}. The Co^{2+} desorbed faster from the cassava waste biomass due to low affinity for the binding sites on the biomass as compared to Cr^{3+} and V^{3+} which where tightly bound on the cassava biomass.

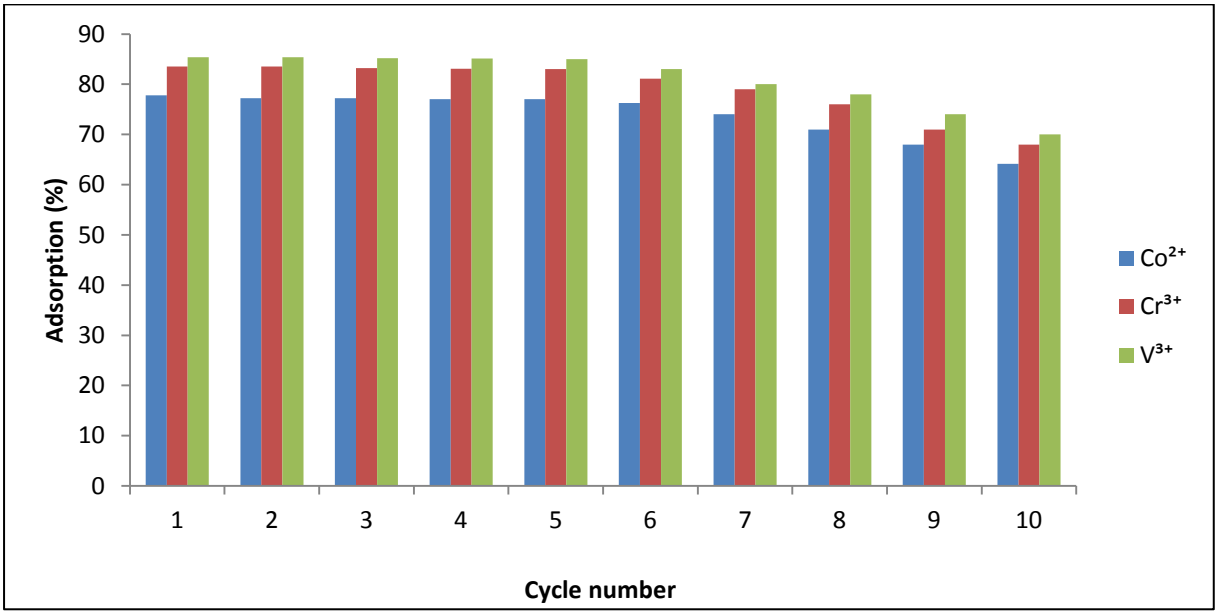

Figure 4.12- Adsorption efficiency of cassava waste biomass for the adsorption-desorption regeneration cycles.

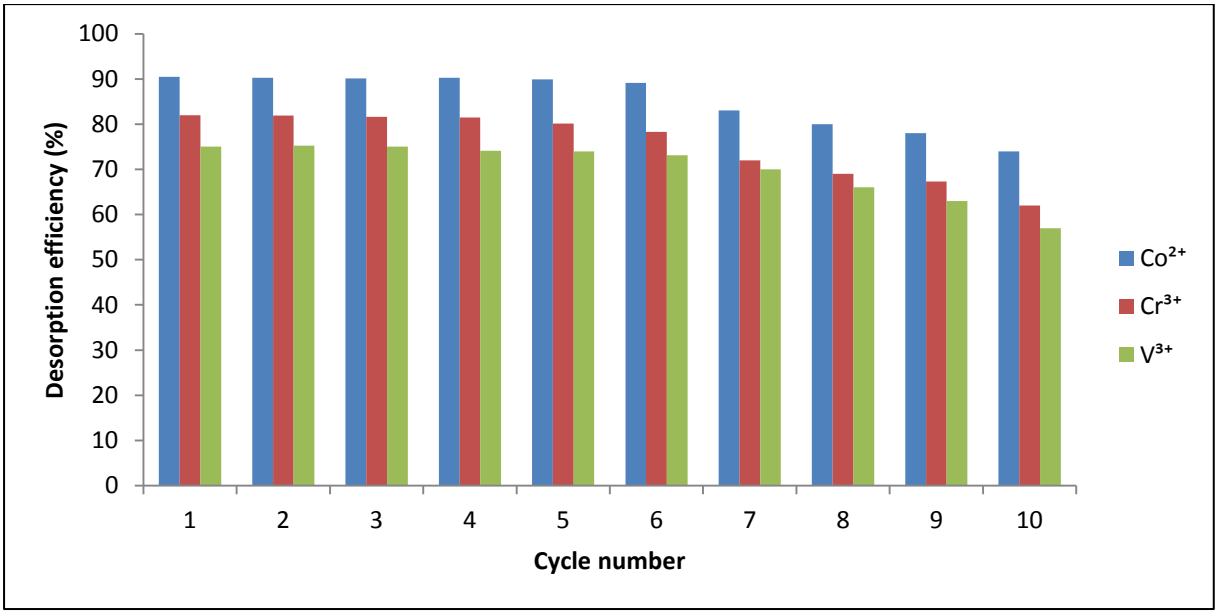

Figure 4.13- Desorption efficiency of cassava waste biomass for the adsorption- desorption cycles using 0.1 mol/L H_2SO_4.

4.3 Summary and Conclusion

The $Co^{2+,}$ Cr^{3+} and V^{3+} ions were effectively removed from aqueous solution using cassava-peel biomass. FTIR analysis of the cassava waste indicated that chemical modification of the biomass resulted in the addition of an –SH group, resulting in an improved metal removal performance of the biomass. Metal uptake was generally found to increase with an increase in pH, agitation speed, biomass and initial metal concentration. The capacity for the sorption of the three metal ions was found to be lower in ternary solution systems as compared to single ion systems suggesting the prevalence of a competitive adsorption effect in mixed solutions.

The presence of the co-cation systems of $Mg^{2+,}$ $Ca^{2+,}$ Na^{+} and K^{+} in aqueous solution decreases the amount of $Co^{2+,}$ Cr^{3+} and V^{3+} adsorbed by cassava-peel biomass. The presence of calcium was observed to have the most negative impact on the adsorption efficiency of the three ion systems studied.

The equilibrium biosorption data could be described by both Freundlich and Langmuir models, but the Freundlich isotherm described the data better. Desorption experiments showed that at low H_2SO_4 concentration it is possible to remove the metal ions bound to the biomass and to regenerate the biosorbent allowing for its successive re-use. The cassava-peel biomass retained its original metal removal capacity for up to six adsorption-desorption cycles. This is a good indication of cassava-peels' potential as biosorbent materials since they can be reused several times while maintaining high overall process efficiency. However, in order to re-use the cassava-peel biomass several times, it is paramount to improve the texture characteristics of the adsorbent material.

CHAPTER FIVE

5 CONTINUOUS ADSORPTION SYSTEMS

5.1 Introduction

Previous adsorption experiments conducted using batch systems showed the ability of acid-treated cassava waste to adsorb Co^{2+}, Cr^{3+} and V^{3+} metal ions. The biosorption capacity of the cassava waste and many other biosorbents obtained from batch equilibrium experiments is useful in providing fundamental information about the effectiveness of metal-biosorbent system (Bharathi and Ramesh, 2013). However, data obtained from batch systems may not be applied directly to most treatment systems (such as column operations) where contact time is not sufficient for the attainment of the equilibrium (Zulfadhly *et al*., 2001; Vinodhini and Das, 2010; Vimala *et al*., 2011; Bharathi and Ramesh, 2013). Furthermore, batch systems are usually limited to the treatment of small quantities of wastewater (Bharathi and Ramesh, 2013). For practical and large scale operations, a continuous system such as a packed column or a semi continuous counter- current system is preferred to batch systems (Mulkoc and Nuhoglu, 2003;Vinodhini and Das, 2010; Vimala *et al*., 2011).

In a semi continuous process, both the adsorbent and liquid solution are continuously fed into the system in a counter current fashion where contact between the two phases occurs (Berk, 2013). Counter current contact maximizes the driving force for mass transfer and, therefore, provides in principle more efficient utilization of the biosorbent capacity than is possible in a simple batch contacting system. However, for counter current contact to be more effective it is necessary to circulate the adsorbent (Ruthven and Douglas, 1984).

Most of the time, biomass cannot be used directly for continuous applications because it is either too soft to withstand pressure in the reactor or has too small a particle size which makes its separation from the treated effluent a difficult task. Thus, the direct use of native biomass is not desirable as it can clog the column. The immobilization of the biosorbent within a suitable matrix can overcome these problems by offering ideal size, mechanical strength, rigidity and porous characteristics to the agricultural material (Malik, 2004). Hence, a packed column with immobilized cassava waste biomass was used in this study.

Packed bed columns make the best use of the concentration difference and allow for more efficient utilization of biosorbent capacity and results in better quality effluent (da Silva *et al*., 2002; Vinodhini and Das, 2010; Vimala *et al*., 2011). In such systems, the concentration

profiles in the liquid and adsorbent phases vary in both space and time (Chu, 2004; Mulkoc and Nuhoglu, 2006). This makes the design and optimization of packed bed difficult to perform without a quantitative modeling approach (Chu, 2004; Mulkoc and Nuhoglu, 2006). Models have an important role in technology transfer from laboratory-scale to industrial-scale (da Silva *et al*., 2002). Appropriate models can also help to analyse and explain experimental data, identify process mechanisms, predict answers to operational conditions changes and optimize processes (Cossich, 2000; da Silva *et al*., 2002).

The purpose of this chapter of the study was to investigate the influence of bed depth and flow rate on the performance of Co^{2+}, Cr^{3+} and V^{3+} adsorption on to immobilized acid treated cassava waste biomass in a fixed bed column. From the perspectives of process modelling, the dynamic behaviour of a packed column is described in terms of breakthrough curve (Chu, 2004; Mulkoc and Nuhoglu, 2006; Vinodhini and Das, 2010). The breakthrough curves for the adsorption of Co^{2+}, Cr^{3+} and V^{3+} were analysed using the Thomas and Bed Depth Service Time (BDST) models.

5.2 Results and Discussion

5.2.1 Surface chemistry structure of immobilized cassava waste biomass

The pattern of sorption of metals onto plant materials is attributable to the active groups and bonds present on them (Krishnani *et al*., 2008). FTIR spectroscopy was, therefore, done for preliminary quantitative analysis of major functional groups present in native immobilized cassava waste biomass used as sorbent of Co^{2+}, Cr^{3+} and V^{3+} in the present studies (Figure 5.1). After the cassava waste biomass was immobilized on sodium alginate, the surface structure did not change as can be seen from Figure 4.1(c) and 5.1(a). The FTIR spectra of cassava waste biomass had not changed after entrapment in sodium alginate beads, therefore, it can be concluded that no chemical reaction had taken place between the cassava waste biomass and sodium alginate beads. The FTIR spectra of metal (Co^{2+}, Cr^{3+} and V^{3+}) loaded immobilized cassava waste biomass were also obtained to determine correspondence of respective metal biosorption at the stretching and bending of active groups present in native immobilized cassava waste biomass (Fig. 5.1 (b)). The FTIR spectra of Co^{2+}, Cr^{3+} and V^{3+} sorbed immobilized cassava waste biomass showed that the peak expected at 3363, 2974, 2563, 1653 and 1443 cm^{-1} had shifted to 3394, 2981, 2630, 1637 and 1438 cm^{-1} due to Co^{2+}, Cr^{3+} and V^{3+} sorption (Fig. 5.1 (a) and (b)). This shift may be attributed to the changes in counter ions associated with carboxylate, hydroxylate and -SH anions suggesting that acidic

groups such as carboxyl, hydroxyl and sulfhydryl are responsible for metal ion uptake. In other words, the changes observed in the spectrum indicate the possible involvement of the stated functional groups found on the surface of the biomass in biosorption process.

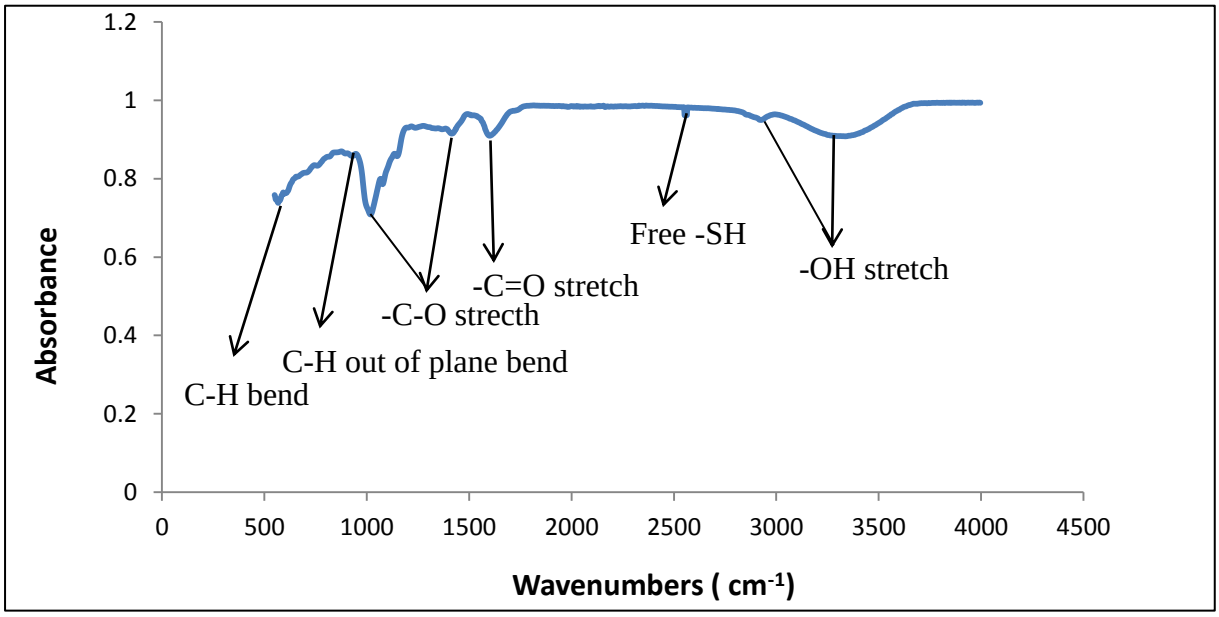

Figure 5.1(a) - Fourier transform infrared spectrum for immobilized cassava waste biomass before loading with Co^{2+}, Cr^{3+} and V^{3+}.

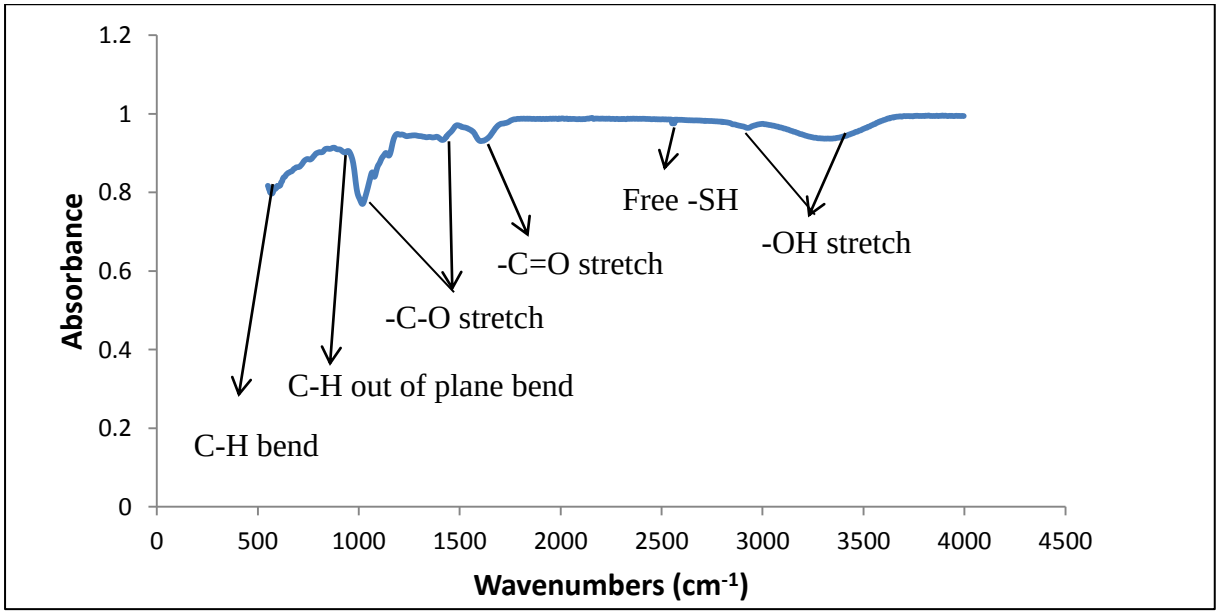

Figure 5.1(b) - Fourier transform infrared spectrum for metal loaded immobilized cassava waste biomass after loading with Co^{2+}, Cr^{3+} and V^{3+}.

5.2.2 BET analysis of immobilized acid treated biomass

The surface area, pore volume and size of the original acid treated, metal loaded and 0.1M eluted immobilized cassava were measured using BET analyser with nitrogen as the adsorbate are represented in Table 5.1.

The results indicated that the surface area of the eluted biomass had a greater surface area as compared to the original acid treated cassava biomass. This is because the sulfuric acid which is used as eluent provides protons upon ionization in aqueous solution which in turn can further open the pores of cassava which increases the surface area of the adsorbent (Muhammad *et al*., 2006). The surface area, pore volume and pore size of 0.1M eluted and original acid treated immobilized cassava biomass did not change after immobilization of cassava with sodium alginate as can be seen from Table 4.4 and 5.1. This might be because there was no chemical reaction between the cassava and the sodium alginate bead. This was also observed in FTIR analysis and the increase in surface area after elution with 0.1M H_2SO_4 is expected to increase the adsorption of Co^{2+}, Cr^{3+} and V^{3+} in subsequent adsorption cycle. After adsorption of metals on the immobilized cassava biomass the BET surface area decreased. The low surface area indicates that the pores of the immobilized cassava are probably blocked by metals.

Table 5.1 Structural characteristics of original acid treated, 0.1M eluted and metal loaded immobilized cassava waste biomass.

	Surface area S_{bet} (m^2/g)	**Pore volume V_t (cm^3/g)**	**Pore size (nm)**
Original acid treated immobilized cassava	0.912	0.00314	476
0.1M H_2SO_4 eluted immobilized cassava	1.683	0.00410	583
Metal loaded immobilized cassava	0.235	0.00490	1418

5.2.3 Semi continuous counter current system

Table 5.2 and 5.3 shows the adsorption of Co^{2+} in single and ternary systems, respectively. The removal of Co^{2+} needed 8 stages to meet the targeted limit of 0.05 mg/L in the effluent discharge. The effluent solution obtained after the 8th stage contained 0.04 and 0.05 mg/L for

single and ternary system, respectively. As can be seen from Tables 5.4 and 5.5, the adsorption of Cr^{3+} needed 6 stages to obtain the targeted limit of 0.05 mg/L. For single and ternary systems, 0.039 and 0.045 mg/L were obtained, respectively. For V^{3+}, the effluent solution at the end of the 4th stage contained 0.005 and 0.018 mg/L for single and ternary systems, respectively (see Table 5.6 and 5.7), with a target limit of 0.1 mg/L. The targeted limits are set by the EPA (2009) for toxic metals in drinking and waste water. The adsorption capacity was slightly lower for ternary metal ion systems as compared to single metal ion systems. This may be attributed to the greater competitive effects of the metal ions for the occupancy of the binding surfaces on the cassava waste. In this case, the number is competitively divided between the different metal ions present in the synthetic wastewater. In terms of affinity for biomass V^{3+} appeared to be easily removable in waste water and only 4 reactors where needed to reach accepted limits by the EPA. The adsorption efficiency obtained from the semi counter current system is higher than that obtained in batch system. It means that there where limited number of active binding sites on the adsorbent for metal adsorption.

In the final reactor, the fresh cassava is put in contact with low grade solution from reactor (n-1). In this reactor the fresh cassava has more active binding sites and can effectively remove trace amounts of Co^{2+}, Cr^{3+} and V^{3+} in solution to 0.04, 0.04 and 0.01 mg/L, respectively, in single metal ion solution.

As cassava waste biomass moves up the train from last reactor to reactor 1 it collects increasing amount of Co^{2+}, Cr^{3+} and $V^{3+}$from solution. As it comes in contact with higher metal ion concentration solutions, it finally reaches its maximum loading in the 1st reactor with the loading at around 20.00 mg/g for Co^{2+}, Cr^{3+} and V^{3+}. The final loaded cassava waste biomass is then removed and eluted with 0.1 M H_2SO_4. Cassava waste biomass adsorbed the metal ions in the following order: $V^{3+}>Cr^{3+}>Co^{2+}$.

Table 5.2– The adsorption of cobalt onto acid treated cassava waste biomass using semi continuous counter current in single system with initial metal ion concentration of 100 mg/L.

No. of stages	**Final concentration (mg/L)**	**Metal uptake (related to effluent movement) (mg/g)**	**Metal uptake (related to cassava movement) (mg/g)**	**% removal per stage**
Tank 1 exit	43.02	11.40	19.89	56.97
Tank 2 exit	30.58	2.49	19.21	28.93
Tank 3 exit	25.42	1.03	18.32	16.89
Tank 4 exit	19.91	1.10	17.30	21.66
Tank 5 exit	10.99	1.78	15.92	34.71
Tank 6 exit	7.89	0.62	14.78	39.31
Tank 7 exit	3.46	0.89	13.78	56.17
Tank 8 exit	0.04	0.68	11.40	98.84

Table 5.3–The adsorption of cobalt onto acid treated cassava waste biomass using semi-continuous counter current in ternary system with initial metal ion concentration of 100 mg/L.

No. of stages	Final concentration (mg/L)	Metal uptake (related to effluent movement) (mg/g)	Metal uptake (related to cassava movement) (mg/g)	% removal per stage
Tank 1 exit	45.32	10.94	20.04	54.68
Tank 2 exit	35.13	2.04	19.26	22.50
Tank 3 exit	26.15	1.80	18.37	20.52
Tank 4 exit	20.78	1.07	17.20	32.3
Tank 5 exit	11.67	1.82	15.84	41.74
Tank 6 exit	8.17	0.70	14.77	54.74
Tank 7 exit	3.69	0.90	12.96	54.77
Tank 8 exit	0.05	0.73	10.94	98.64

Table 5.4 - The adsorption of chromium onto acid treated cassava waste biomass using semi-continuous counter current in single system with initial metal ion concentration of 100 mg/L.

No. of stages	Final concentration (mg/L)	Metal uptake (related to effluent movement) (mg/g)	Metal uptake (related to cassava movement) (mg/g)	% removal per stage
Tank 1 exit	38.15	12.37	19.99	61.86
Tank 2 exit	28.01	2.03	18.98	26.54
Tank 3 exit	20.01	1.60	17.62	28.52
Tank 4 exit	10.18	1.97	16.00	40.58
Tank 5 exit	5.13	1.01	14.40	56.89
Tank 6 exit	0.04	1.02	12.37	99.24

Table 5.5 - The adsorption of chromium onto acid treated cassava waste biomass using semi-continuous counter current in ternary system with initial metal ion concentration of 100 mg/L.

No. of stages	Final concentration (mg/L)	Metal uptake (related to effluent movement) (mg/g)	Metal uptake (related to cassava movement) (mg/g)	% removal per stage
Tank 1 exit	40.16	11.97	20.28	59.84
Tank 2 exit	32.50	1.53	19.08	19.81
Tank 3 exit	21.74	2.15	17.65	33.10
Tank 4 exit	13.26	1.70	15.95	39.02
Tank 5 exit	6.13	1.43	13.80	53.78
Tank 6 exit	0.05	1.22	11.97	99.35

Table 5.6- The adsorption of vanadium onto acid treated cassava waste biomass using semi-continuous counter current in single system with initial metal ion concentration of 100 mg/L.

No. of stages	Final concentration (mg/L)	Metal uptake (related to effluent movement) (mg/g)	Metal uptake (related to cassava movement) (mg/g)	% removal per stage
Tank 1 exit	34.71	13.06	20.00	65.29
Tank 2 exit	18.13	3.32	18.98	47.78
Tank 3 exit	5.13	2.60	16.38	71.75
Tank 4 exit	0.01	1.02	13.06	99.90

Table 5.7 - The adsorption of vanadium onto acid treated cassava waste biomass using semi-continuous counter current in ternary system.

No. of stages	Final concentration (mg/L)	Metal uptake (related to effluent movement) (mg/g)	Metal uptake (related to cassava movement) (mg/g)	% removal per stage
Tank 1 exit	38.85	12.23	20.00	61.15
Tank 2 exit	21.61	3.448	18.60	44.30
Tank 3 exit	6.99	2.924	15.67	67.71
Tank 4 exit	0.02	1.394	12.23	99.74

5.2.4 Adsorption-desorption cycle

To recover Co^{2+}, Cr^{3+} and V^{3+} or reuse the biosorbent, desorption processes should be considered. The loaded cassava waste was removed from the first reactor and washed with distilled water before undergoing elution or desorption of Co^{2+}, Cr^{3+} and V^{3+} using 0.1M H_2SO_4. Figure 5.2 and 5.3 shows the efficiencies of the adsorption and desorption for six cycles, respectively. The adsorption capacity and desorption efficiency remained constant for the first three cycles and then decreased afterwards.

According to Figure 5.3 it is evident that cobalt is easily desorbed from the cassava waste biomass, this was expected since cassava waste biomass has a lower affinity for cobalt as shown in the adsorption results in Figure 5.2 below; hence it is easily displaced from the cassava waste biomass. Cassava waste biomass showed greater affinity for vanadium and chromium and hence their lower desorption efficiencies. The desorption efficiency is a reversal of the adsorption efficiency, i.e., $Co^{2+}>Cr^{3+}>V^{3+}$.

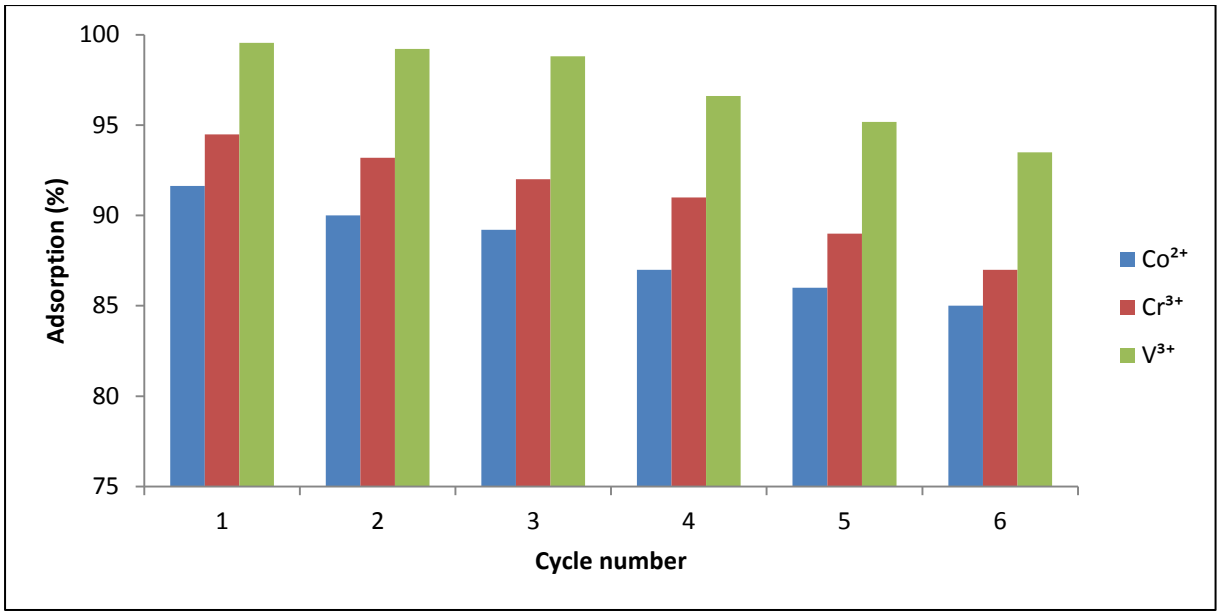

Figure 5.2- Adsorption efficiency of cassava waste biomass for the adsorption-desorption cycles (Semi continuous system).

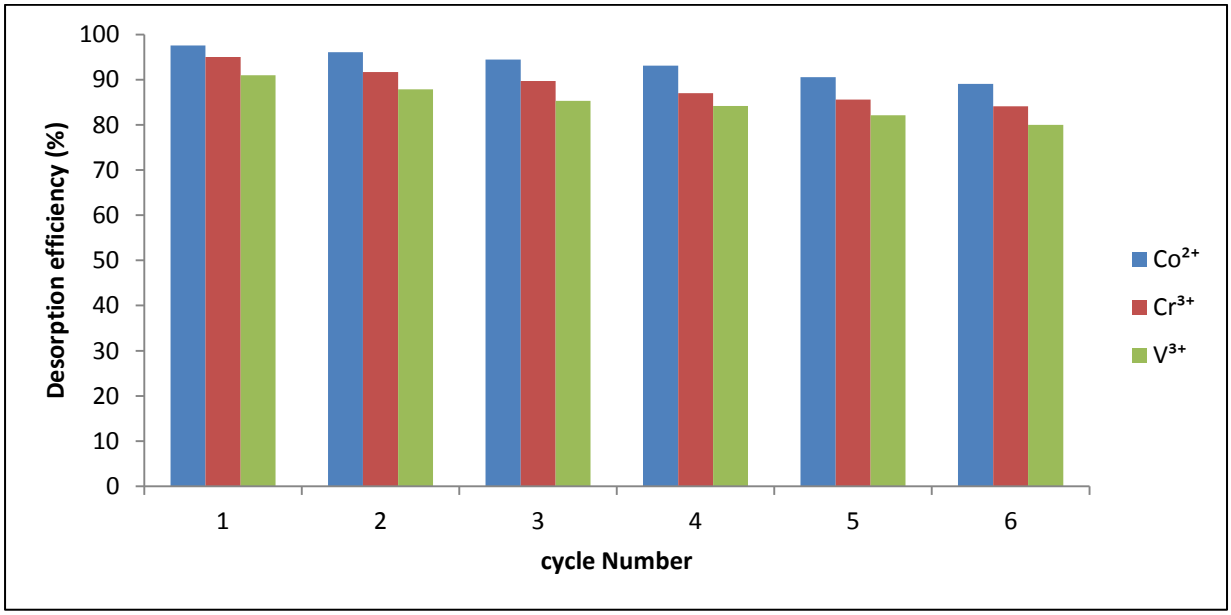

Figure 5.3- Desorption efficiency of cassava waste biomass for the adsorption- desorption cycles using 0.1 mol/L H_2SO_4 (Semi continuous system).

5.2.5 Packed bed column

Effect of flow rate

Flow rate is the most important parameter in evaluating the performance of a biosorption process particularly for continuous treatment of waste water at the industrial scale (Saha *et al.*, 2011). The sorption of Co^{2+}, Cr^{3+} and V^{3+} metal ions from a synthetic solution by

immobilized cassava in a packed bed column were studied by varying the solution flow rate of from 0.83 to 1.61 mL/s, while the bed depth (10 cm) and initial metal ion concentration of 100 mg/L were held constant. The breakthrough curve for the column was determined by plots of dimensionless concentration (C_e/C_0 (where C_e and C_0 are the metal ions concentration of the effluent and influent, respectively)) against time (*t*) at different flow rates, as shown in Figure 5.4 (a) to (c). All the measured breakthrough curves showed an S-shape with two inflexion points. The first location in the lower part of the curve corresponds to the breakpoint or the breakthrough time. This indicates that the packed bed column is becoming saturated. The second inflection point or the exhaustion point located in the upper part of the curves indicates that the bed is completely saturated.

Nonsteady-state conditions prevail in that the immobilized cassava continues to remove increasing amounts of impurities from solution over the entire period of useful operation. The impurity is adsorbed most rapidly and effectively by the first few layers of fresh cassava during the initial stages of operation. These first layers are in contact with the solution at its highest concentration level. The small amounts of solute which escape adsorption in the first few layers of adsorbent are then removed from solution in subsequent strata, and essentially no solute escapes from the adsorber initially ($C_e = 0$) (Walter and Weber, 1974). The primary adsorption zone is concentrated near the influent end of the column. As the polluted feed water continues to flow into the column, the first few layers of cassava become practically saturated with solute and less effective for further adsorption. Thus, the primary adsorption zone moves through the column to regions of fresher adsorbent. The wavelike movement of this zone, accompanied by a movement of the C_0 concentration front, occurs at a rate much slower than the linear velocity of the water or wastewater. As the primary adsorption zone moves through the column, more and more solute tends to escape in the effluent, as indicated in Figure 5.4 and 5.5. The plot of C_e/C_o versus time (for a constant flow rate) or volume of water treated depicts the increase in the ratio of effluent to influent concentrations as the zone moves through the column. The breakpoint on this curve represents that point in operation where for all practical purposes the column is in equilibrium with the influent water, and beyond which little additional removal of solute will occur. At this point it is desirable to reactivate or replace the cassava.

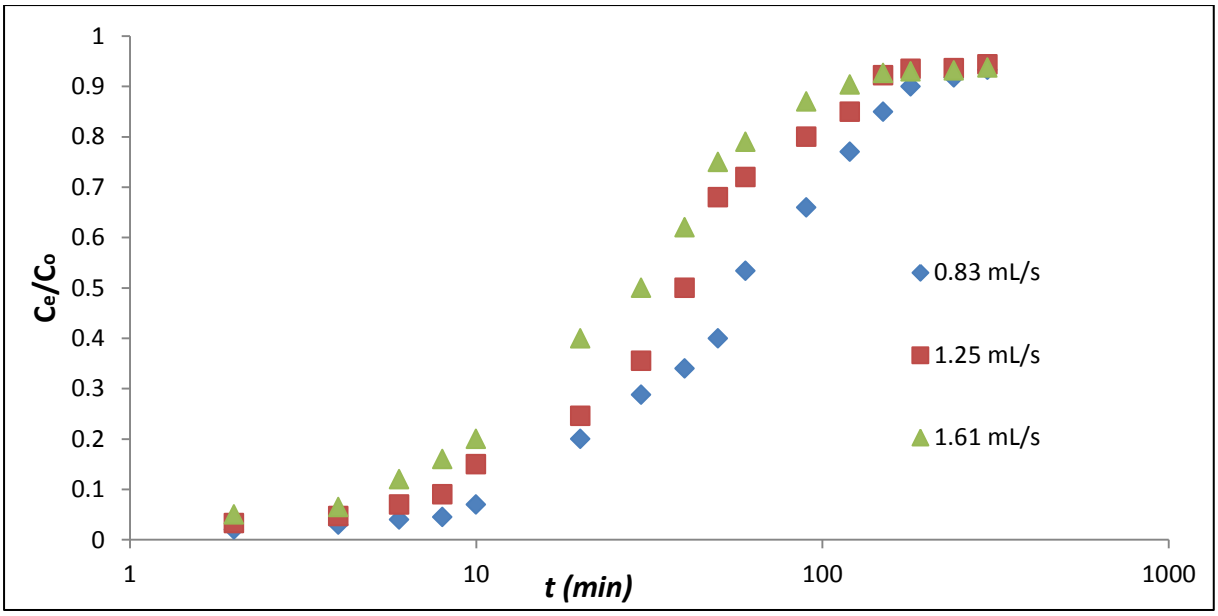

Figure 5.4(a) - Breakthrough curves of Co^{2+} sorption by immobilized cassava waste biomass at different flow rates ([Co] = 100 mg/L, pH = 4 and bed depth = 10 cm).

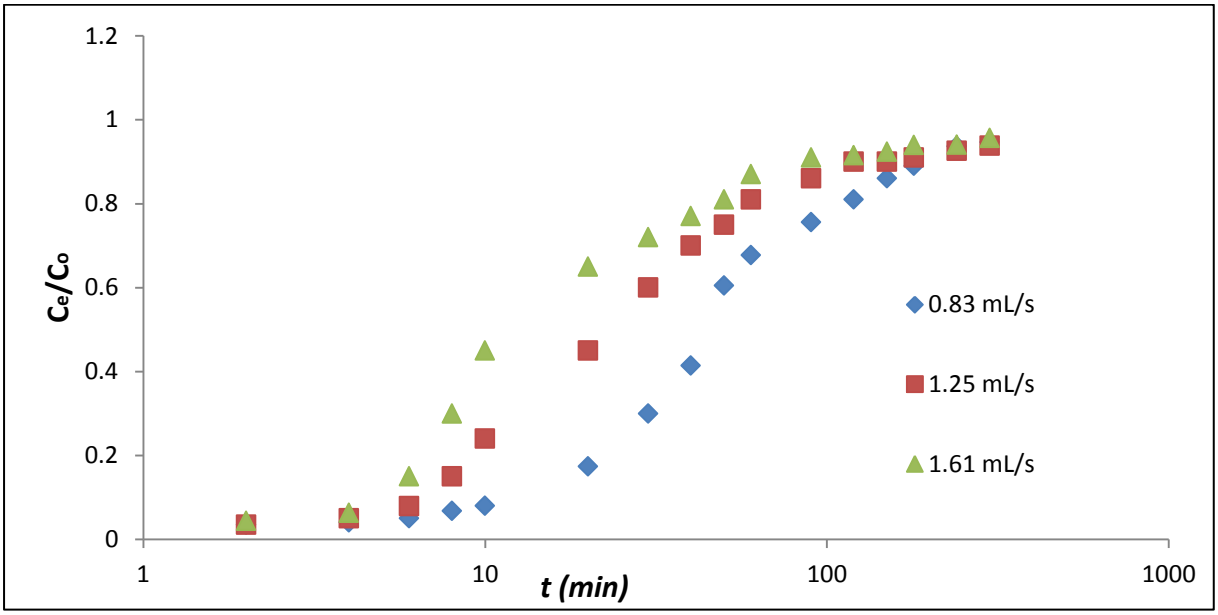

Figure 5.4(b) - Breakthrough curves of Cr^{3+} sorption by immobilized cassava waste biomass at different flow rates ([Cr] = 100 mg/L, pH = 4 and bed depth = 10 cm).

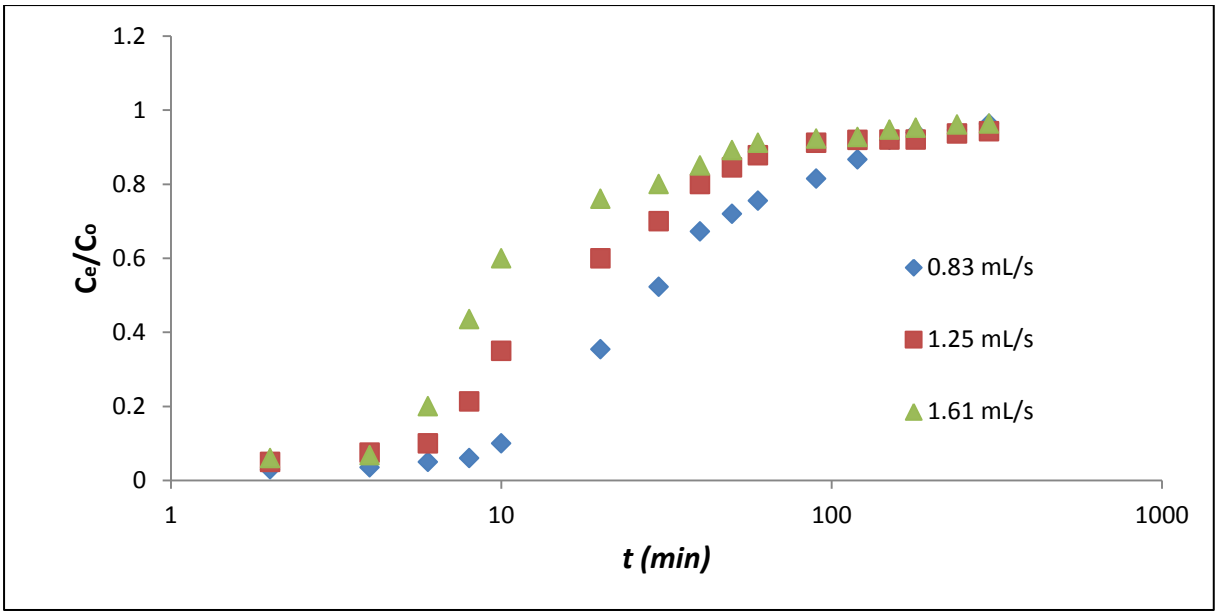

Figure 5.4(c) - Breakthrough curves of V^{3+} sorption by immobilized cassava waste biomass at different flow rates ([V] = 100 mg/L, pH = 4 and bed depth = 10 cm).

As can be seen from the results shown in Figure 5.4 (a) to (c) the removal efficiency is favoured by a lower flow rate of 0.83 mL/s, an increase in flow rate reduced both the breakthrough and exhaustion times resulting in steeper breakthrough curves and shorter zones of mass transfer. The relatively reduced breakthrough and exhaustion time at higher flow rates resulted in comparatively less metal uptake and percent removal. In other words, the adsorption efficiency was lower at higher flow rate. The reduction in metal uptake is attributed to insufficient residence time of the metal ions in the column (Zulfadhly *et al*., 2001; Aksu *et al*., 2002; Vimala *et al*., 2011) and the diffusion limitations of the solute into the pores of the sorbent at higher flow rates (Ko *et al*., 2000; Vijayaraghavan *et al*., 2005). If the residence time of the solute in the column is not large enough for adsorption equilibrium to be reached at the given flow rate, the metal solution leaves the column before the equilibrium occurs. These results are in agreement with that obtained by (Manose, 2012; Ayoob *et al*., 2009; Nwabanne and Igbokwe, 2012).

According to Table 5.8, as the flow rate increased from 0.83 to 1.61 mL/s, there was a decrease in column breakthrough time from 10 to 6 min, 10 to 4 min and 10 to 4 min for Co^{2+}, Cr^{3+} and V^{3+}, respectively. Co^{2+} had a longer residence time as compared to Cr^{3+} and V^{3+}; this is because cobalt has a lower affinity towards the active sites of the biomass. According to this study, flow rates higher than 0.83 mL/s should be avoided since the breakthrough time would decrease. Flow rate lower than 0.83 mL/s is expected to be

beneficial on the removal efficiency. Due to longer residence time at lower flow rates, the metal ions in solution have more time to interact with the available adsorption sites in immobilized cassava waste biomass resulting in better removal efficiencies. This further means a larger amount of solution can be treated before the need to replace the cassava waste becomes imminent and thus impacting on the process cost. Table 5.8 also shows that at higher flow rate the uptake of metal ions onto the biomass decreases. This is due to insufficient retention time for solute to interact with the sorbent and the limited diffusivity of solute into the sorptive sites. This led to premature breakthrough and hence, a reduction in the efficiency and effectiveness of the packed bed column. This again means the operating costs will be higher as the cassava will need to be changed more frequently.

Table 5.8 Parameters for breakthrough curves for the adsorption of Co^{2+}, Cr^{3+} and $V^{3+}$by immobilized cassava waste biomass at different flow rates.

Metals	**Flow rate (mL/s)**	**Breakthrough time (t)**	**Adsorption capacity (mg/g)**	**Breakthrough concentration (mg/L)**
Co^{2+}	0.83	10	45.291	0.12
	1.25	8	35.400	0.09
	1.61	6	23.231	0.07
Cr^{3+}	0.83	10	46.208	0.06
	1.25	6	35.168	0.08
	1.61	4	23.575	0.07
V^{3+}	0.83	10	46.537	0.10
	1.25	6	35.366	0.10
	1.61	4	23.981	0.10

Effect of bed depth

The retention of metals in a fixed-bed column depends on amongst other factors, the quantity of solid sorbent used and on the bed depth of the column (Taty-Costode *et al*., 2005; Nasehir *et al*., 2011; Sankararamakrishnan *et al*., 2008).

The breakthrough curves (C_e/C_o versus time) in Figure 5.5 (a) to (c) were obtained for Co^{2+}, Cr^{3+} and V^{3+} sorption onto immobilized cassava waste biomass at different bed depth (5, 10 and 15 cm), constant influent flow rate (0.83 mL/s) and 100 mg/L metal ion concentration. The Figures show that breakthrough time increase with increasing bed depth from 5 to 15 cm. The increase in metal uptake with increase in bed depth was due to increase in the surface area and adsorption sites owing to the increase in the amount of adsorbent in a larger bed. This further provides a longer contact time and a broadened mass transfer zone. Similar trends have been reported by Taty-Costodes *et al.* (2005); Chowdhurry *et al.* (2012) and Ayoob *et al*. (2009)

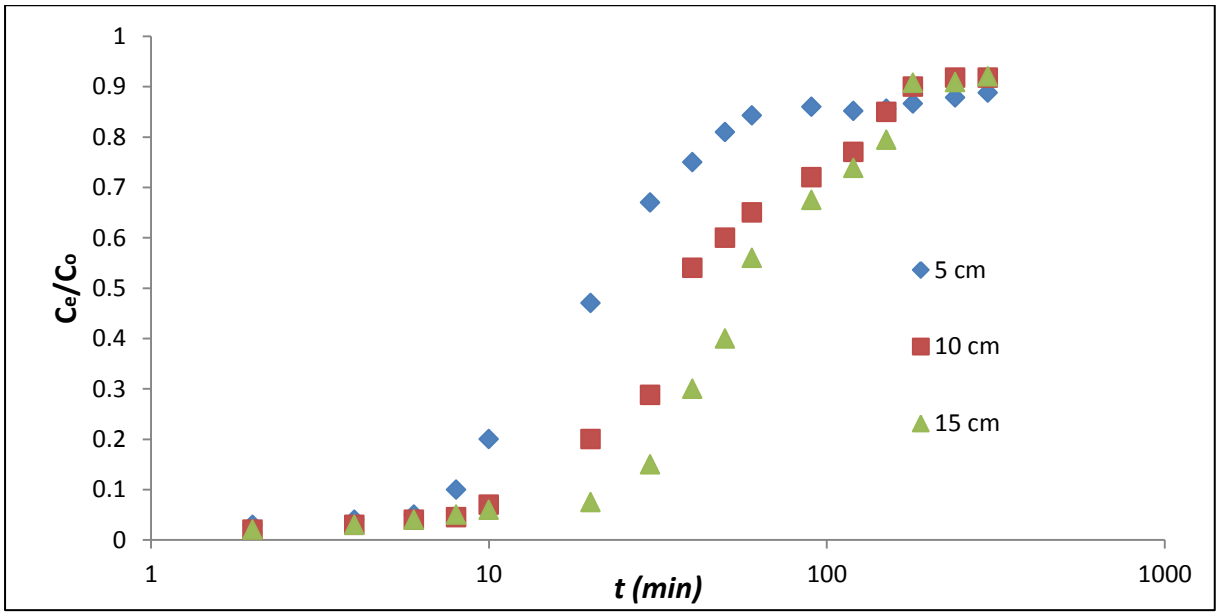

Figure 5.5(a) – Breakthrough curves of Co^{2+} sorption by immobilized cassava waste biomass at different bed depth ([Co] = 100 mg/L, pH = 4 and flow rate = 0.83 mL/s).

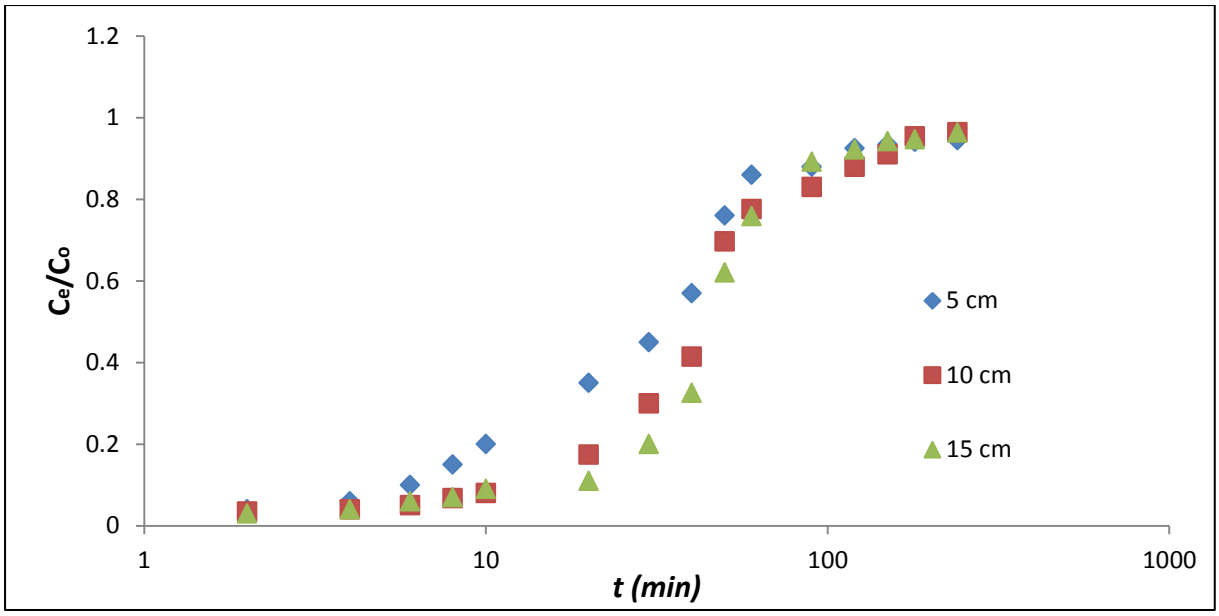

Figure 5.5(b) – Breakthrough curves of Cr^{3+} sorption by immobilized cassava waste biomass at different bed depth ([Cr] = 100 mg/L, pH =4 and flow rate=0.83 mL/s).

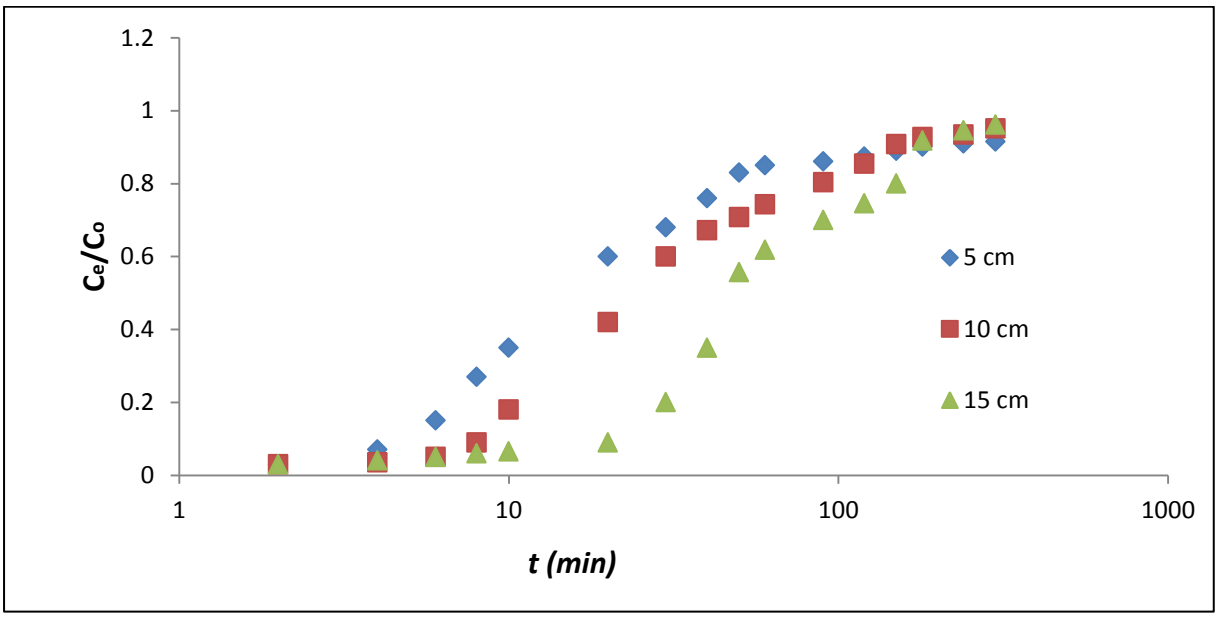

Figure 5.5(c) – Breakthrough curves of V^{3+} sorption by immobilized cassava waste biomass at different bed depth ([V] = 100 mg/L, pH = 4 and flow rate = 0.83 mL/s).

From Table 5.9 it can be observed that the breakthrough time varied greatly with the bed depth. The breakthrough time increased from 8 to 20; 6 to 20 and 4 to 20 for Co^{2+}, Cr^{3+} and V^{3+}, respectively, with increasing bed depth from 5 to 15 cm. There was longer breakthrough time for Co^{2+} at 5 and 10 cm bed depth; this is attributed to the competitive adsorption

towards the active sites between metal ions. For higher bed depth, the increase in the adsorbent mass resulted in an increase in the number of sorption sites thus expected to increase sorption capacity of the system. In this study as the bed depth increased, the metal uptake decreased. This is attributed to decrease of the specific metal concentration shortage in the solution (Gadd *et al*., 1988).

Table 5.9 Parameters for breakthrough curves for the adsorption of Co^{2+}, Cr^{3+} and $V^{3+}$by immobilized cassava waste biomass at different bed depth.

Metals	**Bed depth (cm)**	**Breakthrough time (t)**	**Adsorption capacity (mg/g)**	**Breakthrough concentration (mg/L)**
Co^{2+}	5	8	53.07	0.10
	10	10	27.43	0.06
	15	20	18.34	0.09
Cr^{3+}	5	6	56.48	0.06
	10	10	28.89	0.09
	15	20	19.30	0.11
V^{3+}	5	4	57.06	0.04
	10	8	29.22	0.09
	15	20	19.52	0.09

5.2.6 Application of breakthrough models

Understanding the behavior of concentration–time profile or breakthrough curves is essential for the successful design and operation of any fixed bed adsorption process. However, the breakthrough behavior of packed-bed adsorbents may change under various operational conditions. Hence, a number of pilot-scale experiments are required to evaluate the column performance under various operating conditions to obtain the design parameters. However, this may not always be feasible due to limited time and economic considerations. Nevertheless, mathematical models can be used as an alternative tool for design and analysis of full-scale systems by reducing the number of pilot-scale studies (Maliyekkal and Ligy, 2011). In this study Hutchins bed depth service time (BDST) (Hutchins, 1973) and Thomas

model (Thomas, 1944) are evaluated in terms of their applicability to predict Co^{2+}, Cr^{3+} and V^{3+} by immobilized cassava waste biomass. In all model fittings, linear regression analyses were used to predict the breakthrough behavior and the associated characteristic parameters (Ayoob *et al*., 2007).

Bed depth service time model

The Bed Depth Service Time (BDST) model is a simple model for predicting the relationship between bed depth, and service time, *t*, in terms of process concentration and adsorption parameters (Han *et al*., 2009). This model is used only for the description of the initial part of the breakthrough curve, i.e., up to the breakpoint or 10-50% of the saturation points (Chen *et al*., 2006). The bed depth (Z) and service time (t) holds a linear relationship which is given by BDST model which is expressed as follows:

$$t = \frac{N_0 Z}{C_0 v} - \left(\frac{1}{k_a C_0}\right) \ln\left(\frac{C_o}{C_b} - 1\right) \qquad 5.1$$

where C_b is the breakthrough metal ion concentration (mg/L), C_0 is the initial metal ion concentration, N_0 is the adsorption capacity of the bed (mg/L), Z is the depth of the column bed (cm), *v* is the linear flow velocity of the metal solution through the bed (mL/cm^2s)and k_a is the rate constant (L/mgs).

The BDST model is focused on the estimation of characteristics parameters such as the maximum adsorption capacity and kinetics constant (Suksabye *et al*., 2008) and is based on the assumption that the rate of adsorption is controlled by the surface reaction between the adsorbate and unused capacity of the adsorbent (Goel *et al*., 2005).

The service time was selected as the time when the normalized concentration, C_e/C_0 reached 0.05. A plot of service time versus bed depth at the flow rate of 0.83 mL/s was linear are presented in Figure 5.6(a) to (c). The high correlation coefficient values (R^2 = 0.871, R^2 = 0.9423 and R^2 = 0.9231 for Co^{2+}, Cr^{3+} and V^{3+}, respectively) indicated the validity of the BDST model. The values of N_0 and k_a were calculated from the slope (N/C_0v) and intercept ($(1/k_aC_0)$ *ln* $[(C_0/C_b)-1]$) of the BDST plot, respectively. The values of BDST model parameters are presented in Table 5.10. The value of k_a characterizes the rate of transfer from the liquid phase to the solid phase. For smaller values of k_a, a relatively longer bed is required to avoid breakthrough, whereas the breakthrough can be eliminated even in a smaller bed when the value of k_a is high (Cooney, 1999). The BDST model constants can be helpful to scale up the process for other flow rates without further experimentation.

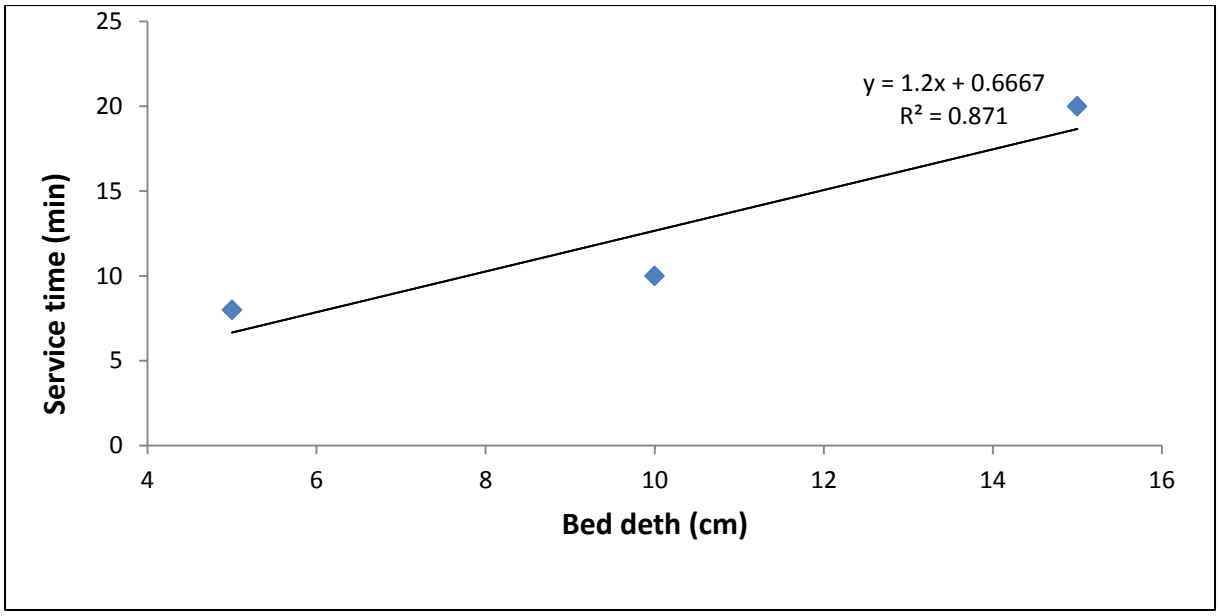

Figure 5.6(a) - Plot of BDST equation for Co^{2+} adsorption on immobilized cassava waste biomass (flow rate = 0.83 mL/s, initial cobalt concentration = 100 mg/L, pH = 4).

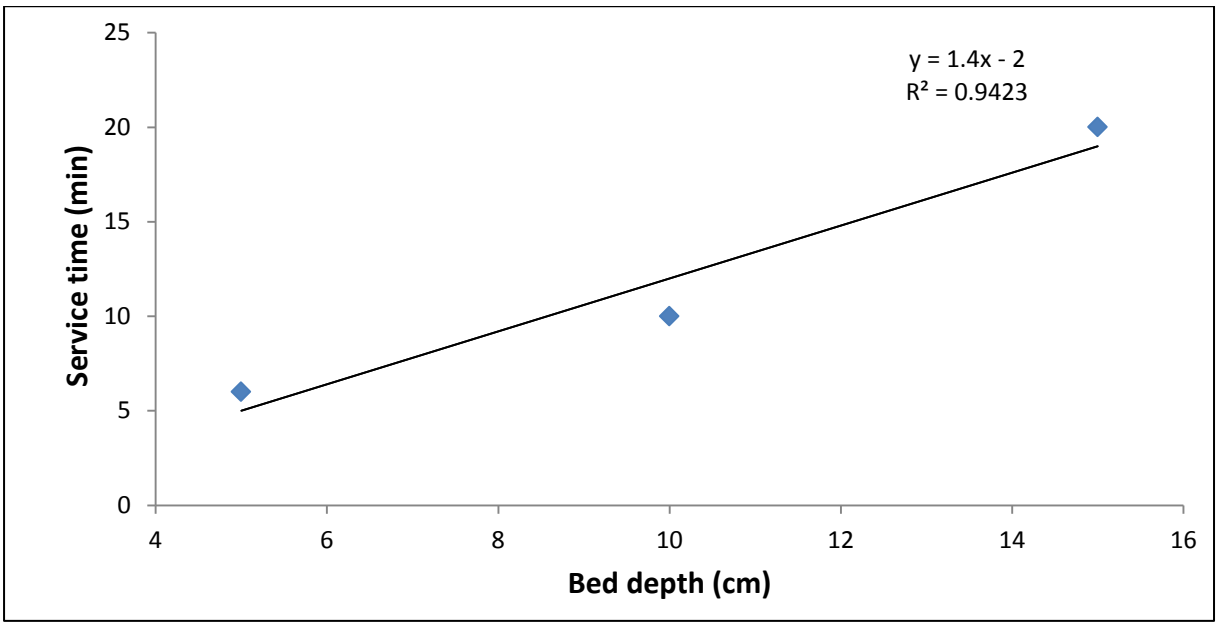

Figure 5.6(b) - Plot of BDST equation for Cr^{3+}.adsorption on immobilized cassava waste biomass (flow rate = 0.83 mL/s, initial chromium concentration = 100 mg/L, pH = 4).

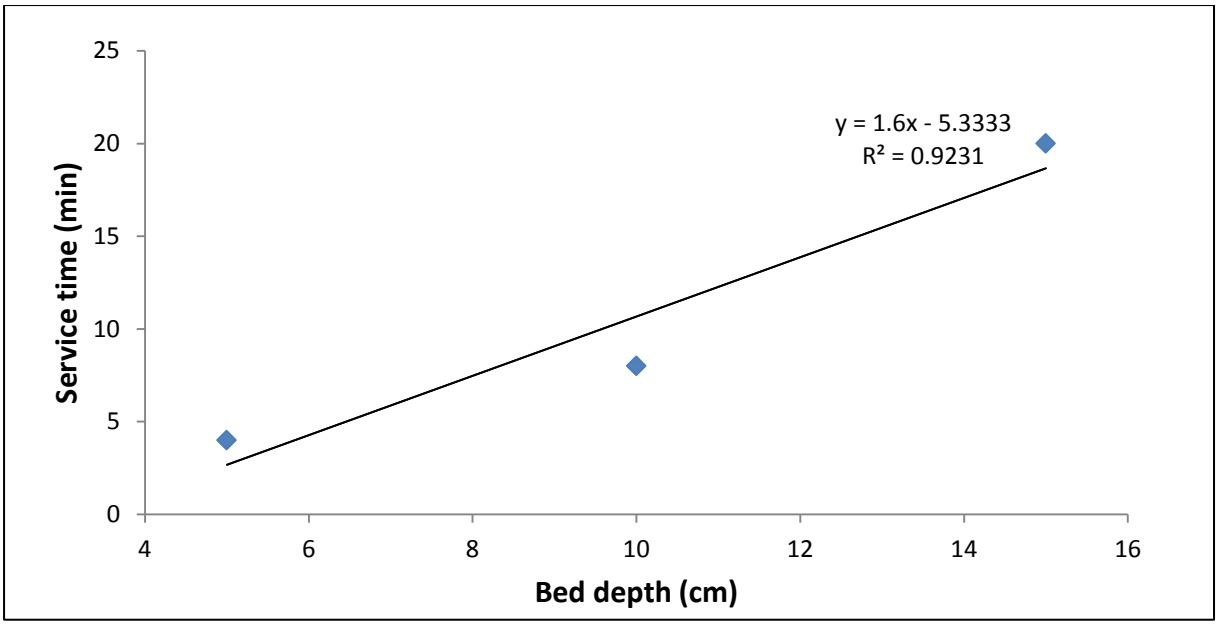

Figure 5.6(c) - Plot of BDST equation for V^{3+}.adsorption on immobilized cassava waste biomass (flow rate = 0.83 mL/s, initial Vanadium concentration = 100 mg/L, pH = 4).

The value of N_0 was higher for V^{3+} in comparison with Co^{2+} and Cr^{3+}. This was attributed to the competitive adsorption towards the active site between the metal ions. Vanadium ion has lower rate constant and high adsorption capacity as compared to Co^{2+} and Cr^{3+} ions, as shown in Table 5.10. These results indicate the possibility of previously adsorbed Co^{2+} and Cr^{3+} having displaced by the V^{3+} ions adsorbed later in the sorption process, due to the greater affinity towards the active sites of the sorbent. These results are in agreement with that obtained by Shahbazi *et al.* (2013) for the adsorption of Cu (II), Pb^{2+} and Cd^{2+} from aqueous solution onto functionalized SDF-15 mesoporous silica.

Table 5.10 The BDST model parameters for the adsorption of Co^{2+}, Cr^{3+} and V^{3+} on immobilized cassava waste biomass.

Metals	**N_0 (mg/L)**	**k_a($Lmg^{-1}s^{-1}$)**	**R^2**
Co^{2+}	99.6	0.032	0.871
Cr^{3+}	116.2	0.011	0.9423
V^{3+}	132.8	0.010	0.9231

Thomas model

One of the simple and generally used models reported by many researchers is the Thomas model, which can be written as (Aksu and Gonen, 2003; Chu, 1994):

$$\frac{C_e}{C_o} = \frac{1}{1} + \exp\left(\left(\frac{k_{TH} q_0 M}{Q}\right)(q_0 M - C_0 V_{eff})\right) \quad 5.2$$

Equation 5.2 can be expressed in linear form as:

$$\ln\left(\frac{C_0}{C_e} - 1\right) = \frac{k_{TH} q_0 M}{Q} - k_{TH} C_0 t \quad 5.3$$

where V_{eff} is the volume of effluent (mL), k_{TH} is the Thomas model constant (mL/mgs), q_0 is the adsorption capacity (mg/g), Q is the volumetric flow rate through column (mL/s), M is the mass of the adsorbent in the column (g), C_0 is the initial metal ion concentration (mg/L) and C_e is the effluent metal ion concentration (mg/L) at any time t (min). The kinetic coefficient k_{TH} and adsorption capacity of column q_0 were determined from a plot of ln [C_0/C_e-1] versus t at a given flow rate and bed depth the model parameters are given in Table 5.11 and 5.12.

The Thomas model has high correlation coefficient (R^2) at the lowest flow rate which gives the validity of the model compared to the higher flow rates for Co^{2+}, Cr^{3+} and V^{3+}, therefore the Thomas model fits experimental data best at low flow rates. The closer the values are to 1 the more accurate the model, which would indicate that external and internal diffusions were not the rate limiting step at lower flow rates. The adsorption was not limited by chemical reaction kinetics. The value of q_0 decreased while k_{TH} increased with increasing flow rate which indicate that mass transport resistance decreases (Aksu and Gonen, 2004; Han *et al*., 2006). The limited resident time experienced by the adsorbent at higher flow rates affected their solid-phase concentration leading to decrease in q_0 as the flow rate increased.

As can be seen in Table 5.11 increase in flow rate (0.83 to 1.61 mL/s) reduced the adsorption capacity of Co^{2+}, Cr^{3+} and V^{3+} by immobilized cassava waste biomass from 54.62 to 45.81 mg/g, 45.13 to 37.78 mg/g and 36.91 to17.88 mg/g, respectively. As the flow rate increased

the Thomas rate constant (k_{TH}) also increased resulting in a decrease in mass transport resistance (Aksu and Gonen, 2004; Han *et al*., 2006). The results are similar to those obtained by Manose (2012) and Yahaya *et al.* (2012).

Table 5.11 Thomas model parameters for the adsorption of Co^{2+}, Cr^{3+} and V^{3+} on immobilized cassava waste biomass at different flow rate (Bed depth = 10 cm, initial metal ion concentration = 100 mg/L).

Metals	**Flow rate (mL/s)**	**q_0(mg/g)**	**k_{TH}($mLs^{-1}mg^{-1}$) x (10^{-4})**	**R^2**
Co^{2+}	0.83	54.62	1.94	0.805
	1.25	52.95	2.19	0.733
	1.61	45.81	2.30	0.608
Cr^{3+}	0.83	45.13	1.83	0.818
	1.25	40.65	1.95	0.771
	1.61	37.78	2.26	0.705
V^{3+}	0.83	36.26	1.70	0.842
	1.25	30.91	1.80	0.716
	1.61	17.88	2.30	0.690

The breakthrough data obtained by varying the bed depth were fitted using the Thomas model. Table 5.12 shows the model constants k_{TH} and q_0 along with correlation coefficient (R^2). Thomas rate constants are dependent on the bed depth. The maximum adsorption capacity q_0 decreased with an increase in bed depth. Similar observations have been reported on this phenomenon by Ayoob *et al*. (2007). High values of regression coefficients were obtained at high bed depth indicating that the Thomas model will be most appropriate for describing the sorption process at high bed depth.

Table 5.12 Thomas model parameters for the adsorption of Co^{2+}, Cr^{3+} and V^{3+} on immobilized cassava waste biomass at different bed depth and (Flow rate = 0.83 mL/s, initial metal ion concentration = 100 mg/L).

Metals	**Bed depth(cm)**	**q_0(mg/g)**	**k_{TH}($mLs^{-1}mg^{-1}$) x (10^{-4})**	**R^2**
Co^{2+}	5	86.23	1.8	0.621
	10	45.76	2.2	0.732
	15	33.09	2.3	0.805
Cr^{3+}	5	61.10	2.1	0.705
	10	38.24	2.4	0.770
	15	25.46	2.6	0.817
V^{3+}	5	61.60	1.9	0.689
	10	34.88	2.1	0.715
	15	28.52	2.3	0.841

5.2.7 Adsorption-desorption cycle

Disposal of the exhausted adsorbent loaded with heavy metal ions creates another environmental problem as it is hazardous material which pollutes the environment. This problem may be overcome to some extent by using one of the elimination methods (e.g. elution, incineration and pyrolysis). The elution of heavy metals is the most common elimination method, allowing both recoveries of solutions of heavy metal ions at higher concentrations for inertisation and recycling of the adsorbent for subsequent uses (Han *et al*., 2005).

In the context of column adsorption, the use of cassava waste biomass as a potential biosorbent depends not only on the biosorptive capacity, but also on how well the biomass is regenerated and used in the metals' recycling process; metal ions binding in the cassava should be desorbed at end of adsorption. Desorbed experiments were performed with 0.1M H_2SO_4 solution. The concentration of 0.1M H_2SO_4 used was based on the batch experiments (see section 4.2.12).

Figures 5.7 and 5.8 show the efficiencies of the adsorption and desorption cycles, respectively. The adsorption capacity of the adsorbent remained constant for the six cycles,

which indicates that there are no irreversible sites on the immobilized cassava waste biomass. Similarly it was shown in batch experiments that after 6 cycles there was a decrease in adsorption. A negligible loss in bed depth and mass of immobilized acid treated cassava was observed after six adsorption-desorption cycles. The desorption efficiency was 79%, 67.8% and 65% for Co^{2+}, Cr^{3+} and V^{3+}, respectively. But desorption efficiency for column experiments were lower than the once obtained in batch experiment's.

The adsorption efficiency increased in the order V^{3+}> Cr^{3+}> Co^{2+} as in batch adsorption process. However, the desorption efficiency is in the reverse order to the adsorption efficiency trends i.e. Co^{2+}> Cr^{3+}> V^{3+}. Co^{2+} desorbed faster from the immobilized acid treated cassava waste biomass as compared to Cr^{3+} and V^{3+}, this was due to its low affinity for the binding sites on the biomass.

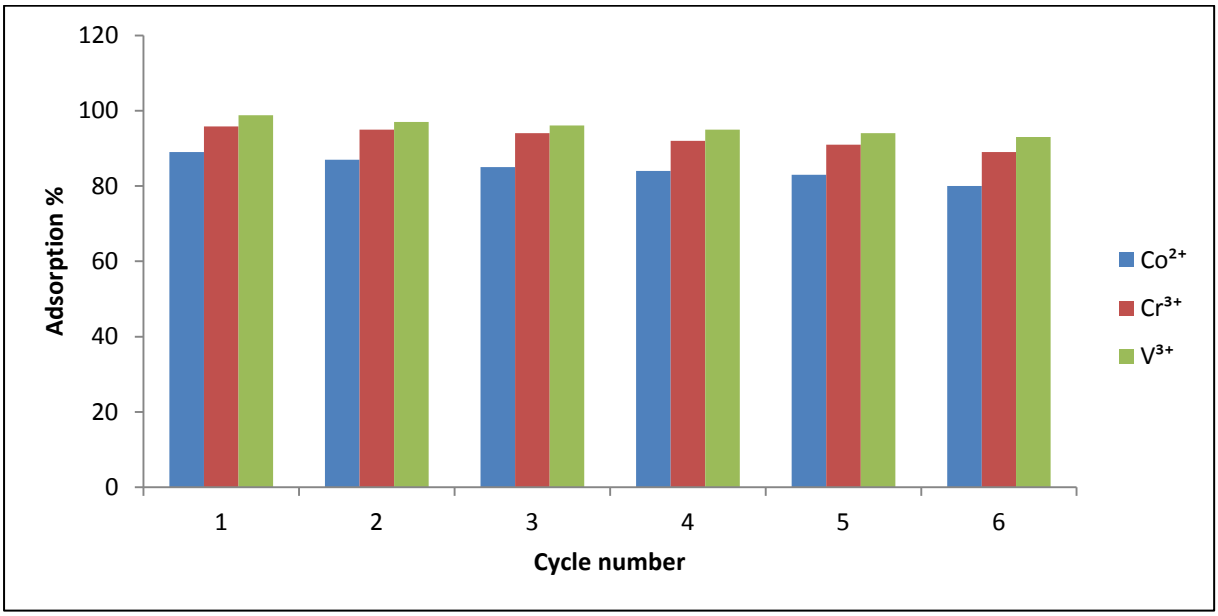

Figure 5.7 - Adsorption efficiency of immobilized cassava waste biomass for the adsorption-desorption cycles (packed column).

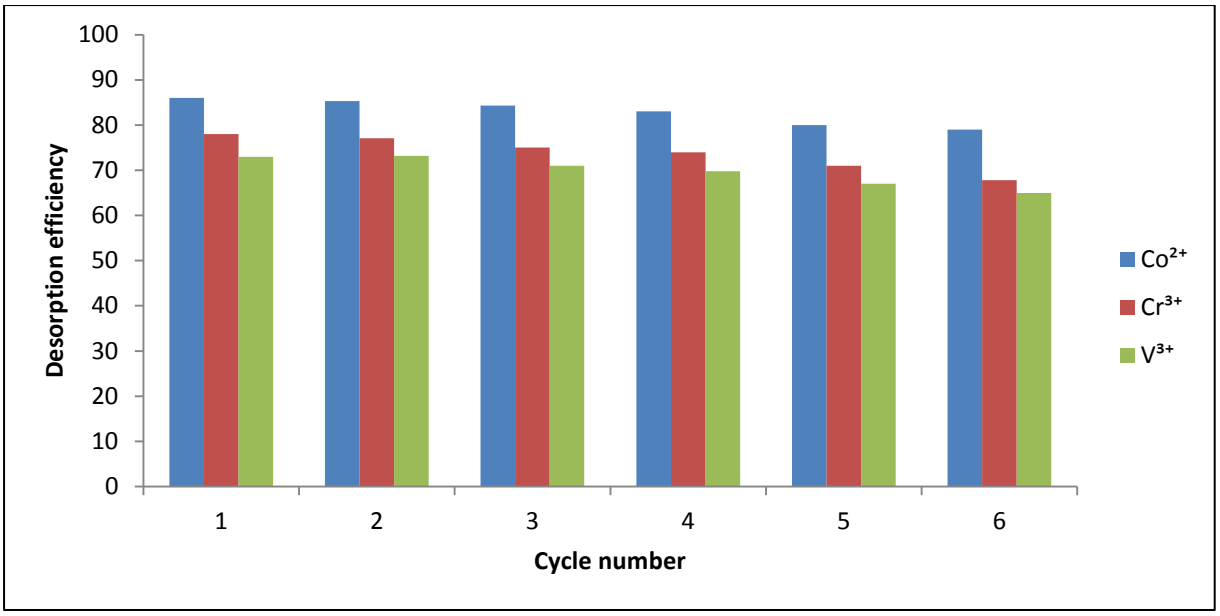

Figure 5.8 - Desorption efficiency of immobilized cassava waste biomass for the adsorption-desorption cycles using 0.1 mol/L H_2SO_4 (packed column).

5.3 Comparison of batch, fixed bed and semi continuous counter current adsorption

Freely suspended cassava waste biomass was initially used for the removal of metal ions in batch and semi continuous counter current systems. Unfortunately, the application of the freely suspended biomass in fixed bed adsorption for the removal of metals was plagued with serious problems. The biomass needed to be separated from aqueous solution and there was a high tendency for the pipeline to be clogged with the biomass. These problems were overcome by immobilization of the cassava waste biomass using sodium alginate. The surface chemistry structure of the cassava before and after immobilization was determined and cassava waste biomass had not changed after entrapment in sodium alginate polymeric matrixes.

The batch operation required less time to reach equilibrium as compared to the fixed bed operation. Overall the sorption capacity observed for the fixed bed system was higher than the batch system for the same initial metal ion concentration. This might be due to the sufficient contact time between the adsorbent and adsorbate in the fixed bed system than in the batch system. For semi continuous counter current system the concentrations limits set by regulators were obtained after 8, 6 and 4 stages for Co^{2+}, Cr^{3+} and V^{3+}, respectively and the adsorption efficiencies obtained were higher than those in batch and fixed bed systems. This was because counter current adsorption maximized the driving force for mass transfer and provided more efficient utilization of the adsorbent capacity.

The adsorbed Co^{2+}, Cr^{3+} and V^{3+} were effectively eluted from the biomass with 0.1M H_2SO_4 and desorption efficiency was generally high. The desorption efficiency obtained was 90, 83 and 75% for batch system; 87, 79, and 73% for fixed bed and 98, 95 and 90% in counter current system for Co^{2+}, Cr^{3+} and V^{3+}, respectively. In the three systems cobalt gave the highest desorption efficiency which may be as a result of low affinity of Co^{2+} ion for the metal binding sites as compared to Cr^{3+} and V^{3+}. Counter current adsorption system gave the highest desorption efficiency as compared to the other two systems. The biosorbent gave a good adsorption-desorption efficiency of 6 cycles in all three systems. The systems proved the suitability of cassava and its potential to withstand extreme condition without losing metal sorption capacity. This was positive towards the evaluation of cassava waste biomass as a potential low cost adsorbent for heavy metal removal.

5.4 Summary and Conclusion

The objectives of this work were to study the adsorption of Co^{2+}, Cr^{3+} and V^{3+}onto cassava waste biomass by means of semi-continuous counter current and column studies. Semi continuous counter current experiments showed that the adsorption of Co^{2+} needed 8 stages to meet the targeted limit of 0.05 mg/L. The Cr^{3+}system needed 6 stages to obtain the targeted limit of 0.05 mg/L whilst for the V^{3+} system required 4 stages to attain the target limit of 0.02 mg/L.

The performance of the packed bed column was analysed using the effluent concentration versus time curves. The packed bed column was found to perform better with lower flow rate and higher bed depth. The uptake analysis revealed a high selectivity for V^{3+}over Cr^{3+} and Co^{2+} at all conditions tested. The experimental data fitted better with the BSDT model than the Thomas model for all the conditions tested. This shows that the rate of adsorption is controlled by surface reaction adsorbate and the unused capacity of the adsorbent.

The adsorption-desorption results showed that the biosorbent can be used repeatedly without significant loss in sorption capacity reflecting its feasibility for commercial application. Furthermore, the easy availability and low cost would make cassava biomass an attractive biosorbent option for heavy metals.

CHAPTER SIX

6 CONCLUSIONS AND RECOMMENDATIONS

6.1 Conclusions

6.1.1 Introduction

Large amounts of plant biomass are produced in excess by the agri-industry and the metal adsorption capacities of different kind of biomass have been identified as potential alternatives to the existing metal removal technology. One such agricultural plant of interest is cassava. The main objective of this work was, to evaluate the adsorption capacity of untreated and acid treated cassava waste biomass for the removal of heavy metal ions (i.e., Co^{2+}, Cr^{3+} and V^{3+}) from synthetic waste water. A review of the literature suggested that cassava waste biomass could be used for the removal of metal ions from wastewater in its original form but adsorption capacity could be improved by chemically modification with thioglycollic acid.

In order to investigate this possibility, the aims of this study were defined as:

- To investigate the effect of various parameters such as: pH, biomass dosage, initial metal ion concentration, agitation and cations in batch system.
- To use counter current system and a packed bed column to upscale the adsorption process.
- To investigate the effect of various parameters such as column bed depth and flow rate of metal solution in a column.
- To look at the possibility of regeneration and re-use of biosorbent.

6.1.2 Batch test works

In laboratory scale experiments, the data showed that cassava waste biomass has potential for the removal of Co^{2+}, Cr^{3+} and V^{3+} ions from aqueous solutions over a range of concentrations for acid treated and untreated biomass. However, acid treatment enhanced the adsorption capacity of the biomass. The characterization of the metal ions adsorption of the acid treated biomass showed that adsorption mechanism is pH dependent and optimum pH of 6, 3 and 3 were obtained for Co^{2+}, Cr^{3+} and V^{3+}, respectively. Furthermore, metal uptake was generally found to increase with an increase in pH, agitation speed, biomass dosage and initial metal concentration. The capacity for the sorption of the three metal ions was lower in ternary

solution as compared to the single ion solution, suggesting prevalence of a competitive adsorption in mixed solution.

The presence of co-cations (Ca^{2+}, Mg^{2+}, Na^{+} ,K^{+}) in aqueous solution decreased the amount of Co^{2+}, Cr^{3+} and V^{3+}adsorbed by cassava. The presence of Ca^{2+} was observed to have the most negative impact on the adsorption of the three metal ion systems.

The equilibrium biosorption data could be described by both Freundlich and Langmuir models, but Freundlich isotherm describes the data better. The metal loaded cassava waste biomass showed remarkable ability for metal recovery using 0.1M H_2SO_4 solution. The metal ions bound to the biomass were recovered and the biosorbent regenerated allowing its successive use. The cassava waste biomass was found to be able to attain the original metal recovery capacity for at-least six adsorption-desorption cycles. This is a good indication of cassava biomass waste potential as biosorbent materials since they can be reused several times while maintaining high overall process efficiency. Thus the possibility of recycling the cassava waste gives the opportunity for a real decontamination of effluent streams at low costs.

The presence of active functional groups responsible for Co^{2+}, Cr^{3+} and V^{3+} adsorption onto original and chemically modified cassava were confirmed by FTIR spectra. FTIR spectra showed that functional groups taking place in sorption included carboxyl and hydroxyl groups when untreated and sulfhydryl groups when treated with thioglycollic acid. Therefore, the additions of these functional groups through chemical modification greatly improved the performance of cassava waste biomass in term of metal removal. BET analysis indicated that surface area increased with increase in the concentration of acid treating agent. The large surface area exhibited more active binding sites for metal binding on the biomass.

6.1.3 Semi- Counter current systems

The required discharge limits were obtained for all metals using semi counter current adsorption system. The minimal accepted limits for Co^{2+}, Cr^{3+} and V^{3+} discharge were reached in 8, 6, and 4 stages, respectively. The adsorption efficiency obtained in the semi counter current system is higher than that achieved in the batch process. Desorption and regeneration can be done to recover metal ions from spent adsorbent. The metal loaded cassava can be regenerated and reused with minimal loss of efficiency for three adsorption /desorption cycles.

6.1.4 Packed Column

The packed bed column breakthrough curves were analyzed at different flow rates and bed depths. The removal efficiency of immobilized acid treated cassava waste biomass from solution strongly depends on the flow rate and bed depth. The breakthrough curves have a typical ‘‘S’’ shape. The breakthrough time increased with a decrease in flow rate while it increased with an increased in bed depth.

Thomas and BDST models were used to predict the breakthrough curves for Co^{2+}, Cr^{3+} and V^{3+} removal in a packed bed of immobilized cassava waste biomass using different flow rate and bed depth. The experimental data best fitted BDST model than the Thomas model, these showed that the rate of adsorption is controlled by the adsorbate and the unused binding sites of the adsorbent. Co^{2+}, Cr^{3+} and V^{3+} adsorbed immobilized cassava waste can be regenerated and reused with minimal loss of efficiency for 6 adsorption-desorption cycle. This is a good indication of cassava waste biomass potential as biosorbent materials since they can be reused several times while maintaining high overall process efficiency. Not only is cassava waste biomass inexpensive and readily available, it also has the potential to remove and recover metal from waste water.

6.2 Recommendations

Based on the obtained results and conclusion, the following recommendations are made:

- It would be necessary to investigate the biosorption of these metals in wastewater or effluent from point sources (heavy-metal polluted rivers, industrial effluent or wastewater treatment plant samples) in order to assess the feasibility of Co^{2+}, Cr^{3+} and V^{3+} adsorption by acid treated cassava waste biomass.
- Acid treated cassava waste biomass could also be investigated for the biosorption of other metal ions (Zn, Cu, Ni, Cd, etc.) which are commonly found in polluted water.
- Evaluation of biosorption kinetics using pseudo-first order and pseudo-second order reaction models.
- The mechanism of adsorption i.e. intraparticle diffusion, chemisorption and homogenous surface diffusion to describe the transport of molecules inside the adsorbent particle should be considered in the future study

- The industrial waste water normally contains other heavy metals (cations and anions) at different concentrations. In this work the effect of cations was studied and showed to decrease the amount of Co^{2+}, Cr^{3+} and V^{3+} adsorbed. It will be necessary to also investigate the effect of anions at different concentrations.
- The process cost should be evaluated in order to assess its potential large scale application.
- The regeneration of cassava waste biomass was investigated and the preliminary findings showed that although the adsorbent can be regenerated, the efficiency decreases after six adsorption-desorption cycles. Desorption studies could be explored as a function of concentration of different eluents such as hydrochloric and nitric acid. Studies in future should explore the best methods of disposing off the adsorbent after re-use.

CHAPTER SEVEN

7 REFERENCES

Abia, A.A., Asuquo, E.D., 2008. Sorption of Pb (II) and Cd (II) ions onto chemically unmodified and modified oil fruit fibre adsorbent: Analysis of Pseudo second order kinetics model. *Indian Journal of Chemical Technology* 15, 341-348.

Abia, A.A., Horsfall, J.M., Didi, O., 2003. The use of chemically modified and unmodified cassava waste for the removal of Cd, Cu and Zn ions from aqueous solution. *Bioresource Technology* 90, 345–348.

Abia, A.A., Horsfall, M., Didi, O., 2002. Studies on the use of agricultural by-products for the removal of trace metals from aqueous solution. *Journal of Applied and Science Environment* 6, 89-95.

Addour, L., Belhocine, D., Boudries, N., Comeau, Y., Pauss, A., Mameri, N., 1999. Zinc uptake by *Streptomyces rimosus* biomass using a packed-bed column. *Journal of Chemistry Technology and Biotechnology* 74, 1089-1095.

Adriano, D.C., 2001. Trace elements in terrestrial environments; biochemistry, bioavailability and risks of metals. Springer–Verlag, New York.

Agency for Toxic Substances and Disease Registry (ATSDR), 2004. Toxicological Profile for Cobalt Atlanta, GA: Department of Health and Human Services, Public Health Service, U.S.

Ahalya, N., Ramachandra, T.V., Kanamadi, R.D., 2003. Biosorption of heavy metals, *Journal of Chemistry and Environment 7*, 71-79.

Akgerman, A., Zardkoohi, M., 1996. Adsorption of phenolic compounds on Fly Ash. *Journal of Chemical Engineering* 41, 185-191.

Ali, A.A., El-Bishtawi, R., 1997. Removal of lead and nickel ions using zeolite tuff, Jordan. *Journal of Chemical Technology and Biotechnology* 69, 27-34.

Ansari, M.I., Masood, F., Malik, A., 2011. Bacterial biosorption: A technique for remediation of heavy metals. Microbes and Microbial Technology, 283-319.

Asku, Z., 1992. The biosorption of Cu (II) by *C. vulgaris* and *Z. ramigera*. *Environmental Technology* 13, 579-586.

Aksu, Z., Gonen, F., Demircan, Z., 2002. Biosorption of chromium (VI) ions by Mowital B30H resin immobilized activated sludge in a packed bed: comparison with granular activated carbon. *Process Biochemistry* 38, 175-186.

Aksu, Z., Gonen, F., 2003. Biosorption of phenol by immobilized activated sludge in a continuous packed bed: prediction of breakthrough curves. *Process Biochemistry* 39, 599-613.

Aksu, Z., Gonen, F., 2004.Biosorption of phenol by immobilized activated sludge in a continuous packed bed: prediction of breakthrough curves. *Process Biochemistry* 39, 599–613.

Aksu, Z., Acikel, U., Kutsal, T., 1997. Application of multicomponent adsorption isotherms to simultaneous biosorption of iron (III) and chromium (VI) on *C. vulgaris. Journal of Chemical, Technology and Biotechnology* 70, 368–78.

Arrascue, M.L., Garcia, H.M., Horna, O., Guibal, E., 2003. Gold sorption on chitosan derivatives. *Hydrometallurgy* 71, 191–200.

Augustine, A.A., Orike, B.D., Edidiong. A.A., 2007. Adsorption kinetics and modeling of Cu (II)ion from aqueous solution by mercaptoacetic acid modified cassava (Manihot Sculenta Cranz) wastes. *Electronic Journal of Environmental, Agricultural and Food Chemistry*, 6 (4), 2221-2234.

Ayoob, S., Gupta, A.K., Bhakat, P.B., 2007. Analysis of breakthrough developments and modeling of fixed bed adsorption system for As (V) removal from water by modified calcined bauxite (MCB). *Journal of Separation and Purification Technology* 52, 430–438.

Bai, R.S., Abraham, T.E., 2003. Studies on chromium (VI) adsorption–desorption using immobilized fungal biomass. *Bioresource Technology* 87, 17-26.

Bailey, S.E., Olin, T.J., Bricka, R.M., Adrian, D.D., 1999.A review of potentially low-cost sorbents for heavy metals. *Water Research* 33, 2469-2479.

Baltpurvins, K.A., Burns, R.C., Lawrance, G.A., Stuart, A.D., 1997. Effect of electrolyte composition on zinc hydroxide precipitation by lime. *Water Resource* 31, 973-980.

Basu, A., Mustafiz, S., Islam, M.R., Bjorndalen, N., Rahaman, M.S., Chaalal, O., 2006. A comprehensive approach for modelling sorption of lead and cobalt ions through Fish scales as an adsorbent. *Chemical Engineering Communications* 193, 580–605.

Benguella, B., Benaissa, H., 2002b. Effects of competing cations on cadmium biosorption by chitin. *Colloids and Surfaces* 201, 143-150.

Bhainsa, K.C., D'souza, S.F., 1999. Biosorption of uranium (VI) by *Aspergillus fumigatus*. *Biotechnology and Technology* 13, 695–699.

Bharathi, K.S., Ramesh, S.P.T., 2013. Fixed-bed column studies on biosorption of crystal violet from aqueous solution by *Citrullus lanatusrind* and *Cyperus rotundus*. *Applied Water Science* 3, 673-687.

Brauckmann, B.M., 1990. Industrial solutions amenable to biosorption. In Volesky B (ed) Biosorption of heavy metals. CRC Press, Boca Ration, FL, USA.

Brigden, K., Labunska, I., Santillo, D., Johnston, P., 2009. Heavy metals and other hazardous chemicals discharged from industrial waste water Treatment Company. The greater pearl river delta, China 1-18.

Brunauer, S., 1945. The adsorption of gases and vapours. University press, oxford.

Bux, F., Kasan, H.C., 1994. Comparison of selected methods for relative assessment of surface charge on waste sludge biomass. *Water SA* 20, 73-76.

Champague, C.P., Gardner, N., 2001. The effect of protective ingredients on the survival of immobilized cells of *Streptococcus thermophilus* to air and freeze-drying. *Electronic Journal of Biotechnology* 4, 146-152.

Calero, M., Hernainz, F., Blazquez, G., Tenoria, G., Martin –Lara, M.A., 2009. Study of Cr (III) biosorption in a fixed bed column. *Journal of Hazardous Materials* 171, 886-893.

Chen, G.Q., Zeng, G.M., Tu, X., Niu, C.G., Huang, G.H., Jiang, W., 2006. Application of a byproduct of *Lentinus edodes* to the bioremediation of chromate contaminated water. *Journal Hazardous Material* 135, 249–255.

Cheremishinoff, N.P., Moressi, A.C., 1978. Carbon adsorption Handbook: 1-53. *Ann Arbor: Science,* 1-53.

Chong, K.H., Volesky, B., 1995. Description of 2-metal biosorption equilibrium by Langmuir-type models. *Biotechnology and Bioengineering* 47,451–60.

Chong, K.H., Volesky, B., 1996. Metal biosorption equilibria in a ternary system. *Biotechnology and Bioengineering* 49, 629-639.

Chowdhury, Z.Z., Zain, S.M., Kan, R.A., Rafique, R.F., Khalid, K., 2012. Batch and fixed bed adsorption studies of lead (II) cation from aqueous solution derived from *Mangostana garcinia* shell. *Bioresource* 7, 2895-2915.

Chu, K.H., 2004. Improved fixed-bed models for metal biosorption. *Journal of Chemical Engineering* 97, 233–239.

Cooney. D.O., 1999. Adsorption Design for Wastewater Treatment. Elsevier Applied Science, Boca Raton.

Cossich, E.S., 2000. Biosorption of Chromium (III) by the Biomass of Marine Alga *Sargassum* sp. University of Campinas, Brazil.

Cresser, M.S., Marr, I.L., 1991. Optical spectrometry in the analysis of pollutants *in* Instrumental Analysis of Pollutants. Hewitt, C.N. (editor). Elsevier Applied Science, London.

Davidson, H.W., Wiggs, P.K., Churchouse, A.H., Maggs, F.A., Bradley, R.S., 1968. Manufactured Carbon. Pergamon, Oxford.

da Silva, E.A., Cossich, E.S., Tavares, C.R.G., 2002. Modeling of copper(II) biosorption by marine alga *Sargassum sp*. In fixed-bed column. *Process Biochemistry* 38, 791–799.

Deans, J.R., Dixon, B.G., 1992. Uptake of Pb^{2+} and Cu^{2+} by novel biopolymers. *Water Research* 4, 26.

Deng, L., Su, Y., Su, H., Wang, X., Zhu, X., 2007. Sorption and desorption of lead (II) from wastewater by green algae *Cladophora fascicularis*. *Journal of Hazardous Material* 143, 220-225.

EPA, 2009. Drinking water contaminants. Online version

<http//water.epa.gov/drink/contaminants/>.Retrieved 09 December 2013

Esposito, A., Pagnanelli, F., Veglio, F., 2002. pH- related equilibria models for biosorption in Single metal systems. *Chemical Engineering Science* 57, 307–313.

Farooqi, A., Masuda, H., Firdous, N., 2007. Toxic fluoride and arsenic contaminated groundwater in the Lahore and Kasur districts, Punjab, Pakistan and possible contaminant sources. *Environmental Pollution* 145, 839-849.

Febrianto, J., Kosasih, A.N., Sunarso, J., Ju, Y.H., 2009. Equilibrium and kinetic studies in adsorption of heavy metals using biosorbent: A summary of recent studies. *Journal of Hazardous Materials* 162, 616-645.

Fiol, N., Villaescusa, I., Martinez, M., Miralles, N., Poch, J., Serarols, J., 2006. Sorption of Pb^{2+}, Ni^{2+}, Cu^{2+} and Cd^{2+} from aqueous solution by olive stone waste. *Separation and purification Technology* 50, 32-140.

Fonseca, B., Teixeira, A., Figueiredo, H., Tavares, T., 2009. Modeling of the Cr (VI) transport in typical soils of the North of Portugal. *Journal of Hazardous Material* 167, 756–762.

Forstner, U., Wittman, G.T.W., 1979. Metal pollution in the Aquatic Environment. Springer-Verleg, Berlin.

Fourest, E., 1993. Study of mechanism of biosorption of heavy metals by the use of industrial fungal biomass in order to purify contaminated aqueous effluent. Thesis of Doctor of Philosophy, University of Science and Technology, Meghalaya, France.

Fourest, E., Roux, J.C., 1992. Heavy metal adsorption by fungal mycelial by-products: influence of pH. *Applied Microbiology and Biotechnology* 37, 399-403.

Friis, N., Myers-Keith, P., 1986. Biosorption of uranium and lead by *Streptomyces longwoodendsis. Biotechnology and Bioengineering* 28, 21-28.

Gadd, G.M., 1993. Interaction of fungi with toxic metals. *New Phytology* 124, 25-60.

Gadd, G.M., 1990. Heavy metal accumulation by bacteria and other microorganisms. *Experiental* 46, 834–840.

Gardea-Torresdey, J.L., Gonzalez, J.H., Tiemann, K.J., Rodriguez, O., Gamez, G., 1998. Phytofiltration of hazardous cadmium, chromium, lead and zinc ions by biomass of *Medicago sativa* (alfalfa). *Journal of Hazardous Material* 57, 29–39.

Ghosh, R., 2006. Principle of Bioseparations Engineering. World Scientific Publishing Company, Singapore.

Godlewska- Zylkiewicz, B., Kozloska, M., 2005. Solid phase extraction using immobilized yeast *Saccharomyces cerevisiae* for determination of palladium in road dust. *Analytical Chemistry* 539, 61-67.

Goel, J., Kadirvelu, K., Rajagopal, C., Garg, V.K., 2005. Removal of lead (II) by adsorption using treated granular activated carbon, Batch and column studies. *Journal Hazardous Material* 125, 211–220.

Gourdon, R., Bhende, S., Rus, E., Sofer, S.S., 1990. Comparison of cadmium biosorption by Gram positive and Gram-negative bacteria from activated sludge. *Biotechnology Letters* 12, 839–842.

Gregg, S.J., Sing, K.S.W., 1982. Adsorption, Surface Area and Porosity. Academic Press, London.

Groen, J.C., Peffer, L.A.A., Pérez-Ramírez, J., 2003. Pore size determination in modified micro and mesoporous materials. Pitfalls and limitation in gas adsorption data analysis. *Microporous and Mesoporous Materials* 60, 1-17.

Gupta, R., Ahuja, P., Khan, S., Saxena, R.K., Mohapatra, H., 2000. Microbial biosorbents: meeting challenges of heavy metal pollution in aqueous solutions. *Current Science* 78, 967–973.

Gurib-Fukim, A., Eloff, J.N., 2013. Chemistry for sustainable development in Africa. Springer, New York.

Han, R., Zhang, J., Zou, W., Xiao, H., Shi, J., Liu, H., 2005. Biosorption of copper (II) and lead (II) from aqueous solution by chaff in a fixed-bed column. *Journal of Hazardous Materials* 133, 262-268.

Han, R., Zou, W., Li, H., Li, Y., Shi, J., 2006. Copper and lead removal from aqueous solution in fixed bed column by manganese oxide coated zeolite. *Journal of Hazardous Materials* 137, 934-942.

Han, R., Wang, Y., Zhao, X., Wang, Y., Xie, F., Cheng, J. & Tang, M., 2009. Adsorption of methylene blue by phoenix tree leaf powder in a fixed-bed column, experiments and prediction of breakthrough curves. *Desalination* 245, 284–297.

Ho, Y.S., Wase, D.A.J., Forster, C.F., 1995. Batch nickel removal from aqueous solution by sphagnum moss peat. *Water Research* 29, 1327-1332.

Holan Z.R., Volesky, B., Prasetyo, I., 1993. Biosorption of cadmium by biomass of marine algae. *Biotechnology and Bioengineering* 41, 819–825.

Holan, Z.R., Volesky, B., 1994. Biosorption of lead and nickel by biomass of marine algae. *Biotechnology and Bioengineering* 43, 1001–1009.

Horsfall Jr, M., Abia, A.A., 2003. Sorption of cadmium (II) and zinc (II) ions from aqueous solutions by cassava waste biomass (*Manihot Sculenta* Cranz). *Water Research* 37, 4913-4923.

Horsfall, M.J., Abia, A.A., Spiff, A., 2003. Removal of Cu (II) and Zn (II) ions from wastewater by cassava (*Manihot Sculenta* Cranz) waste biomass. *African Journal of Biotechnology* 10, 360-364.

Horsfall, M.J., Ogban, F. and Akporhonor, E.E., 2006. Sorption of Chromium (IV) from aqueous solution by cassava (*Manihot Sculenta* Cranz) waste biomass. Chemistry and Biodiversity 3, 161-174.

Hughes, M. N., Poole, R. K., 1989.Metal toxicity. In Metals and Microorganisms. Chapman and Hall, New York.

Hui, K.S., Chao, C.Y.H., Kot, S.C., 2005. Removal of mixed heavy metal ions in wastewater by zeolite 4A and residual products from recycled coal fly ash. *Journal of Hazardous Materials* 127, 89-101.

Huisman, J.L., Schouten, G., Schultz, C., 2006. Biologically produced sulphide for purification of process streams, effluent treatment and recovery of metals in the metal and mining industry. *Hydrometallurgy* 83, 106-113.

Hutchins, R.A., 1973. News method simplifies design of activated carbon systems- bed depth service time analysis. *Chemical Engineering Journal* 80, 133–138.

Iqbal, M., Edyvean, R.G.J., 2004. Biosorption of lead, copper and zinc on loofa sponge immobilized biomass of *Phanerochaete chrysosporium. Minerals Engineering* 17, 217-223.

Jalali, R., Ghafourian, H., Asef, D., Sepehr, S., 2002. Removal and recovery of lead using non-living biomass of marine algae. *Journal Hazardous Material* 92, 253-262.

Johnson, R., 2005. Drinking Water Treatment Methods. Internet version

<http://www.cyber-nook.com/water/Solutions.html>. Retrieved 14 February 2013

Kaduková, J., Virčíková, E., 2005. Comparison of differences between copper bioaccumulation and biosorption. *Environmental* 31, 227-32.

Kapoor, A., Viraraghavan, T., 1995. Fungal biosorption- an alternative treatment option for heavy metal bearing wastewater: A review. *Bioresource Technology* 53, 195-206.

Kim, H.J., Baek, K., Kim, B.K., Yang, J.W., 2006a. Humic substance-enhanced ultrafiltration for removal of cobalt. *Journal of Hazardous Material* 122, 31-36.

Ko, D.C.K., Porter, J.F., McKay, G., 2000. Optimised correlations for the fixed-bed adsorption of metal ions on bone char. *Chemical Engineering Science* 55, 5819-5829.

Kobya, M., 2004. Adsorption, kinetic and equilibrium studies of Cr (VI) by hazelnut shell activated carbon. *Bioresource Technology* 91, 317–321.

Kongsricharoern, N., Polprasert, C., 1995. Electrochemical precipitation of chromium from an electroplating wastewater. *Water Science and Technology* 31, 109-117.

Kotas, J., Stasicka, Z., 2000. Chromium occurrence in the environment and methods of its speciation. *Environmental Pollution* 107, 263-286.

Krishnani, K.K., Xiaoguang, M.X., Christodoulatos, C and Boddu, V.M., 2008. Biosorption mechanism of nine different heavy metals onto biomatrix from rice husk. *Journal of Hazardous Materials*, 153: 1222- 1234.

Ku, Y., Jung, I. L., 2001. Photo catalytic reduction of Cr (VI) in aqueous solutions by UV irradiation with the presence of titanium dioxide. *Water Research* 35, 135-142.

Kumar, P. S., Gayathri, R., Arunkumar, R. P., 2010. Adsorption of Fe (III) ions from aqueous solutionby bengal gram husk powder: equilibrium isotherms and kinetic approach. *Electronic Journal of Environmental, Agricultural and Food Chemistry*, 9, 1047-1058.

Kurniawan, T.A., Chan, G.Y.S., Lo, W.H., Babel, S., 2006. Physico–chemical treatment techniques for wastewater laden with heavy metals. Journal *of Chemical Engineering* 118, 83–98.

Kuyucak, N., Volesky, B., 1990. In Biosorption of Heavy Metals. CRC Press: Boca Raton, FL 173-198.

Kuyucak N., Volesky, B., 1988. Biosorbents for recovery of metals from industrial solutions. *Biotechnology Left* 10, 137-142

Leofanti, G., Padovan, M., Tozzola, G., Venturelli, B., 1998. Surface area and pore texture of catalysts. *Catalysis today* 41, 207-219.

Leusch A., Holan Z., Volesky, B., 1995. Biosorption of heavy metal metals (Cd, Cu, Ni, Pb, and Zn) by chemically-reinforced biomass of marine algae. *Journal of Chemical Technology Biotechnology* 62, 279–288.

Liu, H.L., Chen, B.Y., Lan, Y.W., Chen, Y.C., 2004. Biosorption of Zn(II) and Cu(II) by the indigenous *Thiobacillus thiooxidans. Chemical Engineering Journal* **97**: 195-201.

Liu, H, Wang, J.L., Wen, X.H., 2002b. Study on biosorption of lead by yeast. *Resource Environmental Science* 15, 6–9.

Low, K.S., Lee, C.K., Leo, A.C., 1995. Removal of metals from electroplating wastes using banana pith. *Bioresource Technology* 51, 227–231.

Luef, E.; Prey, T., Kubicek, C.P., 1991. Biosorption of zinc by fungal micelial wastes. *Applied Microbiology and Biotechnology* 14, 688-692.

Maliyekkal, S.M., Ligy, P., 2011. Fixed bed adsorption of Arsenite (As(III)) from drinking water: Breakthrough studies and modelling. 3rd International CEMEPE SECOTOX Conference, Indian Institute of Technology, India.

Mane, P. C., Bhosle, A. B., Jangam, C. M., Vishwakarma, C. V., 2011. Bio adsorption of selenium by pre-treated algal biomass. *Advances in Applied Science Research* 2, 202-207.

Manose, A., 2012. Fixed bed adsorption studies of rhodamine B dye using oil palm empty fruit bunch activated carbon. *Journal of Engineering Research and Studies* 3, 604-613.

Maruca, R., Jo Suder, B., Wightman, J.P., 1982. Interaction of heavy metals with chitin and chitosan. III. Chromium. *Journal of Applied Polymer Science* 27, 4827-4837.

Morrison, R.T., Boyd, R.N., 1992. Organic chemistry, 6th eds. Prentice Hall, London.

Muhammad, N., Mahmood, A., Shahid, S.A., Shah, S.S., Khalid, A.M., Mckay, G., 2006. Sorption of lead from aqueous solution by chemically modified carbon adsorbent. University of Agriculture, Punjab, Pakistan.

Muhamad, N., Parr, J., Smith, D.M., Wheatley, D.A., 1998. Adsorption of heavy metals in slow sand filters. In: proceedings of the WEDC Conference Sanitation and water for all, Islamabad, Pakistan.

Mulkoc, E., Nuhoglu, Y., 2003. The removal of chromium (VI) from synthetic waste water by *Ulothrix zonata. Fresenius Environmental Bulletin* 12, 376–381.

Mulkoc, E., Nuhoglu, Y., 2006. Fixed bed studies for the sorption of chromium (VI) onto tea factory waste. *Chemical Engineering Science* 61, 4363-4372.

Nakajima, A., Baba, Y., 2004. Mechanism of hexavalent chromium adsorption by persimmon tannin gel. *Water Research* 38, 2859–2864.

Nasehir, K.E.M., Yahaya, I.A., Muhamad, F.P.M., Olugbenga, S.B., Mohd, A.A., 2011. Fixed-bed column study for Cu (II) removal from aqueous solutions using rice husk based activated carbon. *International Journal of Engineering and Technology* 11, 248-252.

Ndlovu, S., Simate, G.S., Seepe, L., Shemi, A., Sibanda, V., Van Dyk, L., 2013. Removal of Co^{2+}, V^{3+} and Cr^{3+} from synthetic waste water using cassava waste. *South African Journal of Chemical Engineering* 18, 51-69

Neal, B.G., Lawrence, E.B., Wendt, J.L., 1990. Alkali metal partitioning in Ash from pulverized coal combustion. *Combustion Science Technology* 74, 211- 214.

Noh, J. S., Schwarz, S., 1988. Estimation of the point of zero charge of simple oxides by mass titration. *Journal of Colloid and Interface Science* 130, 157-164.

Noh, J. S., Schwarz, S., 1990. Effect of HNO_3 treatment on the surface acidity of activated carbon. *Carbon* 28, 675-682.

Nwabanne, J.T., Igbokwe, P.K., 2012. Adsorption performance of packed bed column for the removal of lead (II) using Oil Palm Fibre. *International Journal of Applied Science and Technology* 5, 106-115.

O'Hair, S.K., 1995. Cassava: Tropical research and education centre, University of Florida, USA.

Ozer, A., Ozer, D., 2003. Comparative study of the biosorption of Pb (II), Ni (II) and Cr (VI) ions onto *Saccharomyces cerevisiae*: determination of biosorption heats. *Journal of Hazardous Material* 100, 219–29.

Ozer, A., Ozer D., Ekíz H.I., 2004. The equilibrium and kinetic modelling of the biosorption of copper(II) ions on *Cladophora crispata*. *Adsorption* 10, 317-326.

Pagnanelli, F., Esposito, A., Veglio, F., 2002. Multi-metallic modelling for biosorption of binary systems. *Water Research* 36, 4095–4105.

Pagnanelli, F., Toro, L., Veglio F., 2002. Olive mill solid residues as heavy metal sorbent material: a preliminary study. *Waste Management* 22,901-907.

Panda, G.C., Das, S.K., Chatterjee, S., Maity, P.B., Bandopadhyay, T.S., Guha, A.K., 2006. Adsorption of cadmium on husk of *Lathyrus sativus*: Physico-chemical study. *Colloids Surface Biointerfaces* 50, 49-54.

Panday, K.K., Prasad, G., Singh V.N., 1985. Copper (II) removal from aqueous solutions by fly ash. *Water Research* 19, 869-873.

Park, S., Jung, W.Y., 2001. Removal of chromium by activated carbon fibers plated with copper metal. *Carbon Science* 2, 15-21.

Parsons, J.G., Gardea-Torresdey, J.L., Tiemann, K.J., Gamez, G., 2003. Investigation of trace level binding of $PtCl_6$ and $PtCl_4$ to alfalfa biomass (*Medicago sativa*) using Zeeman graphite furnace atomic absorption Spectrometry. *Journal of Analytical chemical Acta* 478, 139-145.

Quek, S.Y., Wase, D.A.J., Forster, C.F., 1998. The use of sago waste for the sorption of lead and copper. *Water SA* 24, 251–256.

Randall, J.M., Reuter, F.C., Waiss, A.C., 1974. Removal of cupric ions from solution by contact with peanut skins. *Journal of Applied Polymer Science* 19, 156–171.

Rangsayatorn, N., Pokethitiyook, P., Upatham, E.S., Lanza, G.R., 2004. Cadmium biosorption by cells of *Spirulina platensis* TISTR 8217 immobilized in alginate and silica gel. *Environmental International 30*, 57-63.

Reed, B.F., Arunnachalam, S., Thomas, B., 1994. Removal of lead and cadmium from aqueous waste streams using Granular activated carbon (GAC) columns. *Environmental Program* 13, 60-65.

Rich, G., Cherry K., 1987. Hazardous Waste Treatment Techologies. Pudvan Publishers, New York.

Richardson, J.F., Harker, J.H., 2002. Chemical Engineering, 5th eds. Butterworth-Heinemann, Oxford.

Rodriguez-Reinoso, F., Linares-Solano, A., 1989. Chemistry and physics of carbon: a series of advances. Marcel Dekker, New York.

Roschin, A.V., 1967. Toxicology of vanadium compound used in modern industry. *Water Research* 32, 26-32.

Ross, I.S., Townsley, C.C., 1986. The uptake of heavy metals by filamentous fungi. In: Eccles H, Hunts (eds) Immobilization of ions by biosorption. IRL Press, Chichester.

Roquerol, J., Rodriguez –Reinso, F., Sing, K.S.W., Unger K.K., 1994. Characterization of Porous Solids II. Elsevier, Amsterdam.

Sag, Y., Kutsal, T., 2000. Determination of the biosorption activation energies of heavy metal ions on *Zoogloea ramigera* and *Rhizopus arrhizus*. *Process* 35, 801-807.

Sağ, Y., Kutsal, T., 1995. Biosorption of heavy metals by *Zooglodea ramigera*: use of adsorption isotherms and a comparison of biosorption characteristic. *Journal of Chemical Engineering* 60, 181–188.

Saha, P.D., Chowdhurry, S., Mondal, M., Sinha, K., 2011. Biosorption of direct red 28 (Congo Red) from aqueous solution by egg shells: Batch and column studies. *Separation science and Technology* 47, 112-123.

Sankararamakrishnan, N., Kumar, P., Chauhan, V.S., 2008. Modeling fixed bed column for cadmium removal from electroplating wastewater. *Separation and Purification Technology* 63,213–219.

Schiewer, S. and Volesky, B., 2000. Environmental Microbe-Metal Interactions. Lovley, D. R., Biosorption processes for heavy metal removal. ASM Press, Washington D.C.

Schwarz, F.J., Kirchgessner, M., Stangl, G.L., 2000. Cobalt requirement of beef cattle- feed intake and growth at different levels of cobalt supply. *Journal of Animal Physiology and Animal Nutrition* 83, 121.

Shahbazi, A., Younesi, H., Badiei, A., 2013. Batch and fixed bed column adsorption of Cu(II), Pb(II) and Cu(II) from aqueous solution onto functionalized SBA-15 mesoporous silica. *The Canadian Journal of Chemical Engineering*91, 739-750.

Sharma, K. R., 2007. Principle of mass transfer. Indian institute of technology, Chennai, India.

Sharma, S.K., Sanghi, R., 2012. Advances in water treatment and pollution Prevention. Jaipur Engineering College and Research Center, Jaipur, India.

Sigel, H., Sigel, A., 1995. Vanadium and its role in life metal ions in biological systemMarcel Dekker, New York.

Sing, K.S.W., Everett, D.H., Haul, R.A.W., Moscou, L., Pierotti, R.A., Rouquerol, J., Siemieniewska, T., 1985. Reporting physisorption data for gas/solid systems with special

reference to the determination of surface area and porosity. *Pure and Application Chemistry* 57, 603-619.

Singh, U., Kaushal, R.K., 2013. Treatment of waste water with low cost adsorbents: A review. *International Journal of Technical and Non- Technical Research* 3, 33-42.

Singh, V.P., Stapleton, J.R., 2002. Biotransformation: bioremediation technology for health and environmental protection. *Industrial microbiology* 36, 219-224.

Sonune, A., Ghate, R., 2004. Developments in wastewater treatment methods, Desalination (167): *World Intellectual Property Organisation 15*, 55-63

Stoeckli, H.F., Guillot, A., Slasli, A.M., Hugi-Cleary D., 2002. The comparison of experimental and calculated pore size distributions of activated carbons. *Carbon* 40, 383-388.

Sud, D., Mahajan, G.,Kaur, M.P., 2008. Agricultural waste material as potential adsorbent for sequestering heavy metal ions from aqueous solutions. *Bioresource Technology* 99, 6017-6027.

Sudha, B.R., Abraham, T.E., 2001. Biosorption of Cr (IV) from aqueous solution by *Rhizopus nitricans*. *Bioresource Technology* 79, 73-81.

Suksabye, P., Thiravetyan, P. and Nakbanpote, W., 2008. Column study of chromium (VI) adsorption from electroplating industry by coconut coir pith. *Journal Hazardous Material* 160, 56–62.

Tact9 media, 2010. Adsorption isotherm. Internet version

<*http://www.chemistrylearning.com/adsorption-isotherm/*>. Retrieved 10 March 2013.

Taty-Costodes, V.C., Fauduet, H., Porte, C., Ho, Y.S., 2005. Removal of lead (II) ions from synthetic and real effluents using immobilized *Pinus sylvestris* sawdust: Adsorption on a fixed-bed column. *Journal of Hazardous Material* 123, 135-144.

Tissue, B.M., 1996. Atomic transitions: Theory. Internet version
<http://elchem.kaist.ac.kr/vt/chem-ed/spec/atomic/aa.htm>. Retrieved 20 March 2013.

Tobin, J.M., Cooper, D.G., Neufeld, R.J., 1984. Uptake of metal ions by *Rhizopus arrhizus* biomass. *Applied Environmental Microbiology* 47, 821-822.

Thomas, H.C., 1944. Heterogeneous ion exchange in a flowing stem. *American Industrial Hygiene Association Journal* 66, 1466-1664.

Tsezos, M., 1990. Engineering aspects of metal minding by biomass: In Enrlich HL and brierley C.L eds. Microbial mineral recovery. McGraw-Hill publishing company, USA.

Tsezos, M., 1983. The role of chitin in uranium adsorption by *Rhizopus arrhizus. Biotechnology and Bioengineering* 25, 2025-2040.

Tsezos, M., Remoudaki, E., Angelatou, V., 1996a. A study of the competing ions effects in the biosorption of metals, *International Biodeterioration and Biodegradation,* 36, 19–28.

Upendra, K., 2006. Agricultural products and by- products as a low cost adsorbent for heavy metal removal from water and wastewater: A review. *Scientific Research and Essay* 2, 33 – 37.

Van der Heen, P., 1977. The removal of traces of heavy metals from drinking water and industrial effluent with ion exchanger. Internet version.

<http://www.ces.iisc.ernet.in/biodiversity/pubs/ces_tr/tr110/tr110_tvr_ces.pdf.> Retrieved 03 March 2013.

Vianna, L.N.L., Andrade, M.C., Nicoli, J.R., 2000. Screening of waste biomass from *Saccharomyces cerevisiae*, *Aspergillus oryzae* and *Bacillus lentus* fermentations for removal of Cu, Zn and Cd by biosorption. *World Journal of Microbiology and Biotechnology* 16, 437–440.

Villegas-Jimenez, A.A., Mucci, A., Paquette, J., 2009. Proton/calcium ion exchange behaviour of calcite. *Physical chemistry Chemical Physics* 11, 8895-8912.

Viggiano, M., Gramham, G., 2003. Joint Service Pollution Prevention Opportunity Handbook. Naval Facilities Engineering Service center, United State.

Vijayaraghavan, K., Yun, Y.S., 2008b. Utilization of fermentation waste (*Corynebacterium glutamicum*) for biosorption of Reactive Black 5 from aqueous solution. *Journal of Hazardous Materials 141,* 45-52.

Vijayaraghavan. K., Jegan. J., Palanivelu. K., Velan. M., 2005. Batch and column removal of copper from aqueous solution using a brown marine alga *Turbinaria ornata*. *Chemical Engineering Journal* 106, 177-84.

Vimala, R., Charumathi, D., Das, N., 2011. Packed bed column studies on Cd(II) removal from industrial wastewater *by Macrofungas pleurotus. Desalination* 275, 291-296.

Vinodhini, V.; Das, N., 2010. Relevant approach to assess the performance of sawdust as adsorbent of chromium (VI) ions from aqueous solutions. *International Journal of Environmental Science and Technology* 7, 85-92.

Volesky, B., 1990. Biosorption and biosorbents, Biosorption of heavy metals. Boca Raton, CRC Press.

Volesky, B., 2001. Detoxification of metal – bearing effluents: biosorption for the next

Century. *Hydrometallurgy* 59, 203-216.

Volesky, B., 2003. Sorption and biosorption. BV Sorbex, Lambert, Quebec, Canada.

Volesky, B., Holan, Z.R., 1995. Biosorption of heavy metals. *Biotechnology Program* 11, 235–250.

Volesky, B., 2004. Sorption and Biosorption. BV Sorbex, Lambert, Quebec, Canada.

Walter, J., Weber, Jr., 1974. Adsorption process.The University of Michigan, College of Engineering, Ann Arbor, Michigan 48104, USA.

Wang, J., Xu, F., Xie, W., Mei, Z., Zhang, Q., Cai, J., Cai, W., 2009. The enhanced adsorption of dibenzothiophene onto cerium/nickel-exchanged zeolite. *Journal of Hazardous Materials* 163, 538-543.

Wang, J., Chen, C., 2006. Biosorption of heavy metals by *Saccharomyces cerevisiae*: A review. *Biotechnology Advances* 24, 427-451.

Wan Ngah, W. S., Hanafiah, M. A. K. M., 2008. Removal of heavy metal ions from wastewater by chemically modified plant wastes as adsorbents: A review. *Bioresource Technology*, 99, 3935-3948.

Warade, A., Gaikwad, R., Sapkal, R., Sapkal, V., 2011. Simulation of multistage counter current liquid-liquid extraction. *Leonardo Journal of Science* 20, 79-94.

Water Science and Technology Board, 2003. Environmental Clean-up at Navy Facilities: Adaptive Site Management. National Academy of Sciences, Washington, D.C.

Wesolowski, D.J., Machesky, M.L., Ridley, M.K., Palmer, D.A., Zhang, Z., Fenter, P., Predota, M., Cummings, P.T., 2008. Ion adsorption on metal oxide surfaces to hydrothermal conditions. *Transitions* 11, 167-180.

Yabe, O. M. J., Oliveira, E., 2003. Heavy metals removal in industrial effluents by sequential adsorbent treatment. *Advance Environmental Resource* 7, 263-272.

Yahaya, N.K.E.M., Abustan, L., Lattiff, M.F.P.M., Bello, O.S., Ahmad M.A., 2012. Study of the removal of Cu from aqueous solution using rice husk based activated carbon. *International Journal of Engineering and Technology 11*, 1-5.

Yin, Y.C., Aroua, M.K., Wan Daud, W.M., 2007. Review of modifications of activated carbon for enhancing contaminant uptakes from aqueous solutions. *Separation and Purification Technology* 52, 403 – 415.

Ying, C.P., 2007. Biosorption of copper (II) and chromium (VI) onto activated sludge isotherms and kinetic models. University of Malaysia, Kuala Lampur, Malaysia.

Zhou, J.L., Kiff, R.J., 1991. The uptake of copper from aqueous solution by immobilized fungal biomass. *Journal of Chemical Technology and Biotechnology* 52, 317-330.

Zhu, Z., Li, A., Yan, L., Liu, F., Zhang, Q., 2007. Preparation and characterization of highly mesoporous spherical activated carbons from divinylbenzene-derived polymer by $ZnCl_2$ activation. *Journal of Colloid and Interface Science* 316, 628–634.

Zulfadhly, Z., Mashitah, M.D., Bhatia, S., 2001. Heavy metals removal in a fixed-bed column by the macro fungus *Pycnoporus sanguineus*. *Environmental Pollution* 112, 463–70.

CHAPTER EIGHT

8 APPENDICES

8.1 Appendix A

Sample calculations

Batch process

The percentage adsorption was calculated using the following equation:

Initial metal ion concentration (C_0) = 100 mg/L

Final metal ion concentration (C_e) = 20 mg/L

$$\%\ adsorption = \frac{C_i - C_e}{C_i} \times 100\%$$

$$\%\ adsoption = \frac{100-20}{100} \times 100\%$$

Therefore % adsorption = 80%

The metal recovery was calculated by the following equation:

Initially sorbed metal ion = 77.78 mg/L

Released metal ions = 70.00 mg/L

$$Metal\ recovery = \frac{Released\ metal\ ions\ (mg)}{Initially\ sorbed\ metal\ ions\ (mg)} \times 100$$

$$Metal\ recovery = \frac{70.00 mg/L}{77.78\ mg/L}$$

Therefore metal recovery = 90%

Precipitation pH of Co^{2+}, Cr^{3+} and V^{3+}

<u>Cobalt</u>

$Co(OH)_2 = Co^{2+} + 2OH^-$

$K_{sp} = [Co^{2+}][OH^-]^2$

K_{sp} For $Co(OH)_2 = 1\times10^{-15}$

100 mg/L of Co^{2+} concentration to mol/L

100 mg/L/1000= 0.1 g/L

Mass of Co^{2+} from $CoSO_4.5H_2O$ = 58.98 g/mol

Mole= mass/ molar mass

Mole = 0.1 g/L/ 58.98 g/ mol

Mole = 1.70×10^{-3} mol/L

$K_{sp}= [Co^{2+}][OH^-]^2$

$1\times10^{-15} = 1.70\times10^{-3}[OH^-]^2$

$[OH-]^2=5.88\times10^{-13}$

$[OH^-] = (5.88\times10^{-13})^{1/2}$

$[OH^-] = 7.66\times10^{-7}$

$pOH = -\log[OH^-]$

$pOH = -\log(7.66\times10^{-7})$

pOH = 6.12

pH = 14-pOH

pH = 7.9

Therefore, cobalt starts precipitating above the pH of 7.9

Chromium

$Cr(OH)_3 = Cr^{3+} + 3OH^-$

$K_{sp} = [Cr^{3+}][OH^-]^3$

K_{sp} For $Cr(OH)_3 = 2\times10^{-30}$

100 mg/L of Cr^{3+} concentration to mol/L

100 mg/L/1000= 0.1 g/L

Mass of Cr^{3+} from $Cr(NO_3)_3$ = 51.996 g/mol

Mole= mass/ molar mass

Mole = 0.1 g/L/ 51.996 g/ mol

Mole = 1.92×10^{-3} mol/L

Ksp= $[Cr^{3+}][OH^-]^3$

$2\times10^{-30} = 1.92\times10^{-3}[OH^-]^3$

$[OH^-]^3=1.04\times10^{-27}$

$[OH^-] = (1.04\times10^{-27})^{1/3}$

$[OH^-] = 1\times10^{-9}$

pOH = -log[OH-]

$pOH = -\log(1\times10^{-9})$

pOH = 9

pH =14-pOH

pH = 5.0

Therefore, chromium starts precipitating above the pH of 5.0

Vanadium

$V(OH)_3 = V^{3+} + 3OH^-$

$K_{sp} = [V^{3+}][OH^-]^3$

K_{sp} for $V(OH)_3 = 4\times10^{-35}$

100 mg/L of V^{3+} concentration to mol/L

100 mg/L/1000= 0.1 g/L

Mass of V^{3+} from VCl_3 = 50.942 g/mol

Mole= mass/ molar mass

Mole = 0.1 g/L/ 50.942 g/ mol

Mole = 1.96×10^{-3} mol/L

$K_{sp}= [V^{3+}][OH^-]^3$

$4\times10^{-35} = 1.96\times10^{-3}[OH^-]^3$

$[OH^-]^3=2.08\times10^{-32}$

$[OH^-] = (2.08\times10^{-32})^{1/3}$

$[OH^-] = 12\times10^{-11}$

pOH = -log[OH-]

$pOH = -\log(12\times10^{-11})$

pOH = 9.89

pH =14-pOH

pH = 4.1

Therefore, vanadium starts precipitating above the pH of 4.1

Fixed bed process

Calculating residence time of the solution in the column

Flow rate (q) = 0.83 mL/s

Volume (V) =80 mL

$$\Theta = \frac{V}{q}$$

$$\Theta = \frac{80\ mL}{0.83\ mL/s} = 96.39\ s$$

BDST model

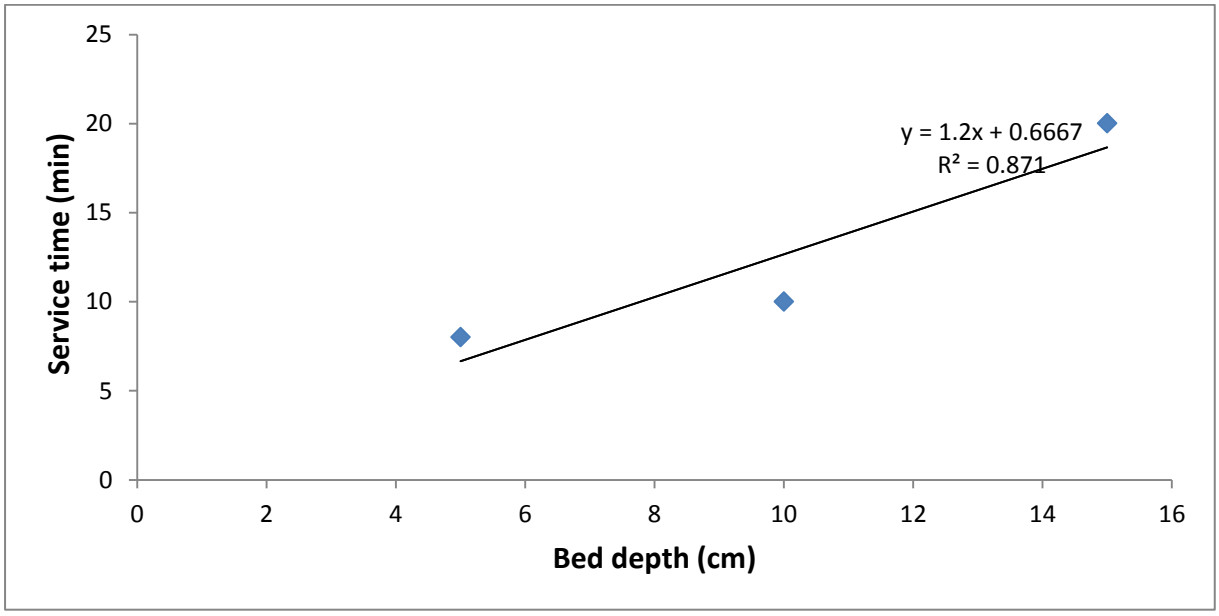

Figure A1 BDST model on breakthrough curve in fixed bed column for Co^{2+} adsorption by immobilized cassava waste biomass

Slope =1.2

Intercept= -0.6667

C_0= 100 mg/L

v= 0.83 mL/s

C_b = 10 mg/L

Calculating adsorption capacity (N_0)

$$Slope = \frac{N_0}{C_0 v}$$

$$N_0 = 1.2 * 0.83 * 100$$

$$Therefore\ N_0 = 99.6\ mg/L$$

Calculating rate constant (K_a)

$$\text{Intercept} = \left(\left(\frac{1}{k_a C_0}\right) \ln\left[\left(\frac{C_0}{C_b}\right) - 1\right]\right)$$

$$\text{Ka} = \left(\frac{1}{0.6667*100} \ln\left[\frac{100}{10} - 1\right]\right)$$

$$k_a = \frac{2.197}{0.6667*100}$$

$$Therefore\ k_a = 0.032$$

Thomas model

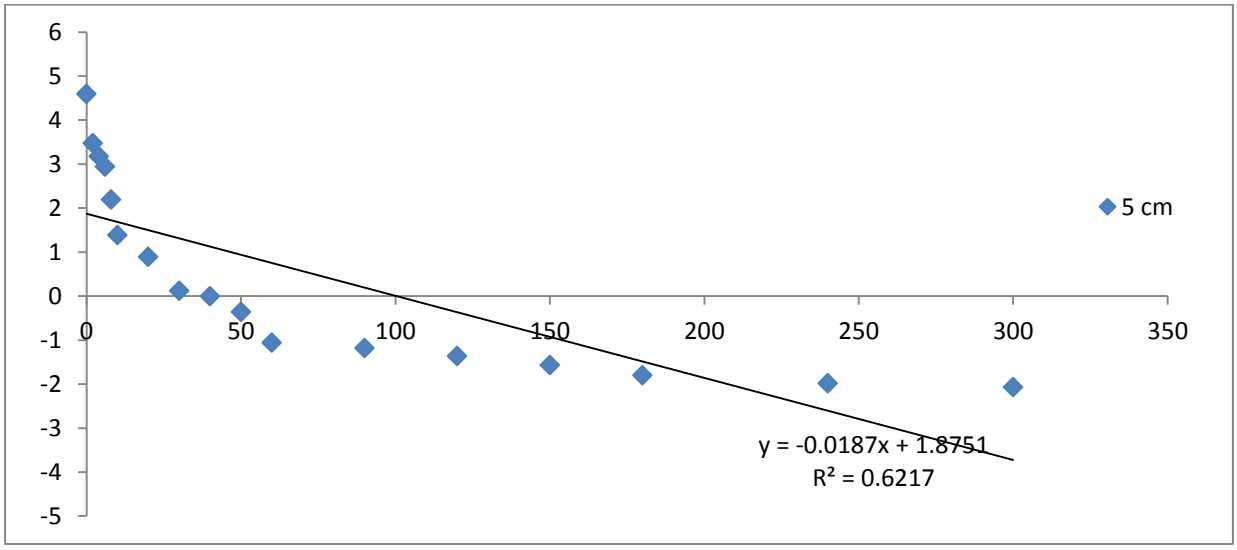

Figure A2 Thomas model for the adsorption of Co^{2+} on immobilized cassava waste biomass: Effect of bed depth.

Calculating Thomas rate constant (k_{TH})

Slope = -0.0187

Intercept = 1.8751

Flow rate (Q) = 0.83 mL/s

Mass (M) = 100.259 g

Initial metal ion concentration (C_0) = 100 mg/L

$Slope = -k_{TH}C_0$

$k_{TH} = \frac{-0.0187}{-100}$

$Therefore\ k_{TH} = 1.9 * 10^{-4}$

Calculating adsorption capacity (q_0)

$\text{Intercept} = \frac{k_{TH}q_0M}{Q}$

$1.8751 = \frac{1.9*10^{-4}q_0100.259}{0.83}$

$q_0 = \frac{1.556}{0.019}$

$Therefore\ q_0 = 81.912$

8.2 APPENDIX B

Flame Atomic absorption spectroscopy (FAAS)

Flame Atomic absorption spectroscopy (FAAS) uses the absorption of light to measure the concentration of gas-phase atoms. Since samples are usually liquid, the metal atoms or ions must be vaporized in a flame. The vaporized atoms absorb ultraviolet or visible light and make transitions to higher electronic energy levels. The metal concentration is determined from the amount of light absorbed by the vaporized atoms (Tissue, 1996). The amount of light absorbed by the atoms is simply the total amount of light produced at the light source (lamp) minus the total amount received by the detector, see Figure A1. The measurable decrease in intensity of the light beam due to absorption at a specific wavelength is characteristic to a specific element according to the Beer-Lambert Law:

$$\log \frac{I_o}{I_t} = \varepsilon . C . I.$$

Where I_o – Incident light intensity,

I_t – Transmitted light intensity,

ε – Species constant as specified wavelength,

C – Concentration of absorbing species,

I – Optical path length.

The percentage transmission (100 x I_o/I_t) which varies linearly with concentration of the element is referred to as absorbance value (Cresser and Marr, 1991). Concentration measurements are usually determined from a working curve after calibrating the instrument with standards of known concentration.

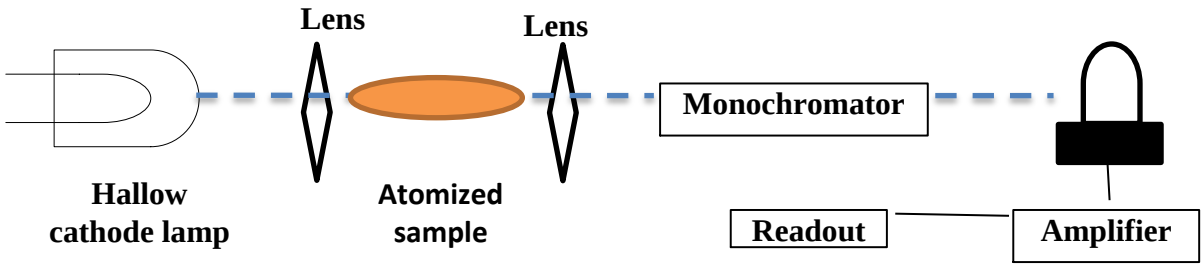

Figure B1 -Schematic of atomic absorption spectrometer (Tissue, 1996).

Light source

The light source is usually a hollow-cathode lamp of the element that is being measured. Lasers are also used in research instruments. Since lasers are intense enough to excite atoms to higher energy levels, they allow AAS and atomic fluorescence measurements in a single instrument. The disadvantage of these narrow-band light sources is that only one element is measurable at a time.

Atomizer

AAS requires that the metal atoms be in a gaseous phase. Ions or atoms in a sample must be vaporized in a high-temperature source such as a flame (2100 – 2400 K) or graphite furnace. Flame AAS can only analyze solutions, while graphite furnace AAS can accept solutions, slurries, or solid samples.

Flame

AAS uses a slot type burner to increase the path length, and therefore to increase the total absorbance (Beer-Lambert law). Sample solutions are usually aspirated with the gas flow into a nebulising/mixing chamber to form small droplets before entering the flame. Table A1 presents examples of different fuels used to produce a flame for the AAS

Light separation and detection

AAS use monochromators and detectors for UV and visible light. The main purpose of the monochromator is to isolate the absorption line from background light due to interferences. Simple dedicated AAS instruments often replace the monochromator with a band-pass interference filter. Photomultiplier tubes are the most common detectors for AAS.

Excitation

A flame provides a high-temperature source for desolvating and vaporizing a sample to obtain free atoms for spectroscopic analysis. In atomic absorption spectroscopy ground state atoms are desired. For atomic emission spectroscopy the flame must also excite the atoms to higher energy levels. The following table lists temperatures that can be achieved in some commonly used flames.

Table B1: Examples of common fuels used in AAS and the temperature of the flames they produce.

Fuel	**Oxidant**	**Temperature, K**
Hydrogen	Air	2000-2100
Acetylene	Air	2100-2400
Hydrogen	Oxygen	2600-2700
Acetylene	Nitrous Oxide	2600-2800

Sample analysis

The flame atomic absorption spectrometer (FAAS) had to be calibrated for each metal before analysing any sample. This was achieved by passing samples of known concentration through the FAAS. These samples were made from standard metal solutions which were diluted to the required metal concentration. The results of analysing these diluted standard solutions gave a calibration curve for each metal.

8.3 APPENDIX C

Summary of experimental results

Table C1 Experimental data on effect acid treated on the removal of Co^{2+} onto cassava waste biomass at initial metal ion concentration of 100 mg/L at 30°C.

Time	Untreated biomass	0.5 M acid treated biomass	1 M acid treated biomass	Biomass (g)	Volume (mL)
0	0	0	0	0.250	50
5	10	15	17.5	0.250	50
10	20	30	30.5	0.250	50
15	25	40	42.5	0.250	50
20	30	45	53.5	0.250	50
25	40	50	60	0.250	50
30	40	50	60	0.250	50
45	40	50	60	0.250	50
60	40	50	60	0.250	50

Table C2 Experimental data on effect acid treated on the removal of Cr^{3+} onto cassava waste biomass at initial metal ion concentration of 100 mg/L at 30°C.

Time	Untreated biomass	0.5M acid treated biomass	1M acid treated biomass	Biomass (g)	Volume (mL)
0	0	0	0	0.250	50
5	12.5	15	17.5	0.250	50
10	25	30	32.5	0.250	50
15	30	45	50	0.250	50
20	35	50	60	0.250	50
25	40.5	60	65	0.250	50
30	40.5	60	65	0.250	50
45	40.5	60	65	0.250	50
60	40.5	60	65	0.250	50

Table C3 Experimental data on effect acid treated on the removal of V^{3+} onto cassava waste biomass at initial metal ion concentration of 100 mg/L at 30°C.

Time	Untreated biomass	0.5M acid treated biomass	1M acid treated biomass	Biomass (g)	Volume (mL)
0	0	0	0	0.250	50
5	10	15	15	0.250	50
10	19	25	36	0.250	50
15	28	45	56	0.250	50
20	36	60	62	0.250	50
25	42	62	70	0.250	50
30	42	62	70	0.250	50
45	42	62	70	0.250	50
60	42	62	70	0.250	50

Table C4 Experimental data on the effect of initial pH on the removal of Co^{2+}, Cr^{3+} and V^{3+} onto cassava waste biomass at initial metal ion concentration of 100 mg/L at 30°C.

Adsorption %								
pH	**2**	**3**	**4**	**5**	**6**	**7**	**Biomass** (g)	**Volume** (mL)
Single metal ion concentration								
Co^{2+}	20	40	50	55	60	42	0.250	50
Cr^{3+}	70	78	71	42	25	12	0.250	50
V^{3+}	80	90	71	45	28	13	0.250	50
Binary metal ions solution								
Co	40	45	55	60	70	30	0.250	50
V	60	74	55	40	30	19		50
Binary metal ions solution								
Co	25	37	50	60	70	80	0.250	50
Cr	70	82	60	53	50	39	0.250	50
Binary metal ions solution								
Cr	57	67	50	45	40	300	0.250	50
V	68	77.2	51.2	44.1	39.8	34.3	0.250	50
Ternary metal ion solution								
Co^{2+}	20	30	40	45	50	75	0.250	50
Cr^{3+}	36.2	30.1	26.5	25.6	23	22.9	0.250	50
V^{3+}	45	50	43.3	42	40	38.8	0.250	50

Table C5 Experimental data on effect of contact time on the removal of Co^{2+}, Cr^{3+} and V^{3+} onto cassava waste

Time	**Co**	**Cr**	**V**	**Biomass (g)**	**Volume (mL)**
0	0	0	0	0.250	50
5	5	5	10	0.250	50
10	10	10	20	0.250	50
15	20	15	30	0.250	50
20	25	20	35	0.250	50
25	32	35	37.5	0.250	50
30	32	35	40	0.250	50
45	32	35	40	0.250	50
60	32	35	40	0.250	50

Table C6 Experimental data on effect of temperature on the removal of Co^{2+}, Cr^{3+} and V^{3+} onto cassava waste biomass

	Adsorption (%)						
	30°C	**35°C**	**40°C**	**45°C**	**50°C**	**Biomass** (g)	**Volume** (mL)
Single metal ion solution							
Co^{2+}	25	45	55	30	10	0.250	50
Cr^{3+}	30	55	61.5	40	20	0.250	50
V^{3+}	34	60	65	45	25	0.250	50
Ternary metal ion solution							
Co^{2+}	25	28	30.3	20.3	18.4	0.250	50
Cr^{3+}	26.6	32	35	25	20.1	0.250	50
V^{3+}	32	45	50	30	23	0.250	50

Table C7 Experimental data on effect of agitation speed on the removal of Co^{2+}, Cr^{3+} and V^{3+} on cassava waste biomass

	Adsorption (%)					
	50 rpm	**100 rpm**	**150 rpm**	**200 rpm**	**Biomass** (g)	**Volume** (mL)
Single metal ion solution						
Co^{2+}	25	45	60	24	0.250	50
Cr^{3+}	40	50	62.5	25	0.250	50
V^{3+}	40.5	55	65	30	0.250	50
Ternary metal ion solution						
Co^{2+}	23.8	27	35	17.6	0.250	50
Cr^{3+}	20.1	26.7	40	19	0.250	50
V^{3+}	32	40	50	26	0.250	50

Table C8 Experimental data on the effect of biomass dosage on the removal of Co^{2+}, Cr^{3+} and V^{3+} on to cassava waste biomass at initial metal ion concentration of 100 mg/L at 40°C.

	Adsorption (%)						
	0.05 g	**0.10 g**	**0.15 g**	**0.20 g**	**0.25 g**	**0.3 g**	**Volume** (mL)
Single metal ion solution							
Co^{2+}	20	40	52	63	70	72	50
Cr^{3+}	21	38	56	65	73	75	50
V^{3+}	25	37	53.1	69.7	74.3	78	50
Ternary metal ion solution							
Co^{2+}	20	21.2	23.8	25.7	27.9	32	50
Cr^{3+}	19.6	20.9	21.3	23.1	24.8	40	50
V^{3+}	20	37	50	52	55	63	50

Table C9 Experimental data on the effect of initial metal ion concentration on the removal of Co^{2+}, Cr^{3+} and V^{3+} on to cassava waste biomass at 40°C.

	Adsorption (%)						
	50 mg/L	**100 mg/L**	**150 mg/L**	**200 mg/L**	**250 mg/L**	**Biomass** (g)	**Volume** (mL)
Single metal ion solution							
Co^{2+}	45	57.5	40	30	27	0.250	50
Cr^{3+}	60	70	50	40	23	0.250	50
V^{3+}	67	75	50	35	20	0.250	50
Ternary metal ion solution							
Co^{2+}	18.7	28.5	12.9	12	12	0.250	50
Cr^{3+}	30	50	39	36	34.3	0.250	50
V^{3+}	56	58	54.9	53.2	52.8	0.250	50

Table C10 Experimental data on the effect of co-cations on the removal of Co^{2+}, Cr^{3+} and V^{3+} on to cassava waste biomass at initial metal concentration of 100 mg/L at 40°C

	Adsorption (%)						
	control	**0.2 g/L**	**0.5 g/L**	**1 g/L**	**2 g/L**	**Biomass** (g)	**Volume** (mL)
Cobalt adsorption							
Ca^{2+}	60	55	40	19	15	0.250	50
K^{+}	60	59.8	59.6	58	57	0.250	50
Mg^{2+}	60	56	55.9	45	40	0.250	50
Na^{+}	60	59.9	59.8	59.4	59	0.250	50
Chromium adsorption							
Ca^{2+}	57	34	25	16	7	0.250	50
K^{+}	57	56	55	54.1	53.8	0.250	50
Mg^{2+}	57	45	30	26	21	0.250	50
Na^{+}	57	56.7	56	55.5	55	0.250	50
Vanadium adsorption							
Ca^{2+}	55	38	27	20	8	0.250	50
K^{+}	55	53	52.3	52	52.1	0.250	50
Mg^{2+}	55	40	32	25	20	0.250	50
Na^{+}	55	54.5	54	53	52.7	0.250	50

Table C11 Experimental data effect of H_2SO_4 concentrations on the desorption efficiency of Co^{2+}, Cr^{3+} and V^{3+} from cassava waste biomass.

	Desorption efficiency (%)						
	0.1 mol/L	**0.5 mol/L**	**1 mol/L**	**1.5 mol/L**	**2 mol/L**	**Biomass** (g)	**Volume** (mL)
Co^{2+}	84	87	95	94.5	95	0.250	50
Cr^{3+}	76.4	77	85	84.9	85	0.250	50
V^{3+}	65.7	67.6	71.6	71.7	71.9	0.250	50

Table C12 Experimental data on the effect of adsorption- desorption efficiency on the removal of Co^{2+}, Cr^{3+} and V^{3+} on to cassava waste biomass at 40°C.

	1	**2**	**3**	**4**	**5**	**6**	**7**	**8**	**9**	**10**	**Biomass** (g)	**Volume** (mL)
Adsorption efficiency												
Co^{2+}	77.8	77.2	77.2	77.0	77.0	76.2	74.0	71.0	68.0	64.1	0.250	50
Cr^{3+}	83.5	83.5	83.2	83.1	83	81.1	79.0	76.0	71.0	68.0	0.250	50
V^{3+}	85.4	85.4	85.2	85.1	85.0	83.0	80.0	78.0	74.0	700	0.250	50
Desorption efficiency												
Co^{2+}	90.5	90.3	90.1	90.2	89.9	89.1	83.0	80.0	78.0	74.0	0.250	50
Cr^{3+}	82.0	81.9	81.6	81.5	80.1	78.3	72	69	67.3	62.0	0.250	50
V^{3+}	75.0	75.2	75.0	74.1	74.0	73.1	70.0	66.0	63.0	57.0	0.250	50

Table C13 Experimental data on the effect of flow rate on the removal of cobalt on the cassava waste biomass at initial metal ion concentration of 100 mg/L and bed depth of 10 cm

Time	**0.83 mL/s**	**1.25 mL/s**	**1.61 mL/s**
0	0.01	0.02	0.03
2	0.02	0.03	0.05
4	0.03	0.05	0.07
6	0.04	0.07	0.12
8	0.05	0.09	0.16
10	0.07	0.15	0.20
20	0.20	0.25	0.40
30	0.29	0.35	0.50
40	0.34	0.50	0.62
50	0.40	0.68	0.75
60	0.53	0.72	0.79
90	0.66	0.80	0.87
120	0.77	0.85	0.90
150	0.85	0.92	0.93
180	0.90	0.94	0.93
240	0.92	0.94	0.93
300	0.93	0.94	0.94

Table C14 Experimental data on the effect of flow rate on the removal of chromium on the cassava waste biomass at initial metal ion concentration of 100 mg/L and bed depth of 10 cm

Time (min)	**0.83 mL/s**	**1.25 mL/s**	**1.61 mL/s**
0	0.01	0.02	0.03
2	0.04	0.04	0.04
4	0.04	0.05	0.06
6	0.05	0.08	0.15
8	0.07	0.15	0.30
10	0.08	0.24	0.45
20	0.17	0.45	0.65
30	0.30	0.60	0.72
40	0.41	0.70	0.77
50	0.61	0.75	0.81
60	0.68	0.81	0.87
90	0.76	0.86	0.91
120	0.81	0.90	0.92
150	0.86	0.90	0.92
180	0.89	0.91	0.94
240	0.94	0.93	0.94
300	0.95	0.94	0.96

Table C15 Experimental data on the effect of flow rate on the removal of vanadium on the cassava waste biomass at initial metal ion concentration of 100 mg/L and bed depth of 10 cm

Time (min)	**0.83 mL/s**	**1.25 mL/s**	**1.61 mL/s**
0	0.024	0.03	0.04
2	0.03	0.05	0.06
4	0.035	0.08	0.07
6	0.05	0.10	0.20
8	0.06	0.21	0.44
10	0.10	0.35	0.60
20	0.35	0.60	0.76
30	0.52	0.70	0.80
40	0.67	0.80	0.85
50	0.72	0.85	0.89
60	0.76	0.88	0.91
90	0.82	0.91	0.92
120	0.87	0.92	0.93
150	0.92	0.92	0.95
180	0.94	0.92	0.95
240	0.95	0.94	0.96
300	0.96	0.94	0.96

Table C16 Experimental data on the effect of bed depth on the removal of Co^{2+} on the cassava waste biomass at initial metal ion concentration of 100 mg/L and flow rate of 0.83 mL/s.

Time (min)	5 cm	10 cm	15 cm
0	0.01	0.01	0.01
2	0.03	0.02	0.02
4	0.04	0.03	0.03
6	0.05	0.04	0.04
8	0.10	0.05	0.05
10	0.20	0.07	0.06
20	0.47	0.20	0.08
30	0.67	0.29	0.15
40	0.75	0.54	0.30
50	0.81	0.60	0.40
60	0.84	0.65	0.56
90	0.86	0.72	0.68
120	0.85	0.77	0.74
150	0.86	0.85	0.80
180	0.87	0.90	0.91
240	0.88	0.92	0.93

Table C17 Experimental data on the effect of bed depth on the removal of Cr^{3+}on the cassava waste biomass at initial metal ion concentration of 100 mg/L and flow rate of 0.83 mL/s.

Time (min)	**5 cm**	**10 cm**	**15 cm**
0	0.02	0.01	0.01
2	0.04	0.04	0.03
4	0.06	0.04	0.04
6	0.10	0.05	0.06
8	0.15	0.07	0.07
10	0.20	0.08	0.09
20	0.35	0.17	0.11
30	0.45	0.30	0.20
40	0.57	0.41	0.33
50	0.76	0.70	0.62
60	0.86	0.78	0.76
90	0.88	0.83	0.89
120	0.93	0.88	0.92
150	0.94	0.91	0.94
180	0.94	0.95	0.95
240	0.94	0.96	0.96
300	0.95	0.97	0.98

Table C18 Experimental data on the effect of bed depth on the removal of V^{3+} on the cassava waste biomass at initial metal ion concentration of 100 mg/L and flow rate of 0.83 mL/s.

Time (min)	5 cm	10 cm	15 cm
0	0.01	0.02	0.02
2	0.03	0.03	0.03
4	0.07	0.035	0.04
6	0.15	0.05	0.05
8	0.27	0.09	0.06
10	0.35	0.18	0.07
20	0.60	0.42	0.09
30	0.68	0.60	0.20
40	0.76	0.67	0.35
50	0.83	0.71	0.56
60	0.85	0.74	0.62
90	0.86	0.80	0.70
120	0.87	0.85	0.75
150	0.89	0.91	0.8
180	0.90	0.93	0.92
240	0.91	0.93	0.95
300	0.92	0.95	0.99

Table C19 Experimental data on the effect of adsorption-desorption efficiency on the removal of Co^{2+}, Cr^{3+} and V^{3+} on the cassava waste biomass at initial metal ion concentration of 100 mg/L, bed depth of 15 cm and flow rate of 0.83 mL/s.

No of cycles	**1**	**2**	**3**	**4**	**5**	**6**
Adsorption efficiency						
Co^{2+}	89	87	85	84	83	80
Cr^{3+}	95.5	95	94	92	91	89
V^{3+}	98.8	97	96.1	95	94	93
Desorption deficiency						
Co^{2+}	86	85.3	84.3	83	80	79
Cr^{3+}	78	77.1	75	74	71	67.8
V^{3+}	73	73.2	71	69.8	67	65

Table C20 Experimental data on the effect of adsorption-desorption efficiency on the removal of Co^{2+}, Cr^{3+} and V^{3+} on the cassava waste biomass using semi-counter current system at initial metal ion concentration of 100 mg/L.

No of cycles	**1**	**2**	**3**	**4**	**5**	**6**
Adsorption efficiency						
Co^{2+}	91.6	90	89.2	87	86	85
Cr^{3+}	94.5	93.2	92	91	89	87
V^{3+}	99.5	99.2	98.8	96.6	95.2	93.5
Desorption deficiency						
Co^{2+}	97.5	96.1	94.4	93.1	90.6	89.9
Cr^{3+}	95	91.7	89.7	87	85.6	84.1
V^{3+}	91	87.8	85.3	84.2	82.1	80

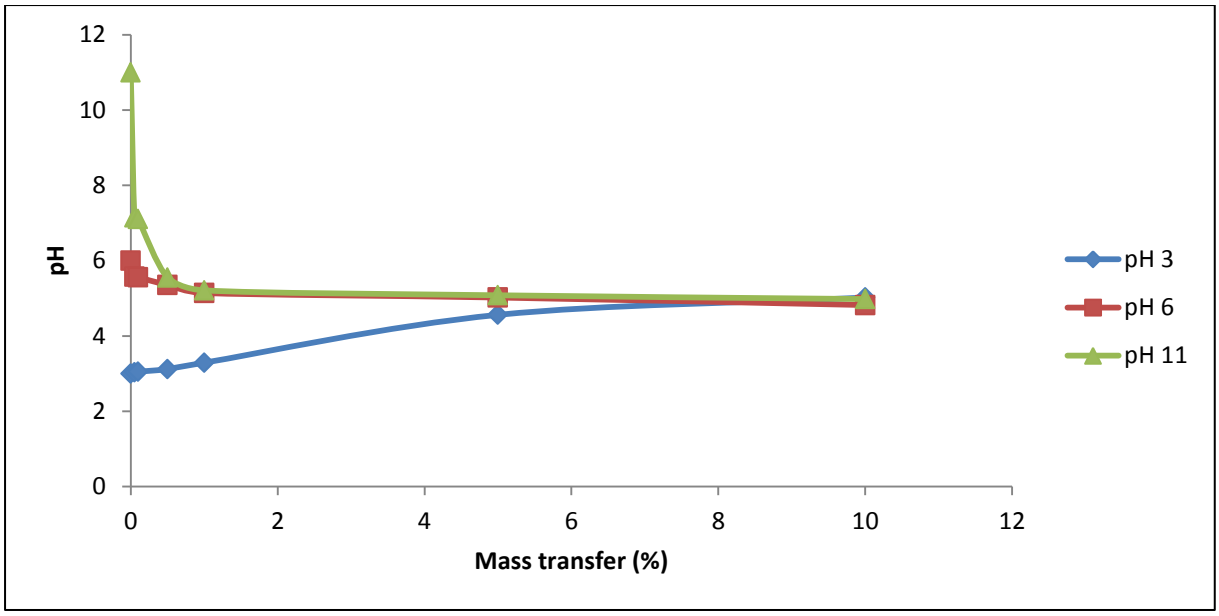

Figure C1 Determining point of zero charge for untreated cassava waste biomass

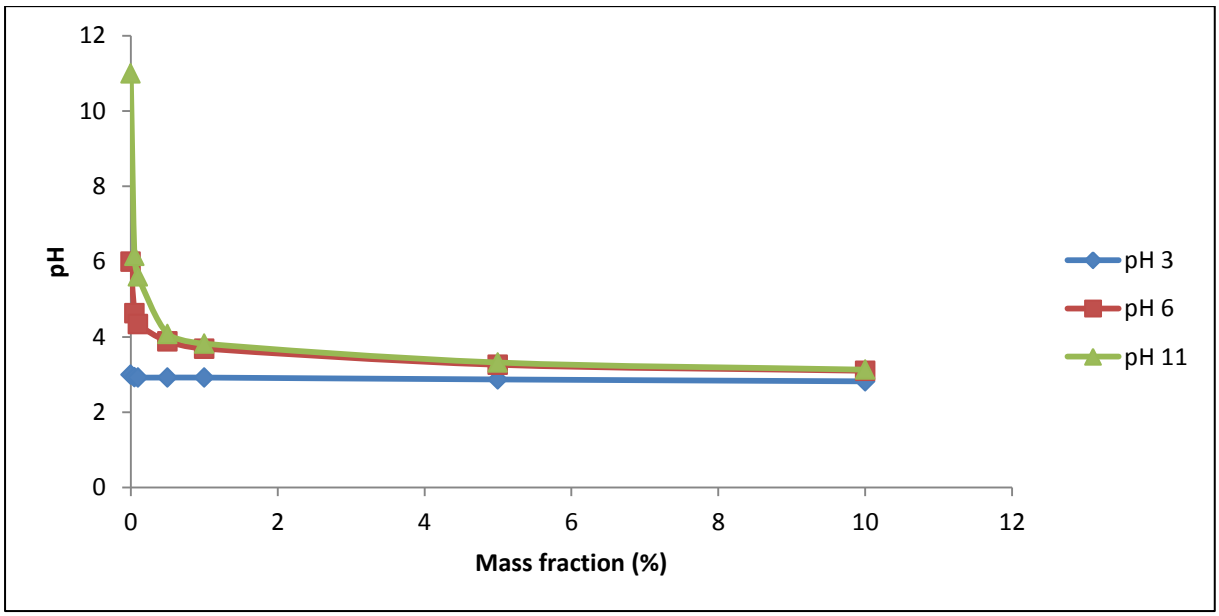

Figure C2 Determining point of zero charge for acid treated cassava waste biomass

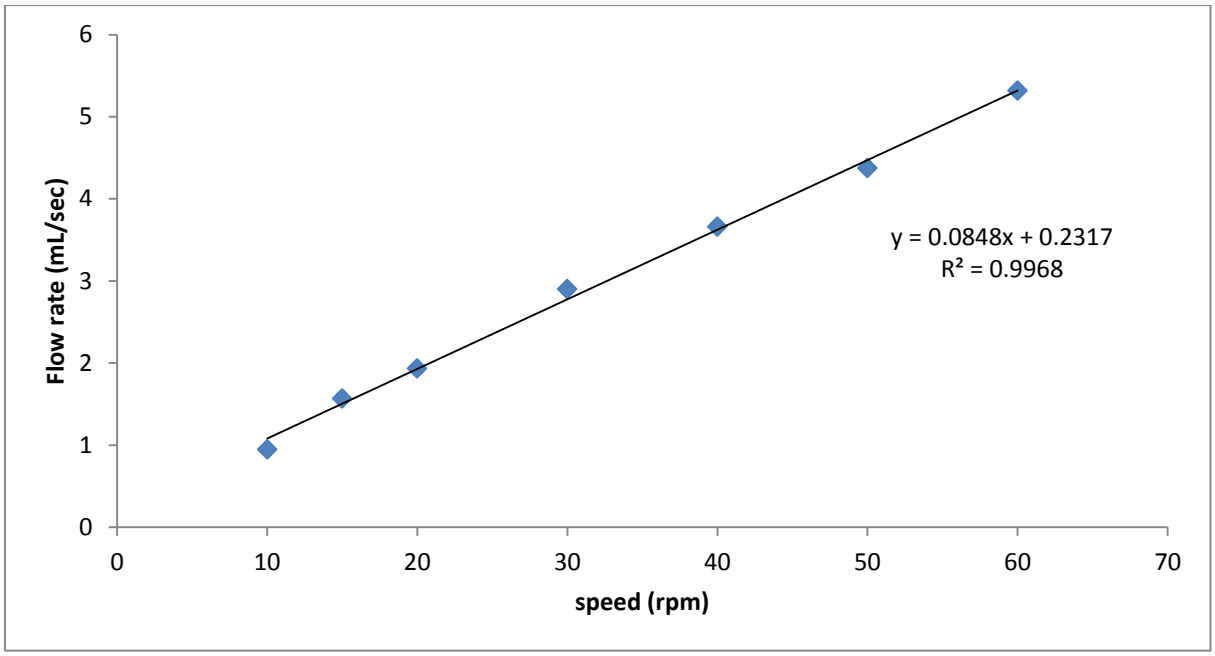

Figure C3 Peristaltic pump calibrations curve

.

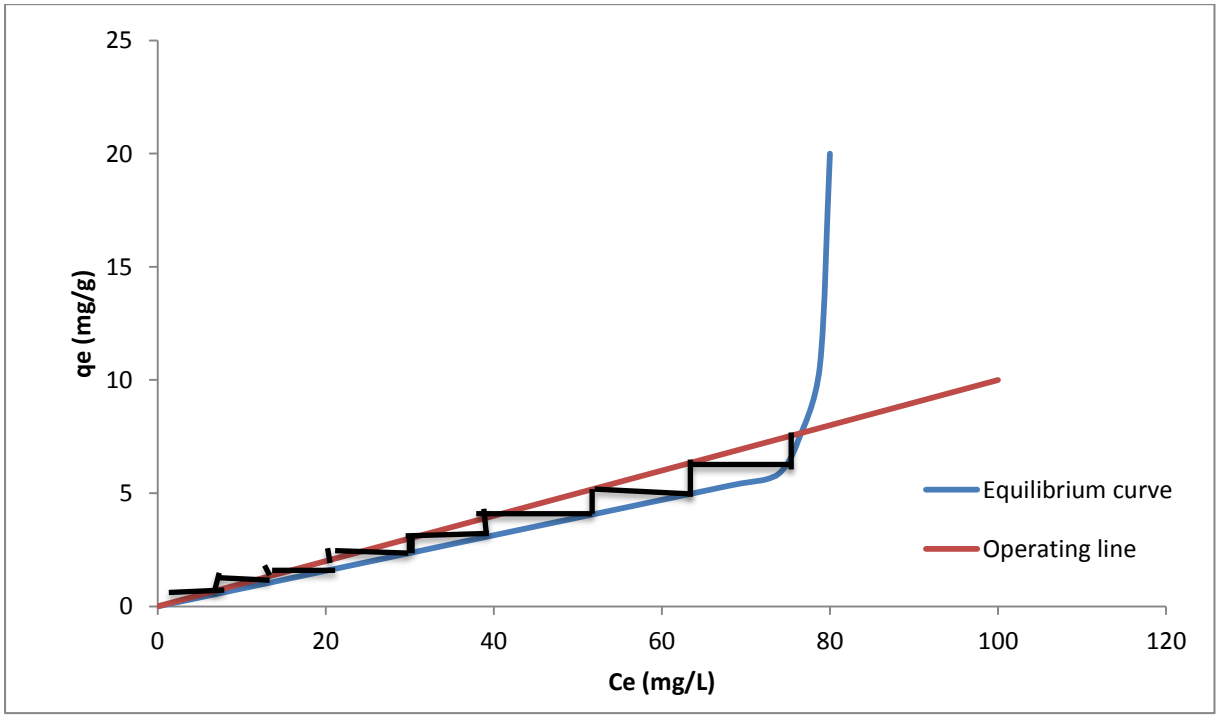

Figure C4 Determining the number of stages for Co^{2+}

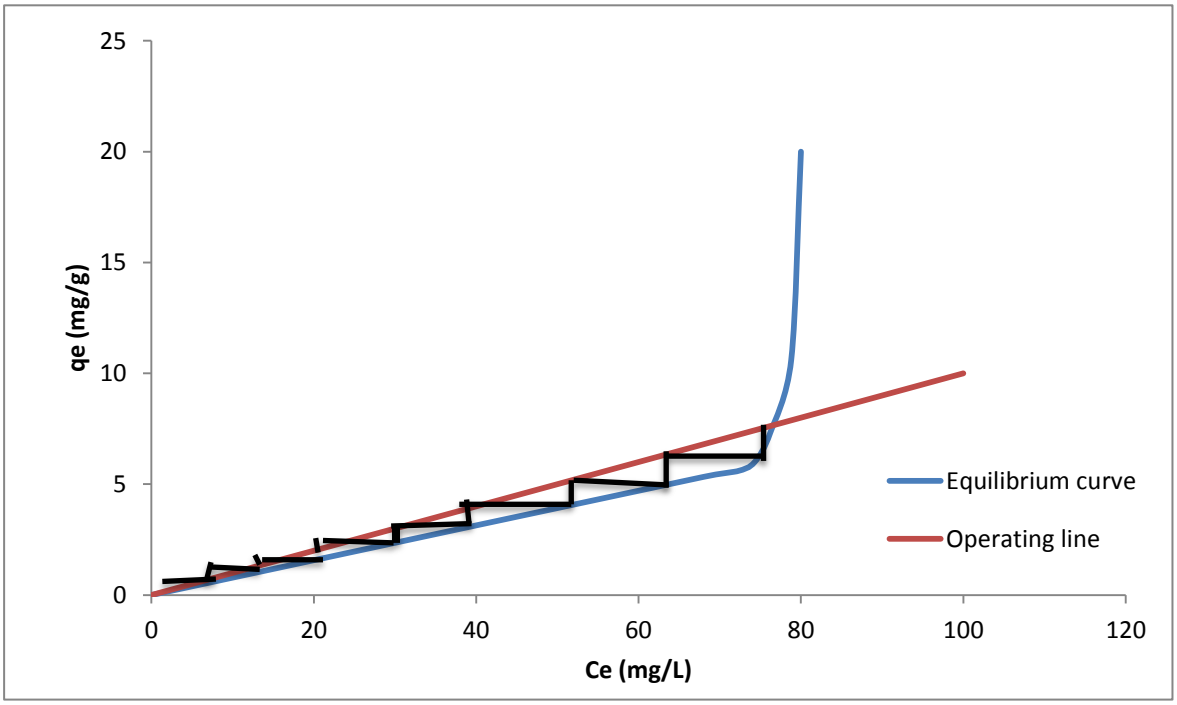

Figure C4 Determining the number of stages for Cr^{3+}

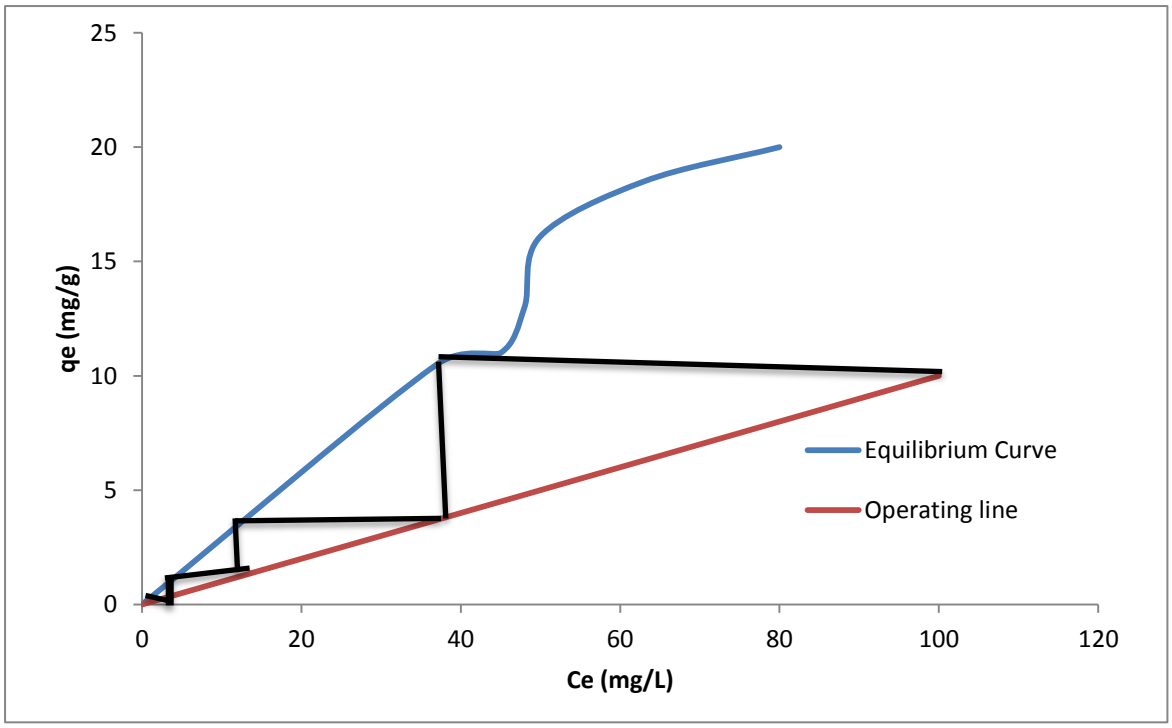

Figure C4 Determining the number of stages for V^{3+}